Cellular effects of the multidomain serine/threonine kinase from *Yersinia enterocolitica*

von

Gerhardt Zenner

Hamburg 2007

Die vorliegende Arbeit wurde zwischen Februar 2003 und Januar 2007 unter Anleitung von Prof. Dr. M. Aepfelbacher am Max von Pettenkofer Institut in München und am Institut für Medizinische Mikrobiologie, Virologie und Hygiene am Universitätskrankenhaus Eppendorf in Hamburg durchgeführt. Die Arbeit wurde betreut und vor der biologischen Fakultät vertreten durch PD Dr. Angelika Böttger (Department Biologie II, LMU, München).

Wesentliche Teile dieser Arbeit sind in folgender Publikation veröffentlicht:

* Trasak, C., <u>G. Zenner</u>, A. Vogel, G. Yuksekdag, R. Rost, I. Haase, M. Fischer, L. Israel, A. Imhof, S. Linder, M. Schleicher, and M. Aepfelbacher. 2007. Yersinia Protein Kinase YopO Is Activated by A Novel G-actin Binding Process. *J Biol Chem*. 282:2268-2277.

* Gleichberechtigte Erstautorschaft die im Verlauf der Dissertation entstanden ist.

Weitere Publikationen:

Ruckdeschel, K., G. Pfaffinger, K. Trulzsch, <u>G. Zenner</u>, K. Richter, J. Heesemann, and M. Aepfelbacher. 2006. The proteasome pathway destabilizes Yersinia outer protein E and represses its antihost cell activities. *J Immunol*. 176:6093-102.

Osiak, A.E., <u>G. Zenner</u>, and S. Linder. 2005. Subconfluent endothelial cells form podosomes downstream of cytokine and RhoGTPase signaling. *Exp Cell Res*. 307:342-53.

Dissertation zur Erlangung des Doktorgrades
an der Fakultät für Biologie
der Ludwig-Maximilians-Universität München
vorgelegt von
Dipl.-Biol. Gerhardt Zenner
aus Arad.

Gutachter:
Erstgutachter: PD Dr. Angelika Böttger.
Zweitgutachter: Prof. Dr. Michael Schleicher
Sondergutachter: Prof. Dr. M. Aepfelbacher

Tag der Einreichung: 05.02.2007
Tag der mündlichen Prüfung: 23.05.2007

Ehrenwörtliche Versicherung

Ich versichere, dass die Dissertation von mir selbständig und ohne unerlaubte Hilfsmittel angefertigt wurde. Die Dissertation habe ich keiner anderen Fakultät oder Universität zur Prüfung vorgelegt. Außerdem habe ich noch nicht versucht, eine Dissertation einzureichen oder mich einer Doktorprüfung zu unterziehen.

Die Arbeit wurde von PD Dr. Angelika Böttger, Department Biologie II, LMU München, betreut.

Hamburg, im Januar 2007

Gerhardt Zenner

A. ABSTRACT

Pathogenic bacteria of the genus *Yersinia* have in common the capacity to overcome the defense mechanisms of their mammalian hosts and to survive and proliferate in lymphoid tissues. Yersiniae employ a type III secretion system to inject effector proteins (Yops) that modulate host cell signaling by unique biochemical activities. One of these effector proteins (YopO) is a 729 amino acid serine/threonine kinase activated by G-actin. Studies of YopO protein organization revealed the following functional domains: Amino acids 1-88 comprise a bacterial secretion/translocation domain also responsible for localization of YopO at the plasma membrane of target cells. The catalytic activity is encompassed by amino acids 89-440 and the C-terminal amino acids 441-729 harbour a Rho GTPase-binding guanine nucleotide dissociation inhibitor (GDI) -like region and an actin binding region.

Here, YopO constructs were established and biochemically characterized with the aim to separate the different YopO activities (kinase, Rho-binding, actin binding) and investigate their cellular effects. In the course of these experiments two separate G-actin binding sites (89-440 and 441-729) were identified and shown to be necessary for effective YopO autophosphorylation on amino acids serine-90 and serine-95.

In infected cells YopO was shown earlier to disrupt F-actin structures and cause a specific phenotype referred to as rounding/arborization where cell retraction occurs without dissolution of focal adhesions. Here the biochemically characterized constructs were individually evaluated for their effects on cell morphology. A YopO construct comprising only the C-terminal Rho-binding GDI-like domain was capable of disrupting F-actin structures. Cell rounding/arborization, however, was specifically dependent on the kinase activity, because the kinase dead YopOD267A/K269A and truncations with reduced kinase activity showed significantly reduced rounding/arborization. Actin binding of YopO itself did not affect F-actin disruption or cell rounding. Using the established constructs we also found that kinase activity was essential for inhibition of YadA-mediated internalization. This internalization mechanism is *Yersinia*-specific and involves bridging of the *Yersinia* adhesin YadA with extracellular matrix to cellular integrin receptors.

Thus, the different structural entities of YopO could be assigned to specific cellular effects and for the first time the kinase activity of YopO could be related to modulation of an immunologically relevant cell function. These results provide a novel piece of information as to the molecular mode of action of a *Yersinia* virulence factor and further our knowledge of the pathogenicity of yersiniae.

B. INTRODUCTION

1. THE GENUS *YERSINIA*

The genus *Yersinia* (named *Pasteurella* until 1964) is named after Alexandre Yersin, who isolated and identified *Yersinia pestis* as the causative agent of plague in the year 1894 (Schleifstein and Coleman 1939; Frederiksen 1964). The genus *Yersinia* belongs to the family of *Enterobacteriaceae* and comprises gram negative, rod shaped, facultative anaerobe, katalase-positive, oxidase-negative, non spore forming bacteria (Brenner 1979; Miller, Finlay et al. 1988).

There are 11 known *Yersinia* species, three of which, *Yersinia pestis*, *Yersinia pseudotuberculosis* and *Yersinia enterocolitica* are pathogenic to humans and rodents causing syndromes ranging from the deadly plague to gastroenteritis (Brenner 1979; Cornelis, Laroche et al. 1987; Knapp 1988). Credible estimates of the number of people killed by *Yersinia pestis* during the course of history approach 200 million (Perry and Fetherston 1997). *Y. pestis* is known to be lethal to non-human primates and many rodents at infecting doses of 10 bacteria or less (Brubaker 1991). *Yersinia* has several chromosomal and plasmid-associated factors (overviewed in Table B1) that are essential to its virulence and survival in mammalian hosts and flea vectors (Brubaker 1991; Straley and Perry 1995).

Y. pestis is an obligate pathogen dependent on an insect-mammal infection cycle. In contrast, *Y. enterocolitica* and *Y. pseudotuberculosis* are free living microorganisms and food-borne pathogens. Contaminated milk and pork products are the main source of *Y. enterocolitica* infections (Black, Jackson et al. 1978). *Yersinia pseudotuberculosis* causes mesenteric adenitis and septicemia, and *Yersinia enterocolitica*, the most prevalent in human infections, causes gastrointestinal syndromes ranging from an acute enteritis to mesenteric lymphadenitis. All three species are invasive lymphotrophic bacteria, which have a common capacity to resist non-specific immune response, in particular phagocytosis and killing by macrophages and polymorphonuclear leukocytes (PMNs) (Cornelis, Boland et al. 1998). The three pathogenic species however differ considerably in invasiveness; while *Y.enterocolitica* and *Y. pseudotuberculosis* can cross the gastro-intestinal mucosa to infect underlying tissue, *Y. pestis* is injected into the body by an insect (e.g. rat flea, *Xenopsylla cheopis*) bite, and thus, does not have to penetrate any body surface on its own (Cornelis, Boland et al. 1998). If *Y. pestis* causes pneumonia in infected persons, the bacteria can be transmitted by exhausted droplets.

Table B1. **Distinguishing properties and virulence determinants of wild-type *Y. pestis, Y. pseudo-tuberculosis*, and *Y. enterocolitica* (Brubaker 1991 with modifications).**

Gene product and location of genes	Established or putative virulence function	*Y. pestis*	*Y. pseudotuberculosis*	*Y. enterocolitica*
pPla plasmid		+	-	-
Pesticin	-	+	-	-
Plasminogen activator	+	+	-	-
Posttranslational degradation of Yops	+	+	-	-
pCD/pYV plasmid		+	+	+
Yops	+	+	+	+
YadA (protein 1 or YopA)	+	-	+	+
V antigen	+	+	+	+
pFra plasmid		+	-	-
Fraction 1 or capsular antigen	+	+	-	-
Phospholipase D	+	+	-	-
Chromosomal determinants				
Pigmentation or peptide F (hemin storage at 26°C)	+ / -	+	-	-
Motility (26°C)	-	-	+	+
Hydrophobic sugars in LPS (26°C)/O-antigen	-	-	+	+
Assimilation of low levels of NH$_4$ (26°C)	-	-	+	+
Constitutive glyoxylate bypass	-	+	-	-
Aspartase	-	-	+	+
Glucose 6-phosphate dehydrogenase	-	-	+	+
Urease	-	-	+	+
Ornithine decarboxylase	-	-	-	+
Host cell invasins				
Invasin (Inv)	+	-	+	+
Attachment invasion locus (Ail)	+	-	-	+
pH 6 antigen/Myf	+	+	+	+
Antigen 5 (catalase)	+	+	+	-
Fermentation of				
Rhamnose	-	-	+	-
Melibiose	-	-	+	-
Sucrose	-	-	-	+
Sorbitol	-	-	-	+
Cellobiose	-	-	-	-
Biosynthesis of				
Methionine	-	-	+	+
Phenylalanine	-	-	+	+
Threonine-glycine	-	-	+	+
Isoleucine-valine	-	-	+	+

Wild-type *Y. pestis* and *Y. pseudotuberculosis* show very high (97 %) chromosomal DNA homology, while chromosomal DNA of *Y. enterocolitica* is significantly less related, indicating that the event of its evolutionary divergence occurred prior to that separating *Y. pseudotuberculosis* and *Y. pestis* (Moore 1979; Achtman, Zurth et al. 1999; Motin, Georgescu et al. 2002).

The medically significant yersiniae grow on suitable media at temperatures ranging from 5 to 42 °C. In contrast to *Y. pestis*, which is immobile independently of the ambient temperature (Cover and Aber 1989; Bottone 1999), the enteropathogenic yersiniae are motile at 27 °C and loose their motility at 37 °C, which is the temperature typical in the host environment (Badger and Miller 1998). The organisms can be identified and differentiated by biochemical and serological reactions and in case of *Y. enterocolitica* also by phage-typing methods (Aleksic and Bockemuhl 1990).

2. *YERSINIA ENTEROCOLITICA* PREVALENCE AND CLINICAL PICTURE

Y. enterocolitica is widely distributed in nature in aquatic and animal reservoirs, with swine serving as a major reservoir for human pathogenic strains (Bottone 1997). Based on biochemical features *Y. enterocolitica* is divided in 6 biogroups, namely 1A (non pathogenic), 1B (highly pathogenic) and biogroups 2, 3, 4 and 5 that are weakly pathogenic (Wauters, Kandolo et al. 1987). Serologically, *Y. enterocolitica* can be separated into almost 60 serotypes of which only 11 serotypes have been most frequently associated with human infection (see Table B2).

On a worldwide basis the majority of these infections are caused by serotypes O:3, O:9, O:5,27 and O:8. In the USA the dominant serotypes are O:4, O:8, O:13, O:18, O:20 and O:21, all belonging to the highly pathogenic biogroup 1B, while the dominant pathogenic serotypes in Europe are O:3, O:5,27 and O:9, which can be assigned to the weakly pathogenic biogroups 2 to 5 (Aleksic and Bockemuhl 1990). However, recently a *Y. enterocolitica* O:8 strain has also been isolated in Germany (Schubert, Bockemuhl et al. 2003). A United States population-based surveillance for *Y. enterocolitica* infections for the years 1996 to 1999 reported an average annual incidence of 3.2 cases/100.000 population and a higher risk for disease in infants and minority populations (Ray, Ahuja et al. 2004).

Table B2. **Virulence of *Y. enterocolitica* correlated with biogroup, serogroup, and ecologic and geographic distribution (Bottone 1999 with modifications).**

Associated with human infections	Biogroup	Serotype(s)	Ecologic distribution
Yes	1B	O:8, O:4, O:13a,13b, O:18, O:20, O:21	Environment, pigs (O:8), mainly in the United States, Japan, Europe
Yes	2	O:9, O:5,27	Pigs, Europe (O:9), United States (O:5,27), Japan (O:5,27), Sweden, The Netherlands
Yes	3	O:1,2,3, O:5,27, O:3	Chinchilla (O:1,2,3), pigs (O:5,27)
Yes	4	O:3	Pigs, Europe, United States, Japan, South Africa, Scandinavia, Canada, The Netherlands
Yes	5	O:2,3	Hare, Europe
No[a]	1A	O:5, O:6,30, O:7,8, O:18, O:46, nontypeable	Environment, pigs, food, water, animal and human feces, global

a *Y. enterocolitica* isolates comprising biogroup 1A may be opportunistic pathogens in patients with underlying disorders.

Infection with *Yersinia enterocolitica* is typically initiated by uptake of contaminated food, following the oral route (Cover and Aber 1989; Aleksic and Bockemuhl 1990). Four to seven days after exposure *Yersinia enterocolitica* causes symptoms from mild self-limiting diarrhea (potentially accompanied by low-grade fever and vomiting) to acute mesenteric lymphadenitis (Bottone 1997). Gastroenteritis, caused by *Y. enterocolitica*, is the most frequent form of Yersiniosis, typically affecting infants and young children. In older children and young adults, acute Yersiniosis can present as a pseudoappendicular syndrome, which is frequently confused with appendicitis. Long-term sequelae, including reactive arthritis, erythema nodosum, glomerulonephritis and myocarditis, are mainly seen in young adults (Fredriksson-Ahomaa, Stolle et al. 2006). Sepsis is a rare complication of *Y. enterocolitica* infection, except in patients who have a predisposing underlying disease or are in an iron-overloaded state. (Winblad 1969; Dequeker, Jamar et al. 1980). In most cases *Y. enterocolitica* infection is self limiting.

3. PATHOGENICITY OF *YERSINIA ENTEROCOLITICA*

In the life cycle of enteropathogenic yersiniae, survival outside the host is essential and in order to achieve this *Yersinia* is able to adapt gene expression to its variable environments. Before ingestion by humans, *Y. enterocolitica* and *Y. pseudotuberculosis* survive in moist natural environments or in food by means of highly adaptable metabolic pathways that are typical for free-living enteric bacteria. Examples for properties that are strongly expressed at ambient temperatures in *Y. enterocolitica* and weakly or not at all at 37 °C are motility, smooth lipopolysaccharide (LPS), some metabolic properties, the adhesin invasin (Inv) and the heat stable enterotoxin Yst (Straley and Perry 1995). The resistance to the immune response of the host, the tropism of the bacteria for lymphoid tissue and the manner in which they are able to spread inside the host are accomplished by pathogenicity factors that are coded on the chromosome and also on extra-chromosomal elements.

One of these chromosomally coded elements is a genomic island, called high-pathogenicity Island (HPI), essential for the mouse-virulence phenotype in *Yersinia*. The HPI is indispensable for pathogenicity of *Yersinia* and also certain pathotypes of *Escherichia coli* (Schubert, Rakin et al. 2004). Strains carrying this HPI, which mediates biosynthesis and uptake of the siderophore Yersiniabactin, are able to adapt to low iron conditions inside the host (Heesemann, Hantke et al. 1993; Carniel, Guilvout et al. 1996).

During colonization *Y. enterocolitica* adheres to intestinal mucin of epithelial cells and passes through the epithelial layer (Hanski, Kutschka et al. 1989; Straley and Perry 1995). This translocation occurs in the small intestine where bacteria cross the intestinal epithelial barrier selectively through the M cells in the follicle-associated epithelium of the Peyer's patches. M cells are specialized cells that take up particles or antigens and transport these components to the gut-associated lymphoid tissue (Neutra, Mantis et al. 2001; Grassl, Bohn et al. 2003). It was shown in mouse models that localized infection of the gut by *Yersinia* was followed by dissemination into other organ sites and the ensuing growth of the organism in the liver and spleen leads to the eventual death of the animal (Autenrieth and Firsching 1996).

The capability of *Yersinia* to resist the non specific immune defense of the host depends on the presence of a 70-kb virulence plasmid (pYV) that encodes a set of secreted proteins, termed Yops (*Yersinia* outer proteins) (Heesemann, Gross et al. 1986), the proteins necessary for injecting the Yops into host cells (termed type III secretion system) and the adhesin YadA (Snellings, Popek et al. 2001; Cornelis 2002; Barnes, Bergman et al. 2006).

4. ADHESION AND INVASION

Many pathogenic bacteria assemble on their surface multifunctional protein structures that function as adhesins and/or defense shields against the various bactericidal weapons of the host. Bacterial adhesins can be found in the form of hair like structures with a diameter of 2-10 nm (also referred to as pili) and as non-pilus-associated adhesins that are mono- or oligomeric proteins anchored to the bacterial outer membrane. Typical members of the non-pilus-associated adhesins are the chromosomally-encoded invasin and the virulence plasmid-encoded *Yersinia* adhesin (YadA) (Hultgren, Abraham et al. 1993; Hoiczyk, Roggenkamp et al. 2000). Especially *Yersinia enterocolitica* as a pathogen that colonizes the small intestine via the oral route needs to be able to adhere to the intestinal mucosa. *Yersinia enterocolitica* employs its surface adhesins to cross the mucosal membrane - preferentially through M cells in the ileum – in order to migrate to the underlying lymphoid tissue in Peyer´s patches (Autenrieth and Firsching 1996).

4.1 Pla and pH6 antigen

Y. pestis expresses neither YadA nor Invasin. The genes encoding these adhesins are present, but are not functional (Rosqvist, Skurnik et al. 1988; Simonet, Riot et al. 1996). Two potential adhesins expressed by *Y. pestis* are Pla (plasminogen activator protease) and pH6 antigen (pH6-Ag). Pla is localized at the outer membrane, has proteolytic activity that activates plasminogen and has been suggested to be important for the ability of *Y. pestis* to infect via flea bites (Sodeinde, Subrahmanyam et al. 1992; Makoveichuk, Cherepanov et al. 2003). It was also reported that adhesion and invasion of *Y. pestis* into epithelial cells was mediated by Pla (Cowan, Jones et al. 2000).

pH6-Ag was first described more than 40 years ago (Ben-Efraim, Aronson et al. 1961) and was initially identified as an antigen expressed only at pH below 6 at 37 °C. Later it was discovered that pH6 antigen fimbrial structures on the surface of *Yersinia pestis* occur at pH 6.7 in host macrophage phagolysosomes as well as extracellularly in abscesses such as buboes (Zav'yalov, Abramov et al. 1996). The operon encoding pH6-Ag has been shown to mediate agglutination of erythrocytes from a wide variety of species and to mediate binding to epithelial cells (Yang, Merriam et al. 1996; Makoveichuk, Cherepanov et al. 2003). The *in vivo* role of pH6-Ag remains to be explored since expression *in vitro* is only seen at 37 °C at slightly acidic pH. Because ph6-Ag binds to apolipoprotein B (apoB)-containing lipoproteins in human plasma (mainly LDL) its suspected function is to prevent *Yersinia pestis* from host cell interaction. Covering the bacterial surface with host lipoproteins has

been speculated to prevent recognition of the pathogen by the host defense systems (Makoveichuk, Cherepanov et al. 2003).

4.2 Attachment Invasion Locus (Ail)

Ail is a chromosomally encoded membrane-associated protein that was shown to play a role in the attachment and subsequent invasion of eukaryotic cells by *Yersinia enterocolitica*. The *ail* gene, if transferred to laboratory *E. coli* strains, was shown to allow normally non adhesive *E. coli* to attach to several epithelial cell types (Hep-2) and efficiently enter select cell lines such as Chinese hamster ovary (CHO) cells (Miller and Falkow 1988). Several years later however it was also shown that non pathogenic strains of *Y. enterocolitica* (lacking the important adhesin invasin) even after introduction and expression of the *ail* gene, were neither able to adhere to nor to invade cultured animal cells. However, these strains became resistant to killing by human serum (Pierson and Falkow 1993).

Epidemiologically the *ail* gene has been shown to be linked exclusively to pathogenic species of *Y. enterocolitica* (Miller and Falkow 1988; Miller, Farmer et al. 1989) and to be able to confer resistance to killing by serum complement not only to *Y. enterocolitica*, but also to *E. coli*. The *ail* gene confers resistance to serum killing also to *Y. pseudotuberculosis* (Pierson and Falkow 1993), but has no role in adherence or uptake in this species (Yang, Merriam et al. 1996). The Ail protein is a 17 kDa outer membrane protein with predicted 8 membrane spanning domains, which is expressed at 37 °C in contrast to invasin (Miller, Bliska et al. 1990; Pierson and Falkow 1993). In the mouse infection model Ail has been demonstrated to be less important for pathogenicity of *Y. enterocolitica* than the other known adhesins invasin and YadA (Pepe, Wachtel et al. 1995).

4.3 Invasin

The chromosomal *inv* gene product invasin, which is generally expressed at low temperature (26 °C, pH 8 or at 37 °C, pH 5.5), but weakly at 37 °C (pH 8), is the principal invasion factor for both *Y. enterocolitica* and *Y. pseudotuberculosis* (Isberg, Voorhis et al. 1987; Pepe and Miller 1993; Revell and Miller 2000). Invasin binds directly to a subset of β1-chain integrin receptors with high affinity, which potentiates the ensuing internalization of bacteria (Isberg and Leong 1990; Van Nhieu and Isberg 1991). In a mouse infection model, a *Y. enterocolitica* *inv* mutant is severely impaired in its ability to cross the intestinal epithelium, but in later stages of disease invasin did not play a role in establishing mouse infection (Pepe and Miller 1993). It was shown that invasin confers the ability to directly bind to the five integrin receptors α3β1, α4β1, α5β1, α6β1, and αvβ1 (Isberg and Leong 1990). In the small intestine,

the only cells presenting β1 chain integrins to the intestinal lumen are M cells, which thus explains the specificity of the microorganism for this cell type during early stages of disease (Clark, Hirst et al. 1998; Isberg and Barnes 2001).

Invasin not only mediates internalization into epithelial cells, but was also shown to, independently of uptake, trigger signaling cascades leading to the activation of NF-κB and the production of various proinflammatory cytokines (Schulte and Autenrieth 1998; Kampik, Schulte et al. 2000; Schulte, Kerneis et al. 2000).

The invasin protein (92 kDa) shares similarity to the intimin family of proteins that were shown to be essential for production of the 'attaching and effacing' histopathology characteristic of pathogenic *E. coli* strains (Yu and Kaper 1992; Zhang, Kohler et al. 2002).
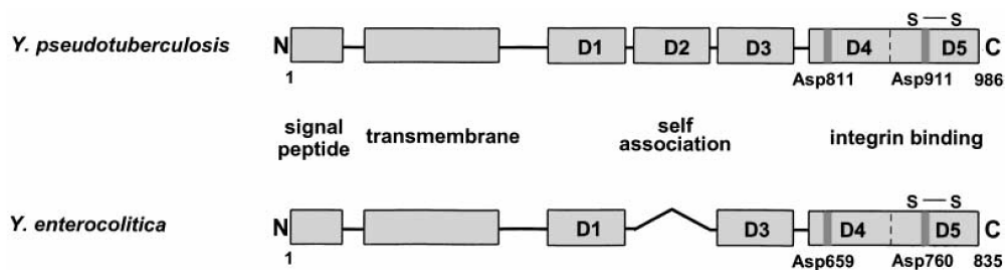
FIGURE 1. **Functional domains of *Yersinia* invasin (Grassl et al., 2003 with modifications).**
The protein is anchored in the outer membrane with its transmembrane amino-terminus.
Y. pseudotuberculosis invasin is made up by five extracellular domains (D1 — D5) with D4 and D5 containing the integrin-binding features (highlighted aspartic acid residues Asp811 and Asp911 are critical for integrin binding). Invasin molecules from *Y. pseudotuberculosis* homomultimerize on domain D2 (self association). The *Y. enterocolitica* protein is highly homologous but the homomultimerization domain D2 is absent. Asp659 and Asp760 are the corresponding amino acids critical for integrin binding.

Between the two enteropathogenic species *Y. pseudotuberculosis* and *Y. enterocolitica* the invasin proteins are highly homologous except for a homomultimerization domain which is only present in *Y. pseudotuberculosis* invasin (Dersch and Isberg 1999). The crystal structure of the C-terminal 497 amino acids, the extracellular part of *Y. pseudotuberculosis* invasin, was solved and it was shown that these amino acids form an 18 nm long rod that is made up of five domains. Domain D1 to D4 form structures similar to immunoglobulin superfamily domains while the C-terminal domain D5 is similar to C-type lectin-like domains of proteins (Hamburger, Brown et al. 1999). Studies with mutant α5β1 integrin receptors and competitive inhibition studies indicate that invasin recognizes a site that is either identical to or overlaps that bound by the natural substrate fibronectin (Van Nhieu and Isberg 1991). Nevertheless, the respective integrin binding regions of invasin and fibronectin seem to be different in three dimensional protein structure. In the case of fibronectin the aspartate at position 1495 (Asp1495) of the Arg-Gly-Asp (RGD) sequence was identified as the most significant

contributor to binding energy besides several other residues located on the same face of the molecule as the RGD sequence (Aota, Nomizu et al. 1994). In invasin the carboxy-terminal D4-D5 adhesion module contains the Asp911 that was shown to be most critical for receptor binding (Leahy, Aukhil et al. 1996; Hamburger, Brown et al. 1999; Isberg and Barnes 2001). The striking difference between invasin and fibronectin is the significantly higher affinity of the bacterial invasin to the integrin receptor, which was shown to be essential for the translocation of bacteria into M cells (Marra and Isberg 1997). High-affinity integrin binding allows invasin to compete efficiently with other ligands for integrin receptors and allows stable contact between host cell and bacterial membranes, which after sequestration of a large number of integrin molecules subsequently leads to signaling events that promote uptake (Isberg and Barnes 2001). A series of studies have shown that the activity of tyrosine kinases (Fincham, James et al. 2000), phosphoinositide 3-kinase (Mecsas, Raupach et al. 1998) and Rho GTPase family members are involved in uptake (Black and Bliska 2000; Von Pawel-Rammingen, Telepnev et al. 2000; Isberg and Barnes 2001).

Latex beads coated with the C-terminal 192 amino acids of *Y. pseudotuberculosis* invasin or with the C-terminal 195 amino acids of *Y. enterocolitica* invasin were shown to be rapidly internalized by epithelial cells and that this type of internalization resembles the zipper mechanism of viable invasin expressing *Yersinia* (Dersch and Isberg 1999; Schulte, Grassl et al. 2000; Wiedemann, Linder et al. 2001; Grassl, Bohn et al. 2003). On the host cell side β1 receptor density was shown to be critical, while on the other side the density of invasin protein on the particles determined if beads were internalized subsequent to attachment (Dersch and Isberg 1999; Isberg, Hamburger et al. 2000). During invasin-mediated phagocytosis Src and Wiskott-Aldrich syndrome (WASP) family proteins, the Arp2/3 complex and the Rho GTPases Cdc42, Rac1 and RhoA were shown to be involved (Alrutz, Srivastava et al. 2001; McGee, Zettl et al. 2001; Wiedemann, Linder et al. 2001).

4.4 *Yersinia* adhesin A (YadA)

The non-fimbrial adhesin YadA of enteropathogenic *Yersinia* species is encoded by a gene on the *Yersinia* virulence plasmid (pYV) in *Y. enterocolitica* and *Y. pseudotuberculosis* strains (Bolin and Wolf-Watz 1984; Balligand, Laroche et al. 1985; Simonet, Riot et al. 1996). The *yadA* gene of *Y. pestis* has a single nucleotide deletion and this frameshift mutation leads to a reduced mRNA half-life, which in consequence leads to a lack of expression of the YadA protein in this highly pathogenic species (Rosqvist, Skurnik et al. 1988). Transcription is dependent on the activator VirF/LcrF that allows the expression of YadA at 37 °C but not below 30 °C (Lambert de Rouvroit, Sluiters et al. 1992). The protein can be detected in the

outer membrane of the bacteria within minutes after temperature shift to 37 °C (Bolin, Norlander et al. 1982).

In a mouse intestinal colonization assay the *Y. enterocolitica* O:9 *yadA* mutant was cleared from the intestine more efficiently than the wild type strain (Kapperud, Namork et al. 1987). YadA was also shown to be an essential virulence factor of *Y. enterocolitica* O:8 and it was observed that the *yadA* mutant initially colonized the Peyer´s patches of mice as efficiently as did the wild-type bacteria, but after 42 hours 10^3-fold more wild-type bacteria were recovered from Peyer´s Patches as compared to the *yadA* mutant (Pepe, Wachtel et al. 1995). In contrast to this, YadA does not appear to be needed for virulence in *Y. pseudotuberculosis* (Han and Miller 1997).
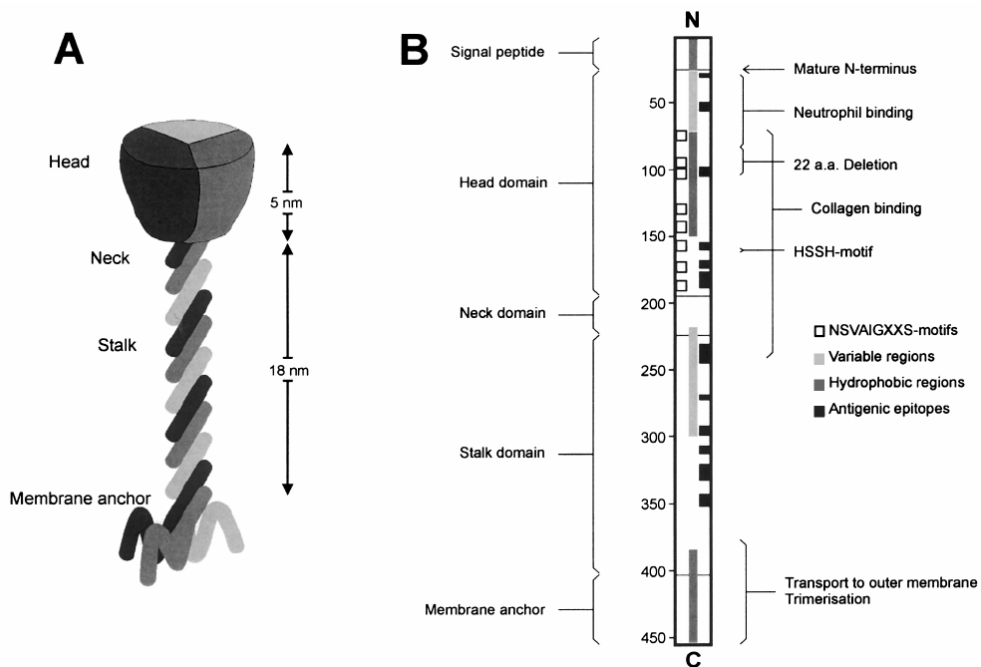
FIGURE 2. **Structure of YadA (El Tahir et al., 2001 with modifications)**.
(A) Hypothetical 'lollipop' structure of the YadA trimer, modified from Hoiczyk et al., 2000. The three intertwined polypeptides are drawn with different shades of grey and the structural domains and their dimensions are indicated. (B) Schematic diagram of one 455-residue YadAYeO3 polypeptide (drawn with the N-terminus up and C-terminus down). The scale at left indicates the positions of amino acid residues. The NSVAIGXXS motifs, the variable and the hydrophobic regions, and linear antigenic epitopes are indicated inside the rectangle. The structural domains of YadA are indicated at the left and functions and properties of its different regions at the right.

The YadA protein is a homotrimeric 200-240 kDa protein that gets expressed as a preprotein and is post-translationally modified, by cleaving off an N-terminal signal sequence of 25 amino acids during incorporation into the outer membrane (Bolin and Wolf-Watz 1984). YadA was described as to form distinct "lollipop"-shaped surface projections with an overall height of ~23 nm (Hoiczyk, Roggenkamp et al. 2000). It consists of an N-terminal head

domain (~5 nm), a rod-like stalk-neck domain (~18 nm long) and a C-terminal membrane anchor that was shown to be responsible for oligomerization and membrane targeting. The stalk is predicted to be formed of a right-handed coiled-coil structure and since the YadA protein has no cysteine residue, the three individual polypeptide chains assemble dependent on ionic and/or hydrophobic interactions (Tamm, Tarkkanen et al. 1993; El Tahir and Skurnik 2001).

The YadA protein is multifunctional and promotes binding to epithelial cells, professional phagocytes, and various extracellular matrix (ECM) molecules, such as laminin, collagen, and fibronectin and additionally protects *Yersinia* against defensins and the bactericidal activity of serum complement, probably by masking surface lipopolysaccharides. (Balligand, Laroche et al. 1985; Roggenkamp, Ruckdeschel et al. 1996; Hoiczyk, Roggenkamp et al. 2000).

Collagen binding

Collagens are major constituents of the ECM, described to have structural and developmental functions, e.g. cell attachment and cell differentiation (Miller and Gay 1987). A collagen binding negative 22 amino acid deletion mutant of YadA was avirulent in a mouse model, demonstrating the importance of this property of YadA to virulence (Tamm, Tarkkanen et al. 1993; Tahir, Kuusela et al. 2000). The high affinity binding of YadA to collagen is resistant to heat (20 min 80 °C), occurs at pH values between 5 and 8 and was shown to be dependent on the 3D structure of trimeric YadA, as any overlapping synthetic (16mer) YadA peptide was unable to bind collagen (Emody, Heesemann et al. 1989; Flugel, Schulze-Koops et al. 1994; Tahir, Kuusela et al. 2000). YadA does not recognize all collagen chains and collagen types; the specific YadA-binding site appears to be located on the α1 collagen chain. Experimental evidence indicates that the interaction of YadA with collagen occurs via the head domain of YadA (aa 26-195), where the histidyl residues in the HSSH motive (aa 159-162) and the repeated NSVAIGXXS motif were shown to play an important role (Schulze-Koops, Burkhardt et al. 1992; Tamm, Tarkkanen et al. 1993; Roggenkamp, Neuberger et al. 1995; Schulze-Koops, Burkhardt et al. 1995; Tahir, Kuusela et al. 2000).

Fibronectin and Laminin binding

Collagen binding-deficient YadA mutants can still retain their ability to bind other ECM proteins, like laminin and fibronectin, and resist complement-mediated serum killing. YadA binds to laminin with significantly lower affinity than to collagen and the NSVAIGXXS motifs of YadA are not required for laminin binding (Tamm, Tarkkanen et al. 1993; Tahir, Kuusela et al. 2000). Similarly to collagen, YadA was shown to bind to immobilized cellular fibronectin with high affinity. The YadA-fibronectin interaction was shown to be heat

resistant (20 min 60 °C), it could be inhibited by a polyclonal anti-YadA antiserum and was shown to not involve the RGDS motif that FN uses to bind to cellular α5β1 integrin receptors (Tertti, Skurnik et al. 1992; Schulze-Koops, Burkhardt et al. 1993).

Independently from uptake in mammalian cells the production of proinflammatory cytokines can by induced by YadA-expressing *Yersinia* and also by non-invasive *E. coli* strains heterologously-expressing YadA on their surface. Inhibitor studies revealed that serine/threonine kinases, as well as phosphatidylinositol-3-kinase are involved in the uptake process and that the YadA induced host cell signaling events leading to cytokine induction involve the same components as in invasin-mediated cytokine signalling, namely Rho GTPases and the MAP kinases MEK1, JNK, and p38 (Bliska, Copass et al. 1993; Yang and Isberg 1993; Eitel and Dersch 2002; Schmid, Grassl et al. 2004).

In contrast to the uptake mediated by direct binding of invasin to β1 integrin cell receptors, YadA mediates a matrix-dependent internalization pathway involving indirect bridging of fibronectin and β1 integrin receptors. The uptake of *Y. pseudotuberculosis* YadA-expressing *E. coli* into HEp-2 cells was first shown to be inhibited by monoclonal antibodies specific against β1 integrin receptors and secondly, in contrast to invasin mediated uptake, to be inhibited by antibodies against human fibronectin (Yang and Isberg 1993; Eitel and Dersch 2002).

Recently a detailed study identified differences between the highly homologues YadA proteins of the enteropathogenic *Yersinia* species. The study identified an internal region in the head domain of YadA of *Y. pseudotuberculosis*, that is critical for YadA-mediated bacterial cell aggregation, the specificity of extracellular matrix (ECM) substrate binding, and bacterial internalization into human Hep-2 cells (Heise and Dersch 2006). This unique N-terminal "uptake domain" (31 amino acids), present in *Y. pseudotuberculosis* YadA and not in *Y. enterocolitica* YadA, was shown to be crucial for mediating uptake in Hep-2 cells. For the internalization, as observed by Heise and Dersch, tight binding of *Y. pseudotuberculosis* YadA to fibronectin bound to α5β1 integrin receptors was required (Heise and Dersch 2006). Binding of *Y. pseudotuberculosis* YadA to the extracellular matrix proteins collagen and laminin was low. The low fibronectin-binding YadA from *Y. enterocolitica*, by contrast, had a higher affinity to collagen and laminin. Therefore, the N-terminal YadA sequence motif (uptake domain) determines matrix adhesion properties and consequently interaction with the respective matrix-associated cellular receptors (Heise and Dersch 2006).

5. TYPE III SECRETION AND TRANSLOCATED EFFECTOR PROTEINS (YOPS)

5.1 Type III secretion and the *Yersinia* needle complex

Type III secretion (TTS) is a mechanism by which gram-negative bacteria inject proteins across bacterial and host cell membranes into eukaryotic host cells. More than 20 type III secretion systems (TTSSs) have been discovered in animal, plant and even insect pathogens, all serving the purpose to interfere with the host cell by injecting effector proteins that generally have more sequence homology to eukaryotic proteins than to bacterial proteins (Cornelis 2002).

The plasmid-encoded TTSS allows *Yersinia* to deliver effector proteins (called Yops for Yersinia outer proteins) into cells of the immune system in order to disturb the dynamics of the cytoskeleton, to block phagocytosis and the production of proinflammatory cytokines, to induce apoptosis, control cell proliferation and exert numerous other effects. This enables the survival and extracellular multiplication of yersiniae in lymphoid tissues and distribution to other organs (Simonet, Richard et al. 1990; Fallman, Andersson et al. 1995; Cornelis 2002). The sequenced *Yersinia enterocolitica* Serotype 0:8 virulence plasmid not only encodes for the device to inject bacterial proteins into cells, referred to as injectisome or needle complex, but also the secreted/injected Yops, their chaperones and additional regulatory factors (Snellings, Popek et al. 2001).

The injectisome is an organelle that is spanning the outer membrane, the peptidoglycan layer and the cytoplasmic membrane of the bacterium. Its basal body, which spans the cytoplasmic inner membrane, consists of proteins that show homology to proteins in the bacterial flagellum. YscN is an essential part of the secretion complex and was shown to resemble the flagellar F^oF1-ATPase proton pump (Woestyn, Allaoui et al. 1994; Aizawa 2001). The basal body is a ring shaped structure with a central pore that connects to a needle which is formed by the polymerization of the proteins YscC and YscF. (Hoiczyk and Blobel 2001). The needle has a hollow centre of about 20 Angstroem and it is generally assumed that the exported proteins travel inside the needle to cross the two membranes and the peptidoglycan layer in one step (Cornelis 2002; Cornelis 2006).
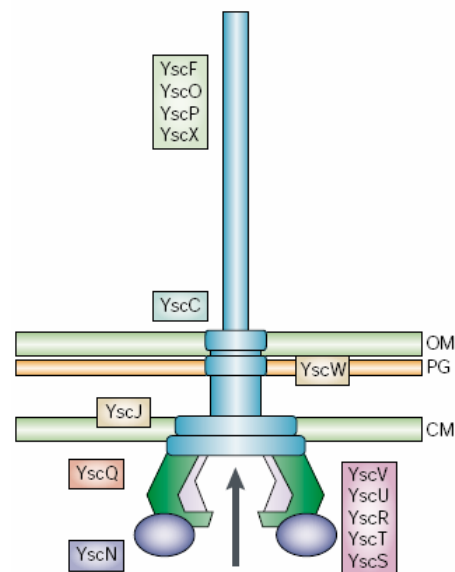
FIGURE 3. **The Ysc injectisome (Cornelis 2002 with modifications).**
Schematic representation of the Ysc injectisome spanning the outer membrane (OM), the peptidoglycan layer (PG) and the cytoplasmic membrane (CM) of the bacterium. The ring spanning the OM is made of the secretin YscC, assisted by the lipoprotein YscW. YscJ is another lipoprotein. YscF, YscO, YscP and YscX are external parts of the injectisome. YscF is the main constituent of the needle. YscV, YscU, YscR, YscT and YscS are proteins of the basal body that are in contact with the CM. YscN is the ATPase of the pump.

In order to translocate effector Yops across the eukaryotic cell membrane the translocator Yops (YopB, YopD and LcrV), that are not an integral part of the injectisome are absolutely required (Hakansson, Schesser et al. 1996). Therefore the injectisome structure can not be considered as a syringe that is able to penetrate the eukaryotic host cell membrane on its own. On the basis of the observation, that YopB and YopD can form pores in artificial liposomes, it was concluded that the injected effectors travel through a pore that is formed by the translocator Yops (Tardy, Homble et al. 1999).

Yersinia do not release Yops when they are incubated in a cell free environment, but only after contact between the pathogen and the mammalian cell the polarized transfer into the eukaryotic cell is induced (Rosqvist, Magnusson et al. 1994). However the injectisome can be triggered to secret Yops *in vitro* by chelating Ca2+ ions in the culture medium. It became clear that the secretion mechanism of the Yops is different from the classical sec-dependent secretion pathway, where upon export the leading signal sequence gets cleaved off (Economou 1999). Studies analyzing whether Yops are recognized specifically by the injectisome by a signal in the N-terminus of the protein or by a signal encoded by the messenger RNA resulted in controversial models (Sory, Boland et al. 1995; Anderson and Schneewind 1997; Anderson and Schneewind 1999). For YopE it was shown that the amino-

terminus and not the 5´ end of YopE mRNA serves as the targeting signal and for YopH it was shown, that bacterial protein synthesis was not required for macrophage inhibition, suggesting that YopH export and translocation are controlled at the posttranslational level (Bliska and Black 1995; Lloyd, Norman et al. 2001). The presence of YopQ in the cytosol of *Y. enterocolitica*, even with a closed secretion apparatus, as well as the post-translational secretion of YopQ could also be demonstrated (Trcek, Wilharm et al. 2002).

Another peculiarity of the *Yersinia* injectisome is that several Yops to be secreted need assistance of specialized chaperones, called Syc proteins for s̲pecific Y̲op c̲haperone. These small acidic proteins have little or no sequence homology between them, but share a putative carboxy-terminal amphiphilic α-helix. They also bear no sequence and functional resemblance to ATP-dependent chaperones, such as heat shock protein 70 (Wattiau, Bernier et al. 1994; Cornelis 2002). Generally, they are encoded by a gene that is located next to the gene encoding the protein they serve and are, in contrast to the Yop protein, not secreted. The observed diameter of the needle is thought to be too small to allow folded, globular proteins to travel through it, so it is assumed that one function of the chaperones is to keep the Yops at least partially unfolded (Hoiczyk and Blobel 2001; Cornelis 2002).

The six effector proteins *Y. enterocolitica* translocates into the host cell upon contact are called: YopM, YopH, YopP (called YopJ in *Y. pestis* and *Y. pseudotuberculosis*), YopE, YopT and YopO (called YpkA in *Y. pseudotuberculosis*).

5.2 YopM – a leucine rich protein

YopM is a leucine-rich repeat (LRR) virulence protein that exhibits heterogeneity of size and sequence among different *Yersinia* strains, while the functional consequences of this variability are not yet known. YopM has a size of approximately 42 kDa and, while being the only effector protein encoding no enzymatic activity, was shown to be necessary for virulence of *Y. pestis* and *Y. enterocolitica* in the mouse model (Mulder, Michiels et al. 1989; Leung, Reisner et al. 1990; Skrzypek, Myers-Morales et al. 2003). The crystal structure of *Yersinia pestis* YopM was resolved and it was shown that the YopM monomer has a horseshoe-like structure with four monomer units stacking together to form a hollow cylinder with an inner diameter of 35 Angstroem (Evdokimov, Anderson et al. 2001).

YopM traffics to the nucleus via a vesicle-associated pathway, but it is not known how nuclear localization is related to YopM's function (Skrzypek, Myers-Morales et al. 2003). Gene transcription microarray analysis performed on macrophages infected with *Y. enterocolitica* obtained divergent results, as one group found evidence that YopM regulates genes involved in cell cycle and cell growth (Sauvonnet, Pradet-Balade et al. 2002), whereas

another group found no evidence for gene regulation by YopM (Hoffmann, van Erp et al. 2004). In recent work the two cytoplasmic kinases PRK2 (protein kinase C-like 2) and RSK1 (ribosomal S6 protein kinase 1) were identified to be direct interaction partners of and their activity to be stimulated by YopM (McDonald, Vacratsis et al. 2003).

The subcellular localization of YopM is distinct from the other Yop effectors. YopM has been demonstrated to be injected into the cytoplasm of cells and translocate to the nucleus via a vesicle-associated pathway (Skrzypek, Cowan et al. 1998). The mechanism for transporting YopM into the nucleus and potential roles in immunomodulation, signaling to cell growth, apoptosis and transcription remain to be shown (Kerschen, Cohen et al. 2004; Viboud and Bliska 2005).

5.3 YopH - a protein tyrosine phosphatase

YopH is a highly active protein-tyrosine phosphatase (PTP) that targets an array of signaling pathways important for innate and adaptive immunity (Guan, Haun et al. 1990; Aepfelbacher 2004; Viboud and Bliska 2005). The protein has 468 amino acids (50 kDa) with defined N- and C-terminal domains, linked together by a proline-rich sequence. The N-terminal domain contains type III secretion signals, a chaperone-binding site and a substrate targeting domain, while the C-terminal region (amino acids 206 to 468) contains the catalytic domain and is similar in structure to PTP catalytic domains found in eukaryotic cells (Black, Montagna et al. 1998; Khandelwal, Keliikuli et al. 2002; Viboud and Bliska 2005). Many YopH substrates are components of focal adhesions, playing a role in regulating the dynamic interaction between the actin cytoskeleton and extracellular matrix-binding integrins (Brakebusch and Fassler 2003). Cytoskeletal uptake structures formed upon interaction of *Yersinia* adhesins with cellular integrins are thought to resemble focal adhesions, and their disruption by YopH may thus explain its antiphagocytic activity (Aepfelbacher 2004).

YopH dephosphorylates focal adhesion kinase (Fak), the adaptor proteins p130Cas and paxillin, Fyn-binding protein (FyB), and the scaffolding protein SKAP-HOM in different cell types such as neutrophils, macrophages, and epithelial cells (Black and Bliska 1997; Persson, Carballeira et al. 1997; Hamid, Gustavsson et al. 1999). Previous studies using *Y. enterocolitica* or *Y. pseudotuberculosis* mutants suggested that YopH is responsible for up to 50 % of the antiphagocytic activity of yersiniae towards neutrophils and J774 macrophages (Fallman, Andersson et al. 1995; Ruckdeschel, Roggenkamp et al. 1996; Aepfelbacher 2004). Inhibition of phagocytosis was shown to be dependent on the enzymatic activity of YopH, when translocation of wild-type YopH but not of the catalytically inactive point mutant

YopHC403S into HeLa cells or J774 macrophages prevented invasin/β1 integrin-mediated uptake of *Yersinia* (Persson, Carballeira et al. 1997; Persson, Nordfelth et al. 1999).

In addition to counteracting signaling pathways activated by phagocytic mechanisms, YopH counteracts other types of immune response pathways in host cells. Among the identified YopH activities are the inhibition of the production of macrophage chemoattractant protein 1 in macrophages infected with *Y. enterocolitica* (Sauvonnet, Pradet-Balade et al. 2002) and the inhibition of signaling cascades associated with T cell or B cell activation by antigen (Yao, Mecsas et al. 1999; Cornelis 2002). YopH-mediated dephosphorylation is very fast and visible within 2 min of infection and this can explain why YopH is among the most effective Yops with regard to mouse virulence and antiphagocytic activity (Andersson, Carballeira et al. 1996; Cornelis 2002; Aepfelbacher 2004).

5.4 YopP - an enzyme that inhibits MAPK and NF-κB signaling pathways

The 33 kDa protein was first identified in *Y. pestis* and called YopJ (Straley and Bowmer 1986) before it was discovered in *Y. pseudotuberculosis* and *Y. enterocolitica* and named YopP (Cornelis, Vanootegem et al. 1987). In the mouse model YopP/J was shown to be important for virulence of the enteropathogenic yersiniae. A *Y. enterocolitica yopP* mutant was attenuated in an oral mouse infection assay (Trulzsch, Sporleder et al. 2004) and accordingly virulence of a *Y. pseudotuberculosis yopJ* mutant was reduced 64-fold in an oral LD50 assay (Monack, Mecsas et al. 1998).

YopP/J functions as a potent inhibitor of the MAPK and NF-κB signaling pathways of the host. Its inhibitory actions result in suppression of cytokine production (IL-8 in epithelial cells and TNF-α in macrophages) and in the induction of macrophage apoptotic cell death (Aepfelbacher, Zumbihl et al. 1999; Orth 2002; Ruckdeschel 2002).

YopP shows limited homology to the ubiquitin-like protease Ulp1 of yeast and therefore was thought to remove ubiquitin or a ubiquitin-like modification from target proteins in host cells. Protein ubiquitination can reversibly activate signaling molecules in addition to marking them for degradation (Orth 2002; Aepfelbacher 2004; Viboud and Bliska 2005). YopP/YopJ associates with members of the MAPK kinase (MAPKK) superfamily, which represent upstream MAPK activators and it furthermore binds and inhibits the IκB kinase-beta (IKK-β), which is the major NF-κB-activating kinase (Orth, Palmer et al. 1999; Aepfelbacher 2004).

Detailed mass spectrometry analysis following the observation that YopJ selectively targets MAPKKs and IKK-b without any obvious changes in their migration on SDS/PAGE (Orth, Palmer et al. 1999; Orth 2002; Navarro, Alto et al. 2005; Viboud and Bliska 2005) provided mechanistic insight into the chemistry of YopJ: It was shown that YopJ acted as an

acetyltransferase to modify the critical serine and threonine residues in the activation loop of the MAPK activator MAPKK6 and thereby was able to block phosphorylation. The acetylation directly competed with phosphorylation and prevented the activation of the modified protein (Mukherjee, Keitany et al. 2006).

5.5 YopE – GAP activity for specific downregulation of Rho GTPases

YopE is a 25-kDa protein (219 amino acids) which, like the homologous domains within exoenzyme S from *Pseudomonas aeruginosa* and SptP from *Salmonella typhimurium*, works as GAP for Rho-family proteins (Fu and Galan 1999; Goehring, Schmidt et al. 1999; Black and Bliska 2000; Von Pawel-Rammingen, Telepnev et al. 2000; Andor, Trulzsch et al. 2001; Aepfelbacher 2004). At the N-terminus residues 54–75 have been shown to be both necessary and sufficient for targeting of YopE to an unidentified perinuclear compartment, while the residues 96 to 219 comprise the Rho GAP domain (Krall, Zhang et al. 2004).

YopE binds to the GTPase and promotes efficient GTP hydrolysis via its GAP domain, where Arg-144 in the "arginine finger" motive is known to be essential for the GAP activity (Scheffzek, Ahmadian et al. 1998; Wurtele, Wolf et al. 2001; Aili, Telepnev et al. 2003; Aepfelbacher 2004). YopE causes disruption of actin filaments, rounding and detachment of infected cells in culture, a phenomenon referred to as cytotoxicity. Studies using epithelial or endothelial cells as model tissues for study of YopE targeting specificity showed that Rac-1 and RhoA can be deactivated by YopE (Black and Bliska 2000; Aepfelbacher 2004; Aili, Isaksson et al. 2006). A YopE GAP mutant (R144A) was shown to be avirulent in mice and unable to induce cytotoxic effects in HeLa cells (Black and Bliska 2000; Von Pawel-Rammingen, Telepnev et al. 2000; Aili, Isaksson et al. 2006). However, recently it was reported that other mutants of YopE lacking *in vitro* GAP activity towards RhoA, Rac1 and Cdc42 were still cytotoxic for HeLa cells (Aili, Telepnev et al. 2003), which suggests that these small GTPases are not the sole targets of YopE during infection (Aili, Isaksson et al. 2006).

YopE contributes to the antiphagocytic activity of *Y. enterocolitica* and *Y. pseudotuberculosis* in cooperation with fellow Yops (Aepfelbacher 2004). Loss of inhibition of phagocytosis in a *Y. enterocolitica* YopE knockout strain was observed in macrophages and neutrophils (Grosdent, Maridonneau-Parini et al. 2002), but in the mouse model, while no single Yop was found to be essential for colonization or persistence in intestinal tissues in single-strain infections, the absence of both YopH and YopE together almost eliminated colonization of all tissues (Logsdon and Mecsas 2003). In the process of Yop effector injection the GAP activity of YopE was shown to counteract the pore-forming activity of the injectisome (Viboud and

Bliska 2001). The fate of the *Y. enterocolitica* translocated YopE, in contrast to YopH and YopP, is determined by host proteasome degradation. This implies the proteasome as integral part of the cellular host immune response against the immunomodulatory activities of a translocated bacterial virulence protein (Ruckdeschel, Pfaffinger et al. 2006).

These findings suggest that YopE has both individual and redundant functions and synergizes with other Yops during the complex infection cycle of yersiniae (Aepfelbacher 2004).

5.6 YopT – a cysteine protease removing the isoprenoid group of Rho GTPases

YopT is a 35 kDa protein (322 amino acids) that belongs to the CA clan of cysteine proteases. It is expressed by *Y. pestis* and *Y. enterocolitica*, but owing to a deletion on pYV is not expressed by virulent serotype O:3 strains of *Y. pseudotuberculosis*, (Iriarte and Cornelis 1998; Shao, Merritt et al. 2002; Viboud and Bliska 2005). Three residues in the catalytic domain of YopT (Cys-139, His- 258 and Asp-274) are required for the enzymatic activity and are conserved among other members of the same clan of cysteine proteases in bacterial plant and animal pathogens (Zhu, Shao et al. 2004; Viboud and Bliska 2005). Cellular overexpression and *in vitro* studies revealed that YopT acts as a cysteine protease to remove the lipid anchor (geranylgeranyl isoprenoid moiety) from RhoA, Rac, or Cdc42 at a cleavage site that is just N-terminal from the cysteine linked to the prenyl group (Shao, Vacratsis et al. 2003; Aepfelbacher 2004).

Before the biochemical activity was characterized, the disruptive effect of YopT on actin stress fibers has been observed (Iriarte and Cornelis 1998). Later it was shown that bacterially translocated YopT *in vivo* has preferential activity for RhoA and less for Rac or Cdc42 (Aepfelbacher, Trasak et al. 2003). Rho GTPase modification by removal of the isoprenoid group has the following consequences in *Yersinia*-infected cells: RhoA is released from the plasma membrane and from its cytoplasmic binding partner guanine nucleotide dissociation inhbitor-1 (GDI-1) and accumulates as a monomeric protein in the cytoplasm (Aepfelbacher, Trasak et al. 2003).

On a cellular level it was shown that YopT-overexpressing *Yersinia* mutants disrupt actin rich phagocytic cups induced by *Yersinia* invasin as well as podosomal adhesion structures required for chemotaxis in macrophages (Aepfelbacher, Trasak et al. 2003). The role of YopT in preventing opsonized and unopsonized phagocytosis of *Y. enterocolitica* by human neutrophils and mouse macrophages was investigated also. Mutant bacteria lacking YopT were phagocytosed in significantly higher amounts than wild-type bacteria both under

opsonizing and nonopsonizing conditions. However, *Yersinia* mutants translocating only YopT were not resistant to phagocytosis by neutrophils or macrophages (Grosdent, Maridonneau-Parini et al. 2002; Aepfelbacher 2004).

A recent study showed that overexpressed Rac1 was not completely inactivated after infection with *Yersinia* expressing solely YopT, but cleaved activated Rac1 molecules entered the host cell nucleus, allowing Rac1 to localize with nuclear guanosine nucleotide exchange factors. The infection of a *Yersinia* strain solely expressing YopT and YopE resulted in a pool of activated, nucleus-localized Rac1 and a pool of inactivated Rac1 in the cytoplasm (Wong and Isberg 2005). While studies on the potential synergistic or competitive cell biological role of YopT in the interplay with other effector Yops have to be pursued, also structural data supporting compartment dependent substrate specificity will have to bring more insight into the specific role of YopT (Aepfelbacher 2004; Viboud and Bliska 2005; Wong and Isberg 2005).

5.7 YopO – a serine/threonine kinase that binds to Rho GTPases and is activated by G-actin

YopO from *Y. enterocolitica* (called YpkA in *Y. pseudotuberculosis*) is an 80-kDa (729 amino acids) protein with multiple functional domains. An N-terminal secretion/translocation/membrane binding region is followed by a serine/threonine kinase catalytic domain in the N-terminal half of the protein (amino acid residues 150–400). The C-terminal half of YopO contains four regions (within amino acids 436–710) with homology to Rho-binding domains (RBDs) that were shown to mimic host cell GDIs (Prehna, Ivanov et al. 2006). The last 20 residues (amino acids 709–729) display some homology to the actin bundling protein coronin (Dukuzumuremyi, Rosqvist et al. 2000; Juris, Rudolph et al. 2000; Aepfelbacher 2004).

The morphological effects in HeLa cells infected with a *Y. pseudotuberculosis* mutant overexpressing YpkA are cell contraction (rounding) accompanied by the formation of pronounced retraction fibers (a phenotype referred to as "arborization"). In these experiments YpkA was localized at the plasma membrane, a property that was later shown to reside in the N-terminal half (amino acids 1-443) of the protein (Hakansson, Galyov et al. 1996; Dukuzumuremyi, Rosqvist et al. 2000; Aepfelbacher 2004).

5.7.1 Serine/Threonine kinase activity

The YopO homolog YpkA (*Yersinia* protein kinase A; 732 amino acids) is the first reported prokaryotic secreted protein kinase that showed extensive homology to eukaryotic serine/threonine protein kinases (Galyov, Hakansson et al. 1993). Mutation of a critical lysine residue in YopO (K269A) or aspartic acid residue in YpkA (D270A), located within the putative catalytic domain, abolished most of the kinase activity (Cornelis, Boland et al. 1998; Dukuzumuremyi, Rosqvist et al. 2000). Binding of actin to YopO is necessary for kinase activation. Removal of the 21 C-terminal amino acids abolish actin binding and actin-induced autophosphorylation (Juris, Rudolph et al. 2000). Autophosphorylation and phosphorylation of basic artificial substrates was the only activity known until recently, when the first physiological substrate of YopO was identified as Otubain1 (Ovarian tumor domain ubiquitin aldehyde binding protein 1), a deubiquitinating enzyme implicated in immune cell clonal anergy (Juris, Rudolph et al. 2000; Juris, Shah et al. 2006).

5.7.2 Rho-binding activity

In yeast two hybrid assays and in immunoprecipitation experiments YpkA associates with the Rho GTPases RhoA and Rac1 but not Cdc42 and conclusively was also shown to reduce the level of GTP-bound RhoA in *Y. pseudotuberculosis*-infected HeLa cells (Barz, Abahji et al. 2000; Dukuzumuremyi, Rosqvist et al. 2000; Aepfelbacher 2004). The C-terminal part of YpkA (amino acids 434-732) was recently crystallized in a complex with Rac1 and the interaction displayed intriguing similarities to the complexes between host cell GDIs and their target Rho family GTPases. However, a structural difference of host cell GDIs and YpkA is that YpkA does not posses any clear analog of the motive necessary to bind the prenyl group of Rho GTPases. (Prehna, Ivanov et al. 2006).

5.7.3 Secretion/Translocation of YopO is dependent on the SycO chaperone

The existence and requirement of a chaperone for YopO was unclear, until recently the open reading frame next to YopO (orf155) was demonstrated to encode the chaperone called SycO. SycO prevents the intrabacterial aggregation of YopO by covering the N-terminal membrane localization domain inside the bacterial cell. The chaperone-binding domain (residues 20-77) within YopO was shown to coincide with the membrane localization domain (Letzelter, Sorg et al. 2006).

5.7.4 Functional role of YopO

YopO synergistically with other Yops contributes to the TTSS-dependent antiphagocytic activity of *Y. enterocolitica*. Increased uptake of *yopO* mutant bacteria by macrophages or neutrophils was most evident when non-opsonized bacteria were used, suggesting that YopO may primarily counteract *β*1 integrin-mediated uptake (Grosdent, Maridonneau-Parini et al. 2002; Viboud and Bliska 2005). It also synergizes with other Yops to confer upon yersiniae the ability to colonize and persist in different tissues (Logsdon and Mecsas 2003; Aepfelbacher 2004). Early mouse oral infection experiments showed that deletion of either the catalytic domain or the C-terminal half of *yopO* in *Y. pseudotuberculosis* resulted in avirulence (Galyov, Hakansson et al. 1993; Galyov, Hakansson et al. 1994). However in recent studies *Y. enterocolitica* and *Y. pseudotuberculosis yopO* null mutants were shown to be able to spread and colonize murine liver or spleen comparable to their respective parental strains (Logsdon and Mecsas 2003; Trulzsch, Sporleder et al. 2004; Viboud and Bliska 2005).

6. STATE OF THE ART - BIOCHEMICAL CHARACTERIZATION OF YOPO

The following chapter (6.1 and 6.2) describes properties of YopO that were characterized together with the cellular effects of YopO that were investigated in this thesis work.

6.1 YopO is activated by G-actin not F-actin

To identify which form of actin stimulates YopO autophosphorylation the recombinant YopO (amino acids 1-729) protein was assayed with G-actin or F-actin. No autophosphorylation occured in the absence of actin and G-actin was shown to be a potent activator of kinase activity, while F-actin did not stimulate YopO autophosphorylation (Trasak, Zenner et al. 2007).

6.2 Identification of autophosphorylated amino acids that regulate kinase activity
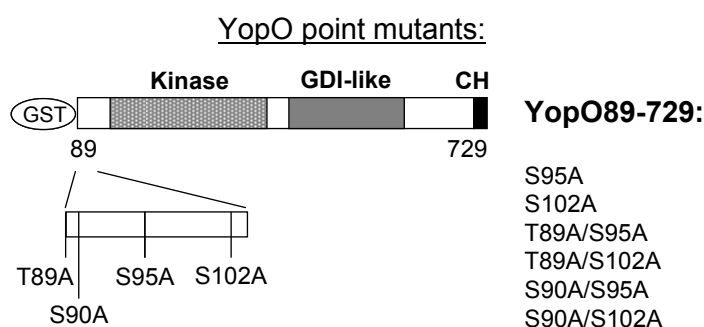
FIGURE 4. **Scheme of YopO point mutants used to identify phosphorylation sites.**
The first and the last amino acids of YopO89-729 and YopO protein organization is depicted. Kinase; region with homology to serine/threonine kinases. GDI-like; region containing homology to Rho GDI. CH; coronin homology region. Point mutants are indicated. cDNA's encoding these constructs were cloned into vectors allowing expression of GST-fusion proteins in *E. coli*.

The YopO protein has 66 serine residues and 34 threonine residues and it has not been known which amino acid(s) are targeted by autophosphorylation and if this occurs by an intramolecular mechanism (cis-phosphorylation) or an intermolecular mechanism (trans-phosphorylation). Despite identification of the first physiological YopO substrate (Otubain1) it has not been known if YopO autophosphorylation regulates the phosphorylation of substrates. Mutants impaired in autophosphorylation had to be tested for their ability to phosphorylate substrates.

FIGURE 5
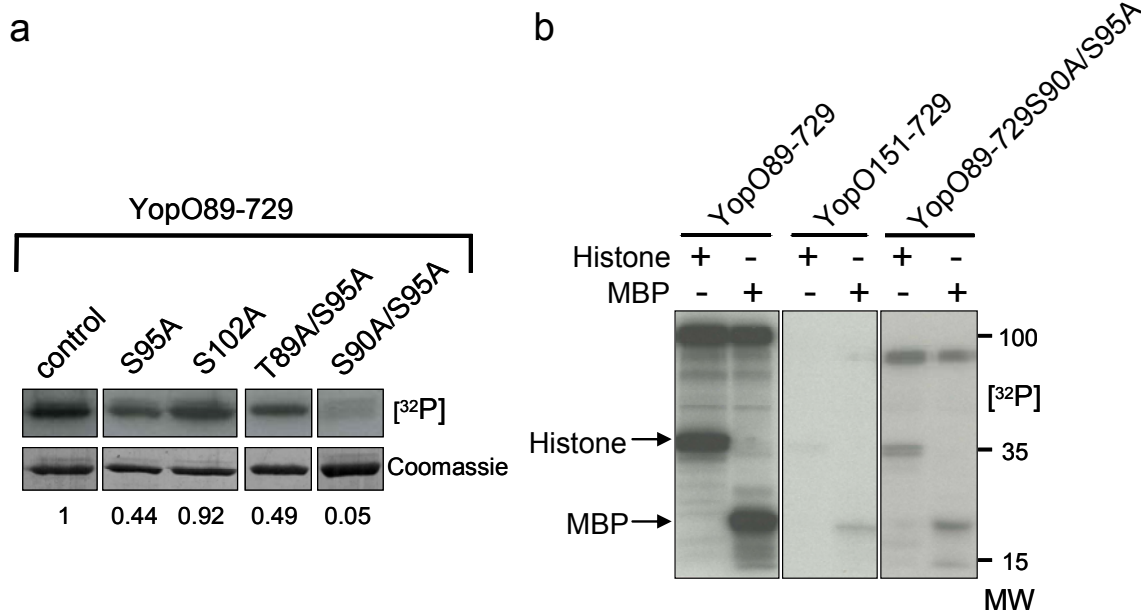
FIGURE 5. **Activity of YopO phosphorylation site mutants (Trasak et al. 2007, with modifications).**
a) Quantified autophosphorylation of YopO single or double point mutants in kinase assay (upper panel radiography, lower panel CoomassieBlue staining, on the bottom values of autoradiography quantification are shown referenced to YopO89-720 control that was set to 1). b) Autophosphorylation of YopO controls substrate phosphorylation. Fully active control YopO89-729, kinase negative YopO151-729 and autophosphorylation deficient YopO89-729S90A/S95A were subjected to kinase reaction in the presence of artificial substrates histone and MBP (radiography shown). Molecular weights (MW) of standard marker proteins are indicated.

Data from mass spectrometry (MS) analysis of *in vitro* phosphorylated YopO89-729 indicated two phosphorylated residues of four possible sites in amino acids 89 to 102 (T89, S90, S95, S102). Furthermore these data suggested that one amino acid lies within amino acids 89-94 and the other one within 95-108 (Trasak, Zenner et al. 2007).

To identify the phosphorylated amino acids by autoradiography equal amounts of the following single or double point mutants of Yop89-729 were subjected to kinase assays: S95A, S102A, T89A/S95A and S90A/S95A. Amino acid substitution S102A showed no reduction in incorporation of radioactivity (figure 5a). Autophosphorylation was reduced by about 50% in YopOS95A and YopOT89A/S95A and greatly diminished by about 95% in S90A/S95A. Values for quantified autophosphorylation were normalized to the fully active YopO89-729 control and displayed on the bottom in figure 5a. Coomassie staining indicates equal amounts of mutant protein. These results identify the autophosphorylation sites serine-90 and serine-95 within YopO89-729 and show that threonine-89 and serine-102 are not involved in autophosphorylation.

Because it was not known if the examined kinase activity, evident by autophosphorylation of YopO, plays a role in the phosphorylation of external substrates, the phosphorylation of artificial substrates was tested (Juris, Rudolph et al. 2000). Autophosphorylation deficient

YopO151-729, fully active YopO89-729 and YopO89-729S90A/S95A were incubated with myelin basic protein (MBP) or histone and [γ-32P] adenosine 5' trisphosphate. Phosphorylation of MBP and histone by YopO89-729 was effective, while the phosphorylation site mutant protein YopO89-729S90A/S95A showed greatly diminished phosphorylation and YopO151-729 showed no phosphorylation of the given substrates (figure 5b).

The data presented in figure 5b show that phosphorylation of artificial substrates is dependent on YopO autophosphorylation at amino acids serine-90 and serine-95 and implicate that the catalytic activity is dependent on the phosphorylation state of serine-90 and serine-95.

7. RHO GTPASES – PRIMARY TARGETS OF YOPS

The Rho proteins constitute ideal targets for pathogens, because they act as eukaryotic switches to control a large variety of cellular processes. Rho GTPases are master regulators of the actin cytoskeleton, but also participate in controlling cell-cell contacts, integrin signaling, endocytosis, intracellular vesicle transport, gene transcription and cell cycle (Symons and Settleman 2000; Aepfelbacher 2004; Schwartz 2004; Aktories and Barbieri 2005).

FIGURE 6
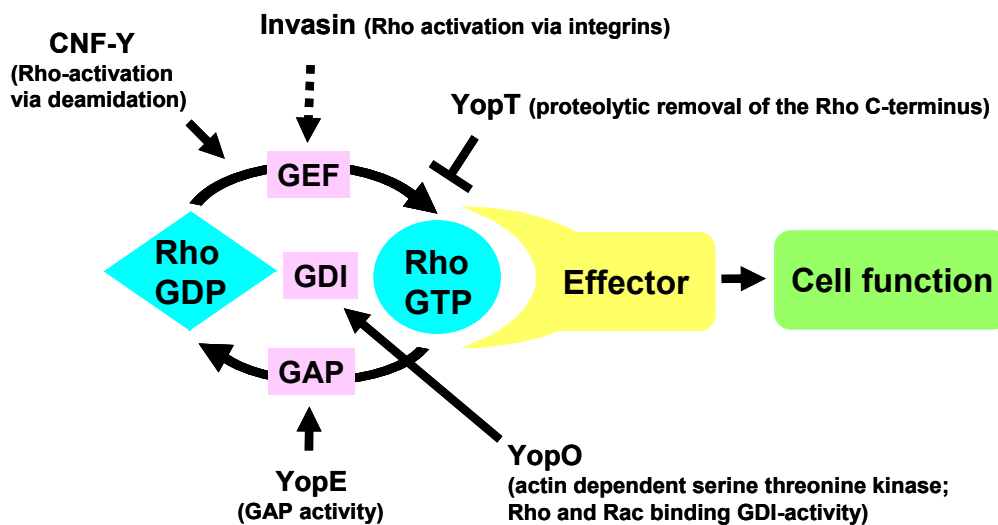
FIGURE 6. **Interference of *Yersinia* virulence factors with the Rho activation/deactivation cycle (Aepfelbacher 2004, with modifications).**
The major biochemical mechanisms by which the respective factors modulate Rho GTPases are in brackets. CNF-Y, cytotoxic necrotizing factor of yersiniae; GAP, GTPase activating protein; GEF, guanine nucleotide exchange factor; GDI, guanine nucleotide dissociation inhibitor; RhoGDP, inactive, GDP-bound Rho GTPase; RhoGTP, active, GTP-bound Rho GTPase; Invasin, *Yersinia* adhesin binding to β1-integrins.

Rho GTPases are inactive in the GDP-bound form, when they are associated with a guanine nucleotide dissociation inhibitor (GDI), and are activated by GDP/GTP exchange caused by guanine nucleotide-exchange factors (GEFs). The active state is terminated by GTPase-activating proteins (GAPs) that greatly enhance the low basal GTPase activity. Furthermore, by binding to GDIs the hydrophobic isoprenoid moiety at the C-terminus of Rho GTPases is neutralized and this is involved in cytosol/membrane cycling (Bishop and Hall 2000; Aepfelbacher 2004). In the GTP-bound state the Rho proteins adopt a conformation that allows interaction and stimulation of a variety of downstream effector proteins, which include protein kinases, lipid kinases, and multidomain scaffolds (Van Aelst and D'Souza-Schorey 1997).

The best-characterized Rho proteins are RhoA, Rac-1, and Cdc42. Each controls the formation of individual cytoskeletal elements in the cell: contractile actin/myosin stress fibers and the organization of focal contacts by RhoA, lamellipodia and focal complexes by Rac-1, and filopodia/microspikes as well as focal contacts by Cdc42 (Ridley, Paterson et al. 1992; Nobes and Hall 1995).

7.1 Rho proteins and actin polymerization

In eukaryotic cells, monomeric G-actin is in dynamic equilibrium with polymerized F-actin. Rapid signal-induced actin polymerization, including that occurring during host–pathogen interactions, can be triggered by different mechanisms, including *de novo* nucleation, which can involve the Arp2/3 (actin-related protein 2/3) complex (Boquet and Lemichez 2003). Rac and Cdc42 lead to morphologically distinct protrusions at the plasma membrane (i.e., lamellipodia and filopodia), but they both initiate actin polymerization through the Arp2/3 complex. In mammalian cells Rho stimulates actin polymerization through diaphanous-related formin (DRF), mDia1 that directly binds actin filaments and promotes filament elongation (Bishop and Hall 2000; Raftopoulou and Hall 2004). A second effector protein directly regulated by Rho is Rho-kinase which in turn regulates LIM kinase-mediated stabilization of filamentous actin structures and myosin light chain phosphatase-mediated actomyosin assembly and contraction (Bishop and Hall 2000).

7.2 Rho proteins and phagocytosis

Rho GTPases have an essential role in phagocytosis as shown in professional phagocytes such as macrophages. Immunoglobulin receptor (FcγR) mediated phagocytosis depends on Cdc42 and Rac, and complement receptor (CR) mediated phagocytosis depends on RhoA (Caron and Hall 1998). Both pathways activate the Arp2/3 complex for actin polymerization but in a Cdc42/Rac- or RhoA-dependent manner (May, Caron et al. 2000; Jaffe and Hall 2005).

The uptake, triggered by *Yersinia* invasin, has been shown to involve Rac, either individually or in cooperation with Rho and Cdc42Hs, dependent on the cell type (Alrutz et al. 2001; McGee et al. 2001; Wiedemann et al. 2001). The central role for Rho-GTPases in assembly and disassembly of peripheral actin filaments is necessary for phagocytosis and consequently can provide an explanation why they are common substrates for bacterial toxins and effectors (Aktories and Barbieri 2005). Phagocytosis mediated by Fcγ receptors is accompanied by an increase in the production of reactive oxygen species leading to the killing of phagocytosed bacteria. This phenomenon known as the phagocytic burst is mediated by membrane-

associated NADPH oxidase complex and was shown to be dependent on Rac proteins (Roberts, Kim et al. 1999; Bokoch and Diebold 2002; Aktories and Barbieri 2005).

Clostridial toxins and exoenzymes from other gram-positive bacteria (C3-like ADP-ribosyltransferases) covalently modify and inactivate Rho GTPases, whereas *Yersinia* YopE acts as a Rho GAP. In both cases this prevents phagocytosis of bacteria (Aktories, Wilde et al. 2004). *Salmonella typhimurium*, on the other hand, is an invasive bacterium exploiting host cell signaling by injecting SopE, which acts as a GEF, to activate Cdc42 and Rac and promote its own internalization (Aktories and Barbieri 2005).

8. AIM OF THIS STUDY

The type III secretion system translocated YopO (729 amino acids) has a secretion/translocation domain at the N-terminus (amino acid 1-88). Sequence alignments predict the location of the kinase domain within amino acids 150-400, it has a C-terminal Rho GDI-like domain (amino acid 431-612) and an N-terminal (within amino acid 89-440) and a C-terminal (within amino acid 440-729) actin binding domain.

YopO was shown to disrupt F-actin and cause rounding in *Yersinia*-infected cells (Hakansson, Galyov et al. 1996). Which of the known biochemical activities of YopO contribute to these cellular effects has not been clear. Whether these activities work independently or synergistically with each other was also unknown and discrepant results with regard to these issues were obtained in previous studies (Dukuzumuremyi, Rosqvist et al. 2000; Juris, Rudolph et al. 2000). Although there was indirect evidence for an antiphagocytic activity of YopO, an effect on a defined phagocytosis mechanism has not been identified (Grosdent, Maridonneau-Parini et al. 2002; Wiley, Nordfeldth et al. 2006).

First it was necessary to establish and biochemically characterize recombinant YopO mutant proteins and eukaryotic expression vectors that allow defining the roles of kinase activity, actin binding, Rho GTPase binding and plasma membrane localization in inducing the known morphological effects of YopO. Furthermore, mechanistically distinct ways of *Yersinia* internalization like Fcγ-receptor-, complement receptor-, invasin- and YadA-mediated phagocytosis had to be evaluated and their sensitivity to YopO tested. The results had to be compiled to a coherent picture of how YopO functions in cells and how this may contribute to immune cell modulation during *Yersinia* infection.

C. RESULTS

1. CHARACTERIZATION OF YOPO CONSTRUCTS USED IN THIS STUDY

1.1 YopO protein organization and constructs

FIGURE 7
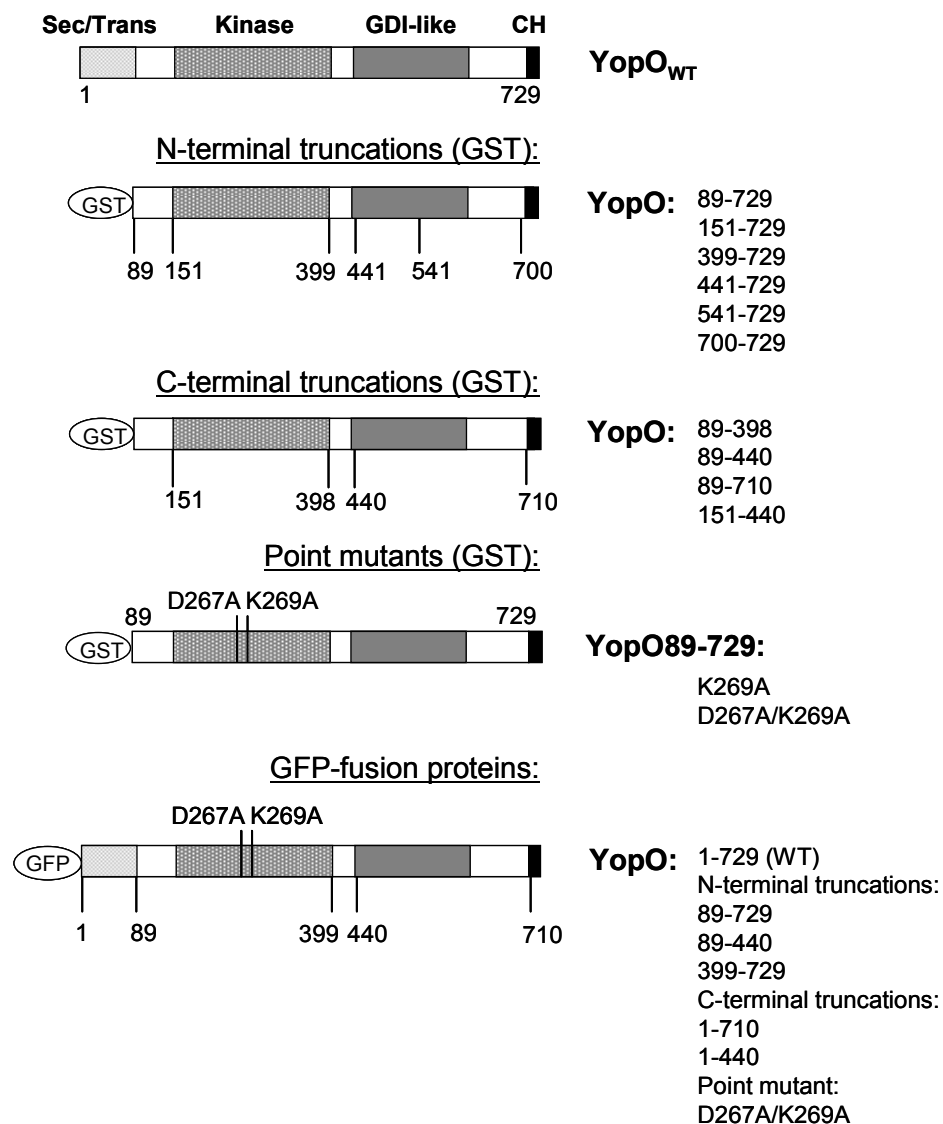
FIGURE 7. **Scheme of YopO protein organisation and YopO constructs used in this study.**
The first and the last amino acids of YopOwt or its fragments and mutants are indicated. cDNA's encoding these constructs were cloned into vectors allowing expression of GST-fusion proteins in *E. coli* or GFP-fusion proteins in host cells. Sec/Trans; secretion and translocation region used by the *Yersinia* type three secretion system. Kinase; region with homology to serine/threonine kinases. D267 and K269 are amino acids critical for catalytic activity. GDI-like; region with homology to Rho GDI. CH; coronin homology region.

1.2 YopO has N- and C-terminal actin binding sites

YopO forms a 1:1 complex with G-actin (Trasak, Zenner et al. 2007). To identify the region(s) in the YopO protein that is(are) involved in actin binding GST-pulldown assays and actin polymerization assays using actin and N- and C-terminal deletion mutants were performed.

Wild type YopO and kinase defective YopO (K269A) bind G-actin with the same efficiency. Progressive truncation of the N-terminal amino acids resulted in mutant proteins that were able to pull down actin (YopO89-729, YopO151-729, YopO399-729, YopO441-729) and proteins that lost the actin binding property (YopO541-729 and YopO700-729). The C-terminal truncations YopO89-710 and YopO89-440 were unable to pull down actin (Trasak, Zenner et al. 2007). The pulldown experiments indicate that YopO amino acids 441 to 729 constitute an actin binding site. In the process of delineating the kinase domain of YopO, YopO89-440 was observed to display autophosphorylation dependent on the presence of G-actin (see figure 8b) indicating that YopO89-440 also does bind actin. An alternative method used to determine G-actin binding of YopO was to measure the polymerization of G-actin to F-actin with fluorescently labeled G-actin monomers in the presence of YopO mutant proteins. The formation of F-actin was dose-dependently inhibited by YopO89-440, confirming the actin binding of the fragment harboring the catalytic domain. Consistent with the pull down data YopO441-729 inhibited F-actin formation. The YopO truncations YopO151-440 and YopO89-398 were shown to have no actin binding activity (Trasak, Zenner et al. 2007).

In conclusion YopO was shown to have two independent actin binding sites, one located N-terminally within amino acids 89-440 and the other located C-terminally within amino acids 441-729 (overview shown in table C1).

Table C1. **Interaction of YopO constructs with G-actin in pulldown and G-actin-polymerization experiments**

Actin binding in pulldown assay			Actin binding in G-actin polymerization assay	
YopO construct	interaction		YopO construct	interaction (K_d)
WT	+		89-729	+ (K_d 1.9 μM)
K269A	+		441-729	+ (K_d 6.1 μM)
89-729	+		700-729	-
151-729	+		89-440	+ (K_d 4.1 μM)
399-729	+		89-398	-
441-729	+		151-440	-
541-729	-			
700-729	-		+ indicating interaction of YopO construct with G-actin. Dissociation constant (K_d).	
89-710	-		- indicating no interaction of YopO construct with G-actin.	

1.3 Kinase activity of N- and C-terminal YopO deletion mutants

In order to characterize the actin-dependent kinase activity, YopO truncations were tested for incorporation of phosphate from radioactively labeled ATP ([γ-32P] adenosine 5' tris-phosphate) in the presence of actin. Bacterially expressed full length YopO (YopOwt) showed considerable degradation and required detergents such as Triton X-100 for purification and stability. Therefore a construct that lacks the N-terminal amino acids 1-88 (YopO89-729) that serve as bacterial secretion and translocation signal was established.

YopO has an N-terminal G-actin binding site comprised by amino acid residues 89-440 and a C-terminal G-actin binding site comprised by amino acid residues 441-729. The YopO deletion mutants YopO89-398 and YopO151-729 have no functional N-terminal actin binding site, the C-terminal truncated YopO89-710 has no functional C-terminal actin binding site.

FIGURE 8
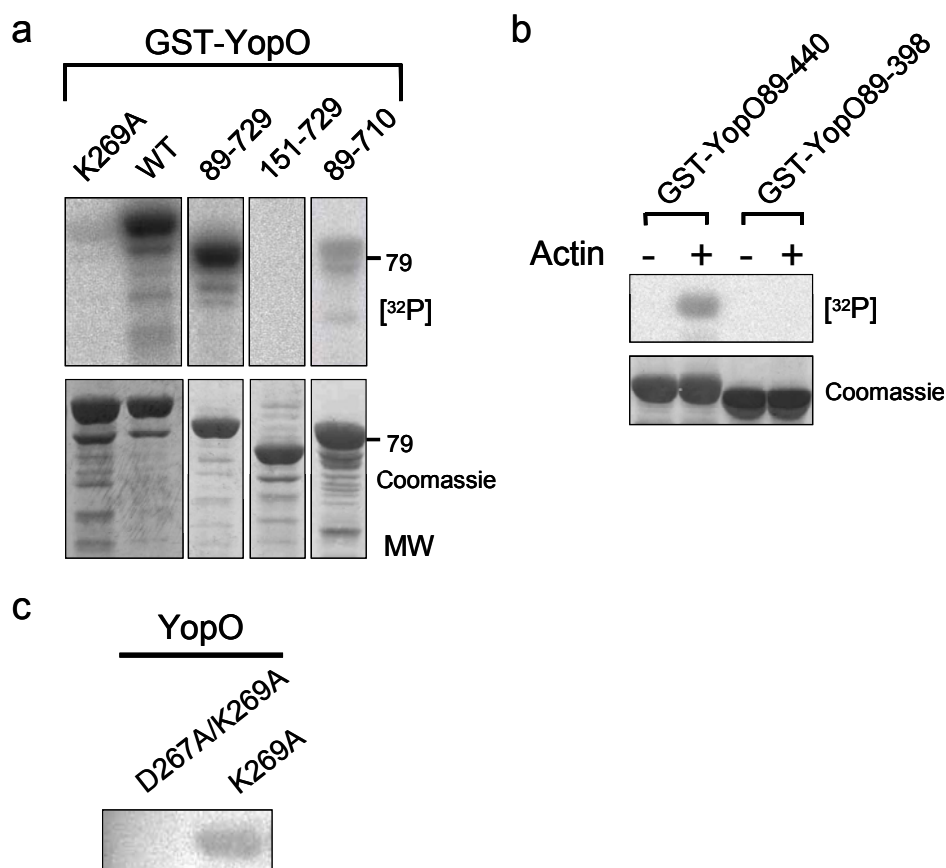
FIGURE 8. **Kinase activity of YopO mutants.**
a) Autophosphorylation of GST-fused YopO mutants in kinase assay (upper panel radiography, lower panel CoomassieBlue staining).
b) Autophosphorylation of GST-YopO89-440 and GST-YopO89-398 in the presence and absence of actin (upper panel radiography, lower panel CoomassieBlue staining). Molecular weights (MW) of standard marker proteins are indicated
c) Autophosphorylation of YopO point mutants. Double point mutant (D267A/K269A) and single point mutant (K269A) are shown.

YopOwt and YopO89-729 have the same actin binding properties and are shown here to incorporate the same amount of [32P]-phosphate during autophosphorylation reactions (Figure 8a). The full length active site kinase mutant YopOK269A showed very low residual autophosphorylation. For complete knockout of kinase activity the active site double mutant YopO89-729D267A/K269A was established and absence of residual autophosphorylation is shown in figure 8c.

The YopO construct comprising amino acids 151-729 (YopO151-729) is kinase dead (figure 8a) which may be caused by the disruption of the N-terminal actin binding site, disruption of the kinase domain, or may be due to the removal of autophosphorylation sites. YopO89-440, consisting of the N-terminal kinase region and actin binding site, was capable of autophoshorylating dependent on the presence of G-actin (figure 8b).

The constructs YopO89-710 and YopO89-440, lacking the C-terminal actin binding site, both show diminished autophosphorylation (compare figure 8a+b). In comparison, YopO89-398, a construct shown to have no actin binding activity, shows no autophosphorylation (figure 8b).

The diminished autophosphorylation activities of constructs YopO89-710 and YopO89-440 compared to YopO89-729 and YopOwt indicate that full actin binding by N- and C-terminal actin binding sites is necessary for full kinase activity.

The point mutant YopOK269A shows drastically reduced autophosphorylation (figure 8c). Introduction of a second mutation in the kinase domain of YopO leads to complete loss of autophosphorylation in YopOD267A/K269A (figure 8c). This double point mutant was used for the evaluation of kinase independent cellular effects.

1.4 Overview of the activities of YopO constructs used in this study

Table C2. **Overview of YopO constructs and their activities**

| YopO construct | PM | kinase | Actin binding | | Rho-binding |
			N-terminal	C-terminal	
WT (1-729)	+	+++	+	+	+
89-729	-	+++	+	+	+
89-710	-	+	+	-	+
89-440	-	+	+	-	-
399-729	-	-	-	+	+
1-710	+	+	+	-	+
1-440	+	+	+	-	-
D267A/K269A	+	-	+	+	+

+ indicating activity; - indicating no activity.

PM; plasma membrane localization. Rho-binding; intact GDI-like domain

An overview of the established YopO constructs with their respective activities is shown in table C2. YopO mutants missing the first 88 N-terminal amino acids are deficient in plasma membrane binding. Truncation at the C-terminus (1-710, 1-440, 89-710, 89-440) leads to constructs with intact kinase domain, but very diminished actin binding. The YopO constructs 1-440, 89-440 with C-terminal truncations lack the GDI-like domain and therefore Rho binding. The isolated Rho-binding GDI-like domain with intact C-terminal actin binding site is present in YopO399-729. Selective inactivation of the kinase was realized with two point mutations in construct YopOD267A/K269A.

2. MORPHOLOGICAL EFFECTS OF YOPO – F-ACTIN AND CELL SHAPE

2.1 Microinjection and Transfection of YopO

In order to examine if transfection of GFP-YopO expressing vectors, leading to eukaryotically expressed YopO fusion proteins, and injection of prokaryotically expressed YopO have the same cellular effects, the actin cytoskeleton and shape of cells was observed after transfection and microinjection. It has not been clear whether eukaryotically expressed YopO fusion proteins are able to elicit the same phenotype as untagged microinjected YopO.

In hitherto performed studies on the effects of YopO in eukaryotic cells, either *Y. enterocolitica* strains expressing YopO, or eukaryotic expression vectors with bi-cistronic expression of YopO and a marker gene were used.

In contrast to the N-terminally truncated YopO89-729 expression and purification of the full length YopOwt (1-729) protein could not be accomplished without detergent. Therefore the full length protein YopOwt was unsuitable for microinjection and YopO89-729 that was shown to have the same *in vitro* activities as YopOwt (see above) was used for microinjection.

2.1.1 Microinjection of YopO89-729 leads to rounding and F-actin disruption

Microinjection of YopO89-729 into endothelial cells (HUVEC) grown on glass coverslips showed two morphological effects. First TRITC-Phalloidin staining showed F-actin disruption in microinjected cells (arrowheads in figure 9a and 9b), secondly the cell shape of microinjected cells showed rounding with apparent retraction fibers (arrows in figure 9a and 9b). Control injections with buffer containing only rat-IgG that was used for the identification of microinjected cells showed none of the effects visible at injection of YopO89-729 (figure 9c and 9d).

FIGURE 9
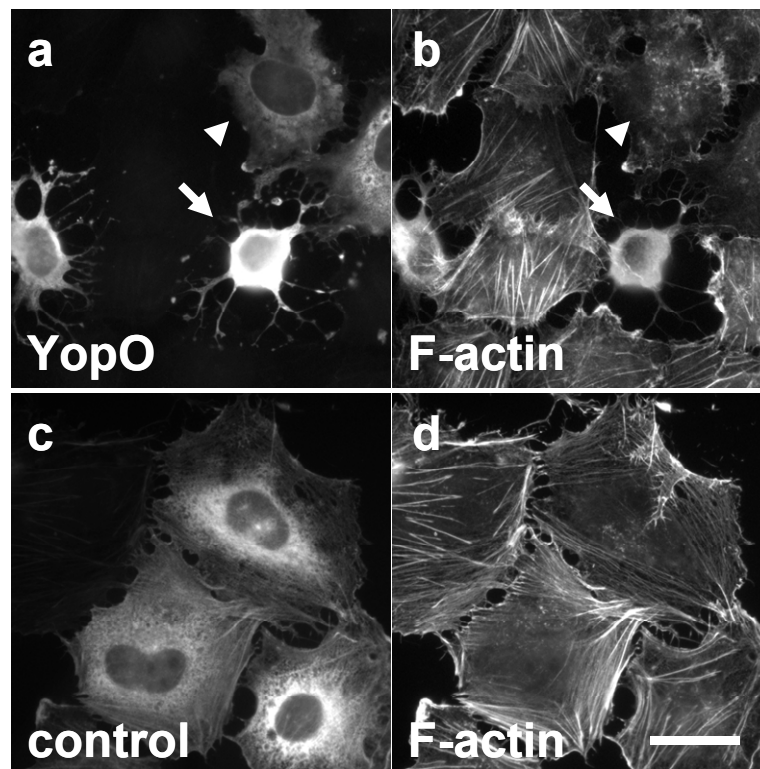
FIGURE 9. **Microinjection of YopO89-729 leads to rounding and F-actin disruption.**
a) Rat-IgG staining showing YopO-injected endothelial cells. b) F-actin staining of
YopO-injected and uninjected cells. Arrow and arrowhead point to an arborized and F-
actin disrupted cell, respectively. c) Immunofluorescence staining of cells injected with
Rat-IgG alone. d) F-actin staining of injected cell and one uninjected control cell to the
left. The bar represents 10 μm.

2.1.2 Transfection of YopO fusion proteins leads to rounding and F-actin disruption

In order to evaluate if the FLAG- or GFP-tag can interfere with the ability of YopO to disrupt
the actin cytoskeleton and induce cell rounding, the phenotype after transfection of FLAG-
tagged and N- or C- terminally GFP-tagged YopO fusion proteins (compare table E7c) was
evaluated in endothelial cells (HBMEC). As a control the empty vector expressing GFP was
used.

N- or C-terminal fusion to GFP had no effect on the ability of YopO to disrupt F-actin and
induce rounding (figure 10). The majority ($89 \pm 5\%$) of the control cells transfected with GFP
show no F-actin disruption and no rounding. A small fraction of cells ($11 \pm 4\%$) showed low
F-actin staining. Low actin staining resembling F-actin disruption may be caused by the
transfection procedure, may represent a motile state of the cell where stress fibers are reduced,
or may simply be a normal variation in the control cells.

FIGURE 10
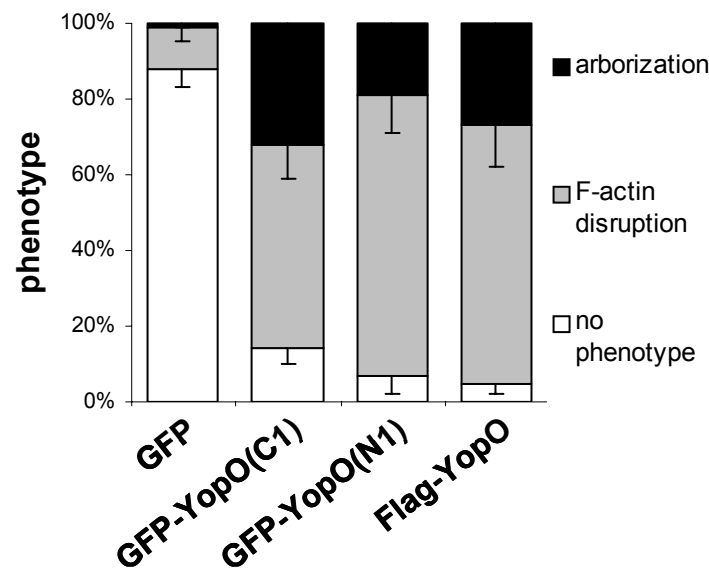
FIGURE 10. **Expression of different YopO-wildtype fusion proteins causes similar cell rounding and F-actin disruption.**
Statistical evaluation of morphological effects upon expression of GFP (control), GFP-YopO(C1), GFP-YopO(N1) and Flag-YopO fusion proteins in endothelial cells (HBMEC). Fraction of cells displaying one of three phenotypes (arborization, F-actin disruption and no phenotype) are shown for every construct. Values are mean ± S.D. of 3 experiments with at least 90 cells evaluated per experiment.

While approximately 10% of the control cells showed reduced actin, less than 1% showed a phenotype that resembled rounding. In contrast, transfection of YopO fusion proteins induced rounding in roughly 30% of the cells (GFP-YopO(C1), GFP-YopO(N1) and FLAG-YopO show rounding in 32 ± 10%, 19 ± 15% and 27 ± 7% of the cells, respectively). The effects of the YopO fusion proteins on the cellular F-actin were drastic: 54 ± 9% (GFP-YopO(C1)), 74 ± 10% (GFP-YopO(N1)) and 68 ± 11% (FLAG-YopO) of transfected cells showed F-actin disruption. Only a small fraction of cells (ranging from 5% to 14%) transfected with the YopO fusion proteins showed no alterations in the actin cytoskeleton and the cell shape.

These data show that the known cellular effects described for YopO introduced by yersiniae are also induced upon expression of the YopO protein fused to a FLAG moiety (7 amino acids) or to GFP (265 amino acids). This validates YopO transfection as a suitable method for the evaluation of the cellular effects of YopO protein domains.

2.2 Cellular effects of N- and C-terminal YopO deletion mutants on F-actin and cell shape

2.2.1 F-actin disruption is mediated by C-terminal Rho-GDI-like domain

Upon transfection of the GFP-fused N- and C-terminal YopO deletion mutants into endothelial cells (HBMEC), their effect on the actin cytoskeleton was visualized by staining of F-actin with AlexaFluor 568-phalloidin. Exemplarily F-actin disruption in a cell expressing GFP-YopO can be seen in figure 11a. In contrast to the GFP-YopO expressing cell, the surrounding cells show normal stress fibers.

FIGURE 11
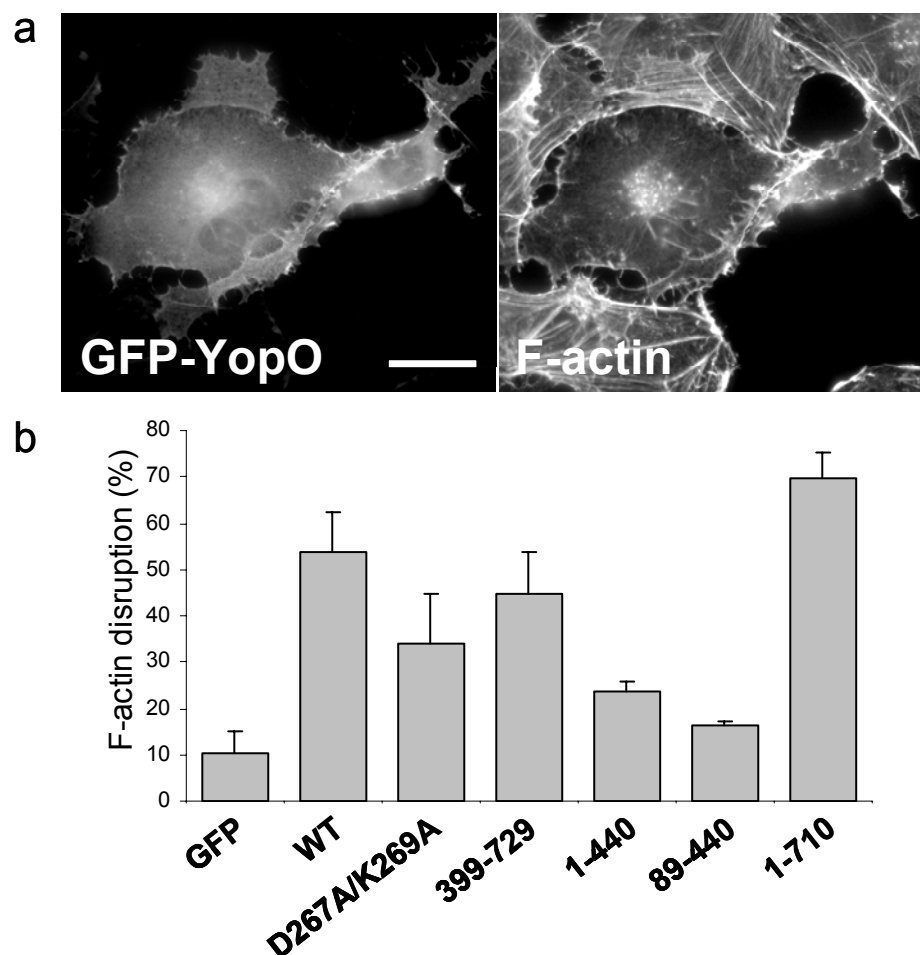
FIGURE 11. **F-actin disruption is mediated by C-terminal Rho-binding domains.**
a) Image of a GFP-YopO expressing cell (left). F-actin staining with AlexaFluor 568 phalloidin of cells in the same field showing F-actin disruption in the transfected cell, but not the surrounding cells (right). The bar represents 10 μm.
b) Statistical evaluation of F-actin disruption for GFP (negative control), GFP-YopOwt (WT) and designated GFP-YopO mutants. The percentage of cells showing clearly visible F-actin disruption is shown. Values are mean ± S.D. of 3 experiments with at least 90 cells evaluated per experiment.

Statistical evaluation shows that in cells containing the GFP-expressing empty vector only a small fraction ($10 \pm 4\%$; figure 11b) showed F-actin disruption, which could be explained by staining artifacts, a possible disruptive effect caused by transfection and/or the fraction of cells that naturally occurs with a diminished amount of F-actin at the moment of staining. YopO constructs carrying the intact C-terminal Rho GDI-like domain (Prehna, Ivanov et al. 2006) showed comparable stress fiber disruption as YopOwt ($54 \pm 9\%$; figure 11b). These constructs include the kinase deficient YopOD267A/K269A ($34 \pm 11\%$), YopO399-729 ($45 \pm 9\%$) and YopO1-710 ($70 \pm 6\%$). The YopO constructs that have residual kinase activity and are lacking the Rho-binding domain, namely YopO1-440 and YopO89-440, showed only minor stress fiber disruption with $24 \pm 2\%$ and $16 \pm 1\%$, respectively. From the fact that the low actin binding constructs YopO1-710 and YopO399-729 disrupt stress fibers very effectively it can be concluded, that F-actin disruption is not dependent on the actin binding capacity of YopO.

Conclusively these results show that the C-terminal Rho GDI-like domain alone is capable of inducing F-actin disruption and that this effect is independent on the YopO kinase activity and actin-binding activity.

2.2.2 F-actin disruption can be rescued by RhoAV14

The constitutive active RhoAV14 mutant is known to induce stress fibers (Ridley, Paterson et al. 1992). To test if RhoAV14 can prevent F-actin disruption caused by YopOwt, endothelial cells were co-transfected with mRFP-YopOwt and GFP-RhoAV14 and the F-actin staining was evaluated.

Co-expression of GFP-RhoAV14 and mRFP-YopOwt is shown in figure 12a. The double-transfected cell (arrow in figure 12a) shows characteristic GFP-RhoAV14 and mRFP-YopO staining together with an amount of F-actin comparable to the adjacent untransfected cell to the right (arrowhead in figure 12a). Upon cotransfection of RhoAV14 and YopO the disruptive effect of YopO on F-actin structures was no longer visible.

For statistical evaluation the percentage of cells showing F-actin structures (stress fibers) was scored for cells expressing GFP (empty vector control), GFP-RhoAV14, GFP-RhoAV14 and mRFP-YopO (co-expression), mRFP-YopO and mRFP (empty vector control). The majority of the GFP-RhoAV14 expressing cells ($78 \pm 8\%$; figure 12b) as expected showed distinct cytoplasmic F-actin structures. Upon cotransfection of GFP-RhoAV14 and mRFP-YopOwt the phenotype of single transfected GFP-RhoAV14 was observed, with the majority ($81 \pm 9\%$) of the co-transfected cells showing induced F-actin (figure 12b).

FIGURE 12
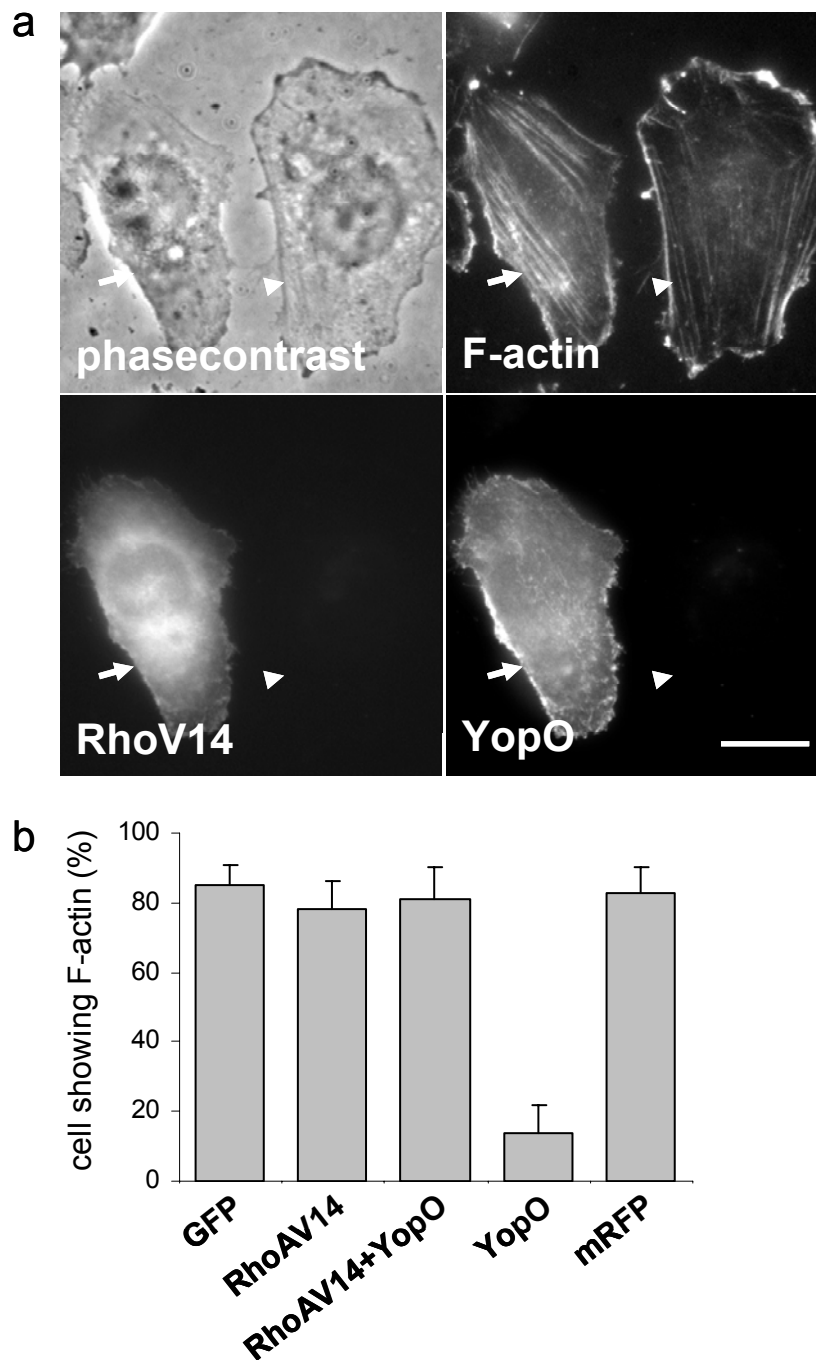
FIGURE 12. **F-actin disruption can be rescued by RhoAV14.**
a) Image series of an endothelial cell (HBMEC) expressing GFP-RhoAV14 (lower left)
and mRFP-YopO (lower right) stained for F-actin (upper right) and visualized by
phasecontrast microscopy (upper left). Arrow indicates double-transfected cell
(RhoAV14+YopO coexpression) with F-actin fibers. Arrowhead indicates untransfected
cell with F-actin fibers. The bar represents 10 μm.
b) Statistical evaluation of cells showing F-actin fibers. Cells expressing GFP (empty
vector), GFP-RhoAV14 (RhoAV14), GFP-RhoAV14 and mRFP-YopO (RhoAV14
+YopO), mRFP-YopO (YopO) and mRFP (empty vector) were evaluated for formation
of stress fibers. The fraction of cells showing F-actin fibers is displayed. Values are mean
± S.D. of 3 independent experiments. For every designated construct 90 cells were
evaluated per experiment.

This shows that co-expression of RhoAV14 and YopO does not result in F-actin disruption. Single expression of mRFP-YopOwt induced F-actin disruption in $86 \pm 8\%$ of the cells with only $14 \pm 8\%$ (figure 12b) of the cells showing cytoplasmic F-actin fibers. The control cells expressing the respective vector controls showed no reduction in stress fiber formation (GFP empty vector: $85 \pm 6\%$; mRFP empty vector: $83 \pm 7\%$).

These data show that F-actin disruption mediated by YopO can be rescued by co-expression of constitutive active RhoAV14. Hence the RhoA inhibiting activity of YopO does not effect the interaction of RhoA with its downstream targets.

2.2.3 Rounding/Arborization is dependent on kinase activity

Transfection of GFP-YopO into endothelial cells not only leads to the described F-actin disruption, but also to a rounded phenotype with articulate retraction fibers. This phenotype is shown by cells that are retracting or rounding up without completely dissolving their focal adhesions that attach them to the substratum. Cells rounding up in this specific way end up showing a fine branching (arborized) structure, a treelike shape that resembles the form of dendrites of a nerve cell (figure 13a).

Statistical analysis was performed and the fraction of arborized cells determined and displayed in figure 13b. Cells transfected with the GFP empty vector as negative control were scored for rounding and showed a minimal fraction of arborized cells of $1 \pm 0.8\%$. Cells transfected with the full length, fully-active GFP-YopOwt construct showed a degree of arborization of $32 \pm 10\%$. Compared to GFP-YopOwt the kinase dead GFP-YopOD267A/K269A showed significantly less arborization ($5 \pm 4\%$). GFP-YopO1-440, GFP-YopO89-440 and GFP-YopO1-710 displaying greatly reduced kinase activity all showed significant reduction of arborization compared to YopOwt (figure 13b).

These data indicate that the full degree of arborization is dependent on YopO kinase activity which in turn is dependent on actin binding.

FIGURE 13
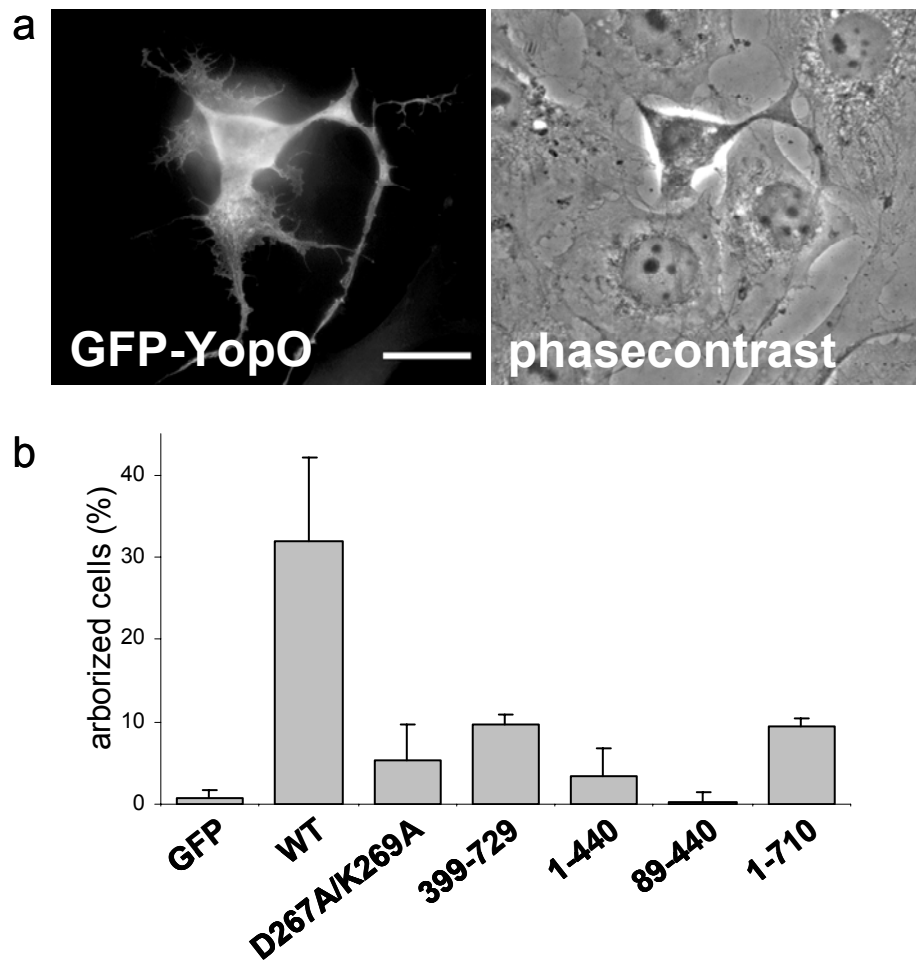
FIGURE 13. **Rounding/arborization is dependent on kinase activity of YopO.**
a) Image of GFP-YopO expressing cell (left). Phasecontrast image of cells in the same field showing rounding of the transfected cell (right). The bar represents 10 μm.
b) Statistical evaluation of cell rounding/arborization for GFP (negative control), GFP-YopOwt (WT) and designated GFP-YopO mutants. Values are mean ± S.D. of 3 experiments with at least 90 cells evaluated per experiment.

3. FUNCTIONAL ROLE OF YOPO IN PHAGOCYTOSIS

3.1 Fcγ-Receptor (FcγR)- and Complement Receptor (CR)-mediated phagocytosis

Phagocytosis, the uptake of particles (>0.5 μm) into cells, is a conserved cellular function that is driven by actin polymerization (Kaplan 1977; Castellano, Chavrier et al. 2001; May and Machesky 2001) and is important for host defense mechanisms as well as for tissue repair and morphogenetic remodeling. The molecular activators and effectors of the actin cytoskeleton involved in phagocytosis are very similar to those regulating other cell functions and include the small GTPases of the Rho family (Castellano, Chavrier et al. 2001).

Two of the best characterized phagocytic receptors in macrophages, the complement receptor 3 (CR3) and Fc-gamma receptors (FcγRs), are involved in the uptake of opsonized microorganisms during infection. CR3 binds C3bi on complement-opsonized targets, whereas FcγRs bind to the conserved Fc domain of immunoglobulin G (IgG) coated targets. Although both uptake processes require actin polymerization, complement-receptor-mediated phagocytosis is morphologically distinct from that mediated by FcγRs. FcγR mediated phagocytosis is characterized by a dramatic, actin-dependent extension of the plasma membrane around the particle and is followed by the production of superoxide and the release of inflammatory cytokines, while complement-opsonized particles 'sink' into the phagocyte; there is minimal membrane disturbance, and internalization does not usually lead to an oxidative burst or inflammatory response (Caron and Hall 1998; May and Machesky 2001). Two distinct mechanisms of phagocytosis with regard to Rho GTPases and actin reorganization involved were identified by Hall in the year 1998: Type I phagocytosis, used by the immunoglobulin receptor is mediated by Cdc42 and Rac and type II, used by the complement receptor (CR), is mediated by Rho (Caron and Hall 1998). Both mechanisms are favorable targets for pathogens that have the strategy to avoid phagocytosis.

YopO was shown to have a dramatic impact on the actin cytoskeleton and the cells ability to form or maintain cytoskeletal F-actin structures. To elucidate if F-actin disruption caused by YopO has a functional role in phagocytosis, CR- and Fcγ-R-mediated internalization of sheep red blood cells (SRBC) in the presence of YopO was quantified.

3.1.1 FcγR-induced actin polymerization is not inhibited by YopO

Actin polymerization at the phagocytic cup is necessary to drive the uptake process. FcγR-mediated phagocytosis is morphologically accompanied by articulate, actin-dependent extensions of the plasma membrane around the internalized particle. The pronounced F-actin structure formed is referred to as actin cup (May and Machesky 2001).

YopO has drastic effects on F-actin structures in endothelial cells, but it was not known if YopO can inhibit the formation of phagocytic actin cups.

Before Fcγ-R and CR-dependent internalization was evaluated, the effect of YopO on the formation of phagocytic actin cups during Fcγ-R mediated phagocytosis was evaluated.

FIGURE 14
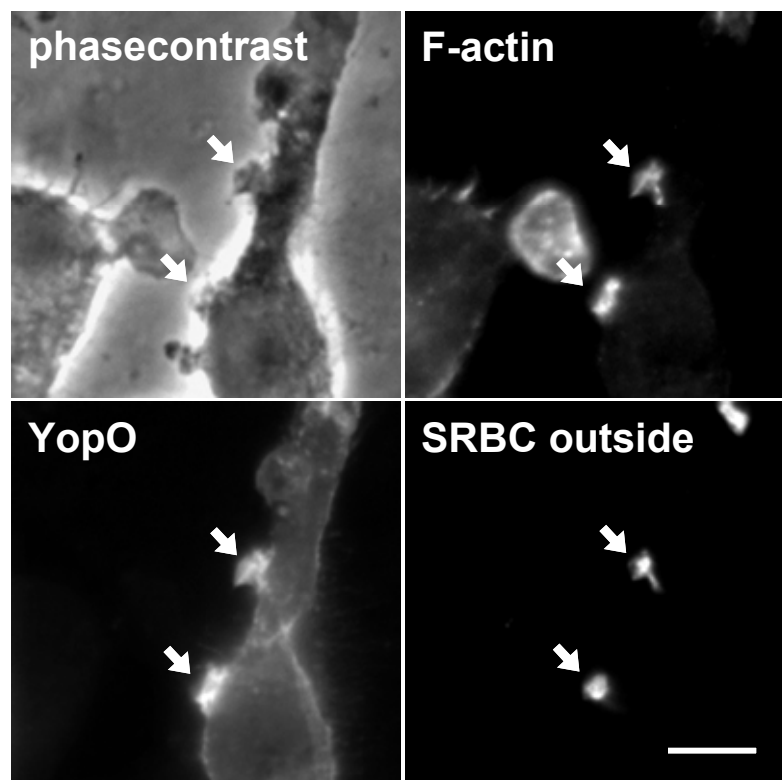
FIGURE 14. **Actin cup formation during Fcγ-R- mediated uptake is not inhibited by YopO.** Image series showing GFP-YopO expressing macrophage (lower left), AlexaFluor 568 outside-stained SRBC (lower right), Marina Blue F-actin staining (upper right) and phasecontrast image (upper left). External SRBC triggering actin polymerization are marked with arrows. The bar represents 10 μm.

The process of phagocytic F-actin cup formation during the FcγR-mediated uptake of IgG-coated SRBC into a GFP-YopO transfected macrophage is visualized in figure 14. Outside staining (arrows, lower right) shows external SRBC that trigger the formation of F-actin at the site of attachment (arrows, upper right). The GFP-YopO expressing macrophage can be identified by green fluorescence (b/w capture, lower left). Phasecontrast (upper left) identifies

the GFP-YopO expressing macrophage and an adjacent untransfected macrophage. Attached IgG-coated SRBC (marked by arrows) were able to trigger actin polymerization in GFP-YopO transfected macrophages.

Thus *de novo* formation of F-actin structures surrounding the ingested SRBC is shown here to occur in the presence YopOwt.

3.1.2 FcγR and CR-mediated phagocytosis are not inhibited by YopO

To quantify the effects of YopO on the two distinct uptake mechanisms mediated by the phagocytic receptors FcγR and CR (complement receptor), the uptake of IgG- and complement-coated sheep red blood cells (SRBC) into GFP-YopOwt expressing human macrophages was evaluated. The adapted microscopic method employed allows to analyze phagocytosis of defined particles (SRBC) via defined receptors on the cellular level (Greenberg, el Khoury et al. 1991; Braun, Fraisier et al. 2004). Phagocytosed SRBC can be distinguished from attached SRBC by the use of fluorescence staining and phasecontrast. A peculiar property of SRBC is that they become visible by phase contrast inside a cell as swollen particles in vacuoles, but are almost invisible outside of cells. After fixation the attached external SRBC are fluorescently stained and appear only detectable by fluorescent staining and not by phase contrast. Internalized SRBC appear negative for staining, or weekly stained, but are detectable as distinct round particles by phase contrast.

Potential inhibition of uptake by GFP-YopO can be caused by interference in phagocytic signaling, or by inhibition of macrophage-SRBC interaction. The latter is not the case for GFP-YopO transfected macrophages. Binding and uptake of particles in GFP-YopO transfected cells is not impaired as can be observed in figure 15a. Attachment and uptake is visualized for IgG-coated SRBC. A considerable amount of phagocytosed SRBC (arrows in figure 15a) and several attached SRBC (arrowheads) can be seen in the GFP-YopO transfected as well as in the untransfected cell.

The number of phagocytosed and attached SRBC was determined for control cells expressing GFP or cells expressing GFP-YopO in three independent experiments. Statistical analysis of phagocytosis of IgG- and complement-coated SRBC was performed. Internalization in transfected cells was normalized to internalization in control cells and the fraction of phagocytosed SRBC in GFP-YopO expressing cells compared to the intracellular fraction in control cells (displayed in figure 15b). Phagocytosis of IgG-coated SRBC (FcγR-mediated phagocytosis) was not significantly inhibited in GFP-YopOwt transfected cells, which showed $93 \pm 9\%$ SRBC internalization compared to the control. Complement receptor mediated

phagocytosis was also not significantly inhibited by GFP-YopO. Compared to control cells, internalization of complement-coated SRBC appeared to be lower in GFP-YopO transfected cells ($80 \pm 11\%$), but statistical analysis of internalization data revealed no significant reduction.

These data indicate that GFP-YopOwt has no inhibitory effect on FcγR- and Complement Receptor-mediated phagocytosis in macrophages.

FIGURE 15
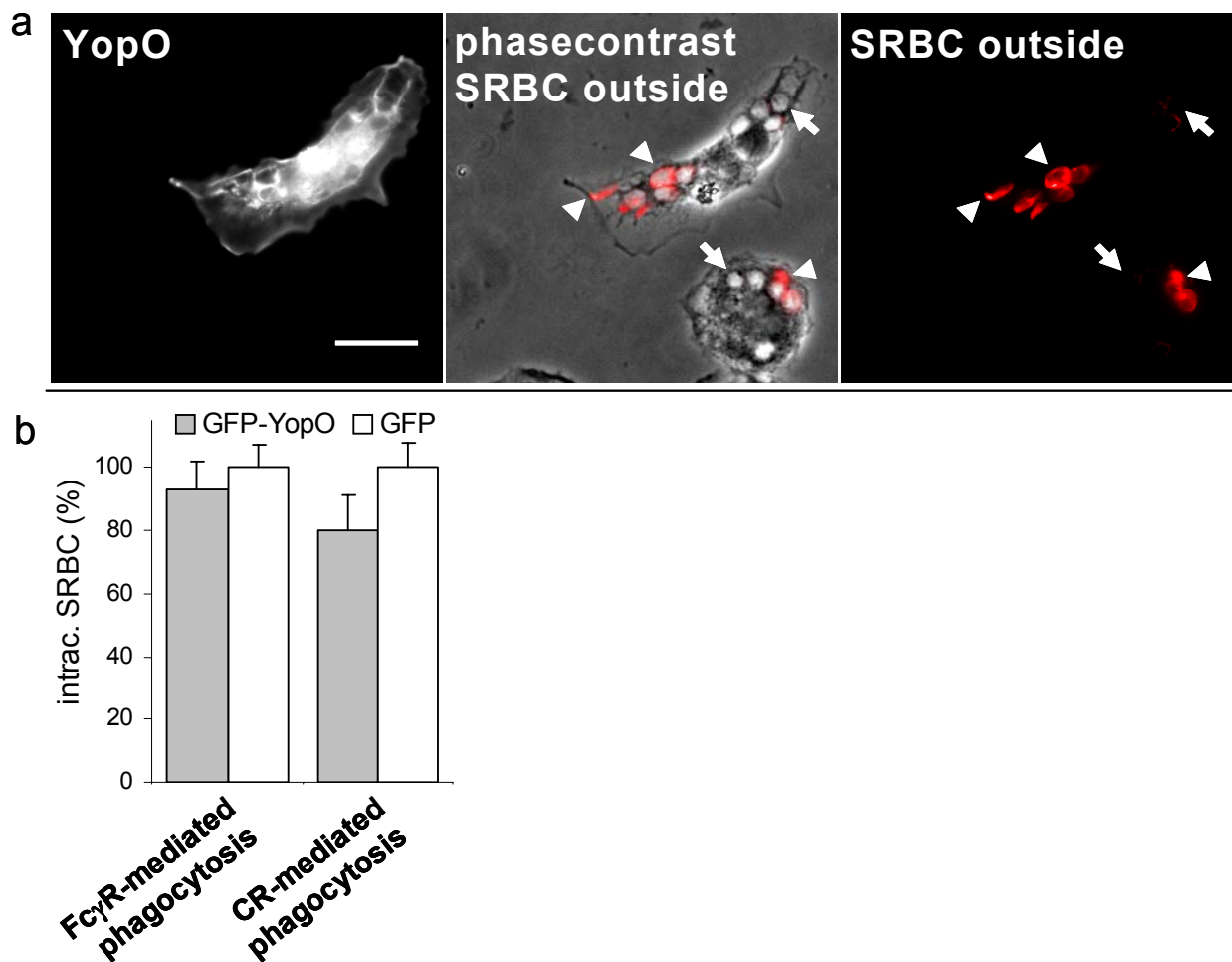
FIGURE 15. **Fcγ-R and CR-mediated phagocytosis are not inhibited by YopO.**
a) Image series showing a GFP-YopO expressing macrophage (left), phasecontrast image merged with outside staining of SRBC (middle) and AlexaFluor 568 outside-stained SRBC (right). The bar represents 10 μm. Arrows indicate internalized SRBC. Arrowheads indicate external SRBC.
b) Statistical evaluation of internalization for GFP (control) and GFP-YopOwt (YopO) expressing macrophages. Uptake is shown as the percentage of total cell associated SRBC that is intracellular. Uptake was normalized to control (GFP expressing cells) that was set to 100%. Values are mean ± S.D. of 3 independent experiments with 90 cells evaluated per experiment.

3.2 Invasin mediated phagocytosis

3.2.1 Invasin-beads and Invasin-*E. coli* show similar invasion properties

Heterologously expressed invasin can be coupled to the sulfate groups on the surface of fluorescent microspheres (beads). The advantage of fluorescent beads for microscopic evaluation of internalization is that the beads can be better detected and quantified in phasecontrast, do not have to be fluorescently stained and additionally do not get degraded after uptake. Internalized bacteria start to lose their antigenic epitopes upon degradation by lysosomal proteases. To evaluate fluorescent beads for internalization assays, triggering of phagocytic cups and uptake kinetics of beads coated with invasin (Invasin-beads) was examined and compared to Invasin-*E. coli*.

After attachment of Invasin-beads the formation of actin cups is triggered with similar efficiency and kinetics as with Invasin-*E. coli*. Phasecontrast and F-actin staining in figure 16a show Invasin-beads (marked by arrows, upper pictures) that trigger the formation of distinct F-actin structures (actin cups) around them. The formation of actin cups at sites of Invasin-*E. coli* attachment is also shown in figure 16a (lower pictures).

After it was shown that the actin cups triggered by attachment of Invasin-beads and Invasin-*E. coli* are similar, uptake kinetics in endothelial cells (HBMEC) was determined. At several time points (10, 30 and 60 minutes) after attachment of Invasin-beads and Invasin-*E. coli*, cells were fixed and the respective uptake evaluated (displayed in figure 16b). Invasin-coated beads showed comparable uptake kinetics as Invasin-*E. coli*. After 10 minutes $51 \pm 9\%$ and $64 \pm 8\%$ of the attached particles were internalized for Invasin-*E. coli* and Invasin-beads, respectively. After 60 minutes the majority of attached Invasin-*E. coli* ($87 \pm 7\%$) and Invasin-beads ($92 \pm 11\%$) were localized inside the cell.

Taken together the identical internalization morphology and the uptake kinetics, fluorescent Invasin-beads were shown to be a suitable model system to examine invasin-mediated phagocytosis on a cellular level.

FIGURE 16
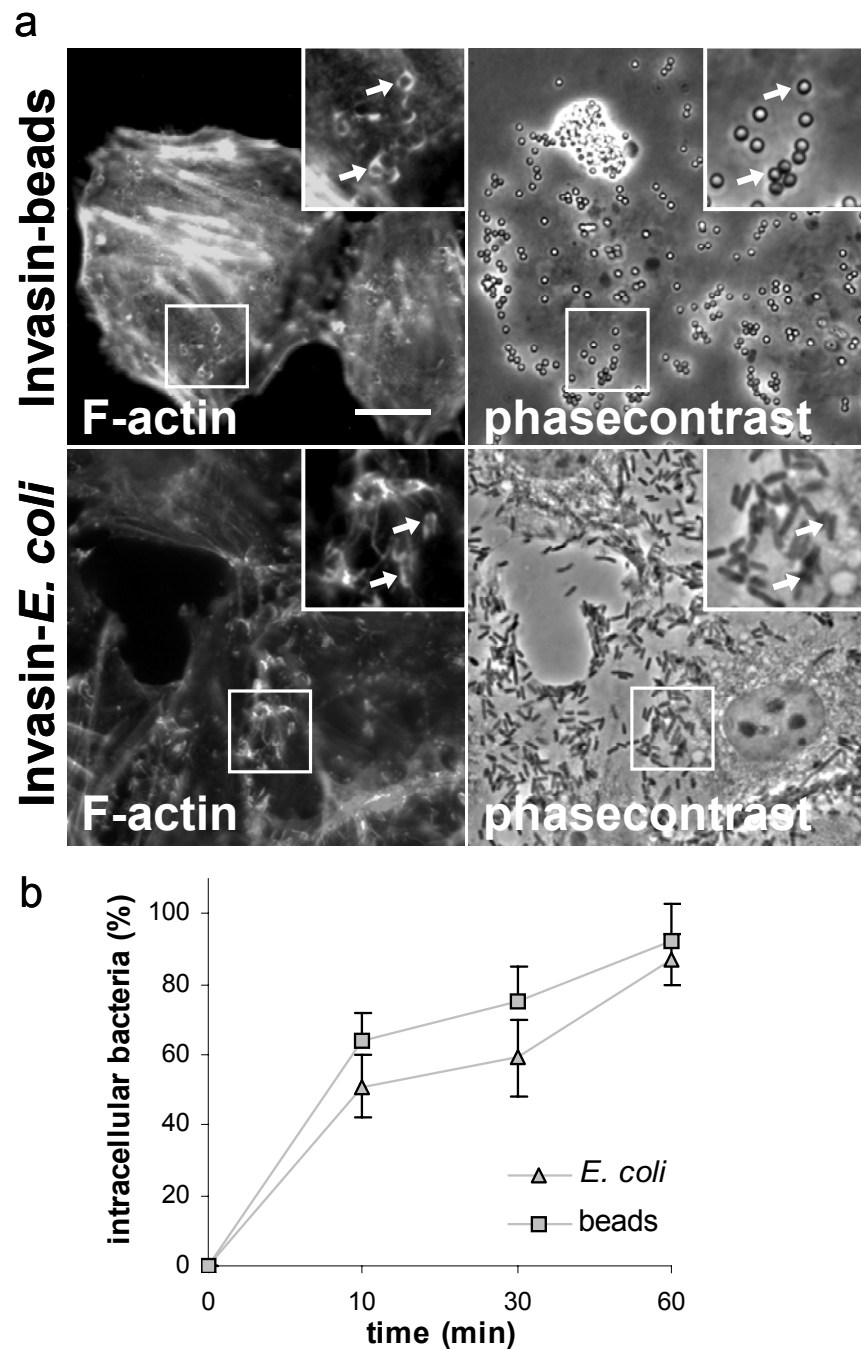
FIGURE 16. **Invasin-beads and Invasin-*E. coli* show similar invasion properties.**
a) Morphological effects in endothelial cells (HBMEC) induced by Invasin-beads (upper panels) and Invasin-*E. coli* (lower panels). AlexaFluor 568 F-actin staining shows discrete actin cups at sites of attached Invasin-beads (upper left). Beads are visible by phasecontrast (upper right). AlexaFluor 568 staining shows F-actin accumulation at sites of Invasin-*E. coli* attachment (lower left). Bacteria are visible in phasecontrast (lower right). Arrows indicate sites of Invasin-bead/*E. coli*-triggered actin polymerization. The bar represents 10 μm.
b) Uptake kinetics of Invasin-*E. coli* and Invasin-beads. Internalization was quantified after 10, 30 and 60 minutes by double fluorescence staining. Uptake is shown as the percentage of total cell associated bacteria that is intracellular. Values are mean ± S.D. of 3 experiments with at least 90 cells evaluated per experiment.

3.2.2 Localization of YopO to phagocytic cup depends on amino acids 1-88

YpkA has been shown to localize to the plasma membrane dependent on the amino acids 1-443 (Dukuzumuremyi, Rosqvist et al. 2000). Localization of YopO to specific *Yersinia*-induced phagocytic structures has not been examined. Whether recruitment to phagocytic structures occurs and if it is dependent on the N-terminal membrane localization domain, the kinase domain, or the C-terminal Rho GDI-like domain has also not been known.

It is shown here that GFP-YopO localization to invasin-induced uptake structures is dependent on the amino acids 1-88 and further that GFP-YopO1-440, which lacks the C-terminal Rho GDI-like domain is enriched at theses sites (figure 17).

FIGURE 17
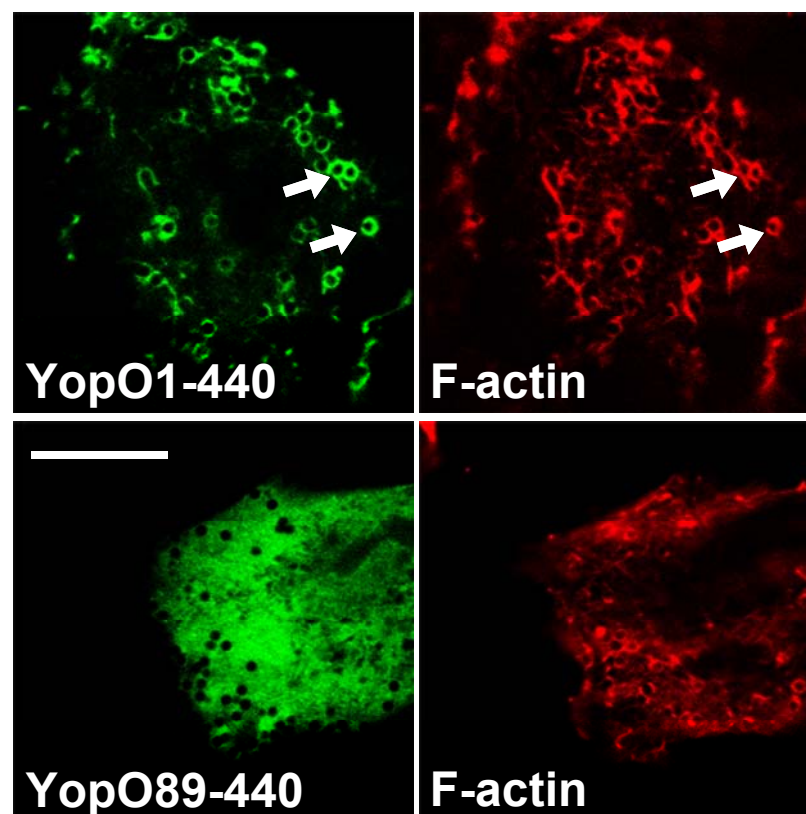
FIGURE 17. **Localization of YopO to phagocytic cup depends on amino acids 1-88.** Localization of GFP-YopO1-440 to invasin-induced phagocytic cups (upper panels) versus diffuse cytoplasmic localization of GFP-YopO89-440 (lower panels). GFP-YopO1-440 is accumulated around attached beads (upper left). Alexa568 phalloidin staining shows Invasin-bead-induced F-actin cups (upper right and lower right). YopO89-440 shows no discrete accumulation at sites of Invasin-bead attachment (lower left). Arrows indicate YopO localization to invasin-induced actin cups. The bar represents 10 μm.

Confocal images of invasin-beads attached to endothelial cells (HBMEC) show phagocytic actin cups (red color) and accumulation of GFP-YopO1-440 (green color) at the sites of bead attachment (arrows, figure 17). This distinguished accumulation at the site of Invasin-bead

attachment is not visible for GFP-YopO89-440 indicating that amino acids 1-88 are necessary for targeting YopO to the phagocytic cup. GFP-YopO89-440 shows diffuse cytoplasmic localization (figure 17). Localization of the full length GFP-YopO to the invasin-induced uptake structure can be seen in figure 18.

In conclusion the localization of YopO to the invasin-induced phagocytic cup is shown to be dependent on the N-terminal amino acids 1-88.

3.2.3 Invasin-induced actin cup formation is not inhibited by YopO

Interaction of Invasin-beads with endothelial cells causes actin polymerization at the site of attachment. In contrast, YopO causes drastic depolymerization of F-actin. To find out if YopO can inhibit the polymerization of actin at the site of bead attachment, GFP-YopO transfected cells (HBMEC) were inoculated with Invasin-beads.

FIGURE 18
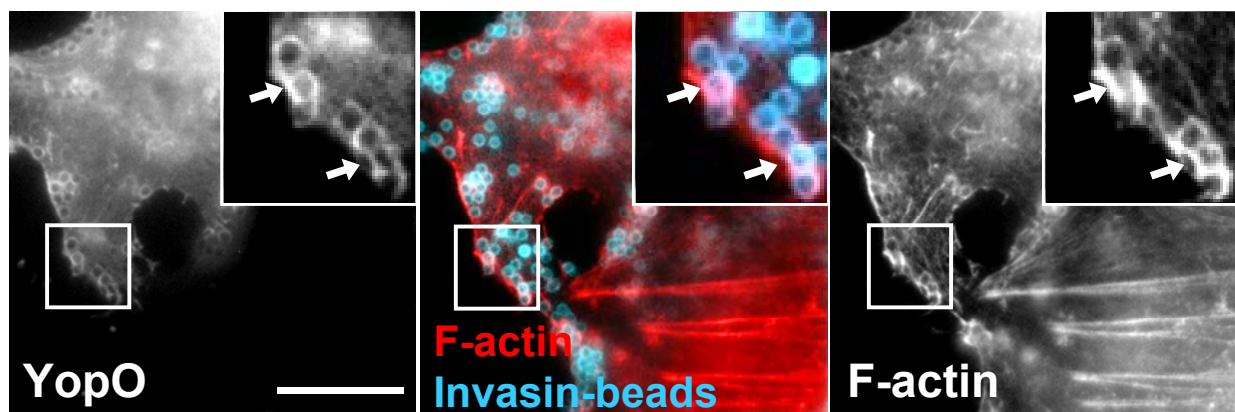
FIGURE 18. **Invasin-induced actin polymerization is not inhibited by YopO.**
Image series showing GFP-YopO expressing cell (left), merged F-actin in red and Invasin-bead staining in blue (middle) and single channel with AlexaFluor 568 phalloidin stained F-actin (right). YopO expressing cell shows polymerization of actin at sites of Invasin-bead attachment (arrows) despite disruption of cytoplasmic F-actin fibers. Accumulation of GFP-YopO at the sites of Invasin-bead attachment is visible in the left picture (arrows). The bar represents 10 μm.

Cells showing cytoplasmic F-actin disruption were examined for the formation of actin cups at the site of Invasin-bead attachment (figure 18). The GFP-YopO expressing cell (left picture) stained for F-actin (right picture) shows articulate F-actin disruption. Attached Invasin-beads (arrows), visualized in blue in the middle picture, were able to trigger the polymerization of actin in the GFP-YopO expressing cell. GFP-YopO localization at the site of bead attachment is visible in the left frame.

In conclusion, in cells showing obvious F-actin disruption caused by YopO, invasin-induced actin cup formation at the site of Invasin-bead attachment (arrows) was not inhibited.

3.2.4 Invasin-mediated internalization is not inhibited by YopO

To test if YopO can interfere with the uptake triggered by invasin, GFP-, GFP-YopOwt- and GFP-RacN17 expressing endothelial cells (HBMEC) were microscopically evaluated for internalization of Invasin-beads. Internalization was normalized to GFP-control that was set to 100%. The uptake of Invasin-beads was described to be dependent on the small GTPase Rac1 (McGee, Zettl et al. 2001). Microinjection of dominant negative RacN17 inhibited actin cup formation upon uptake of Invasin-beads (Wiedemann, Linder et al. 2001). As a control for uptake inhibition, cells expressing GFP-RacN17 were evaluated for Invasin-bead internalization.

FIGURE 19
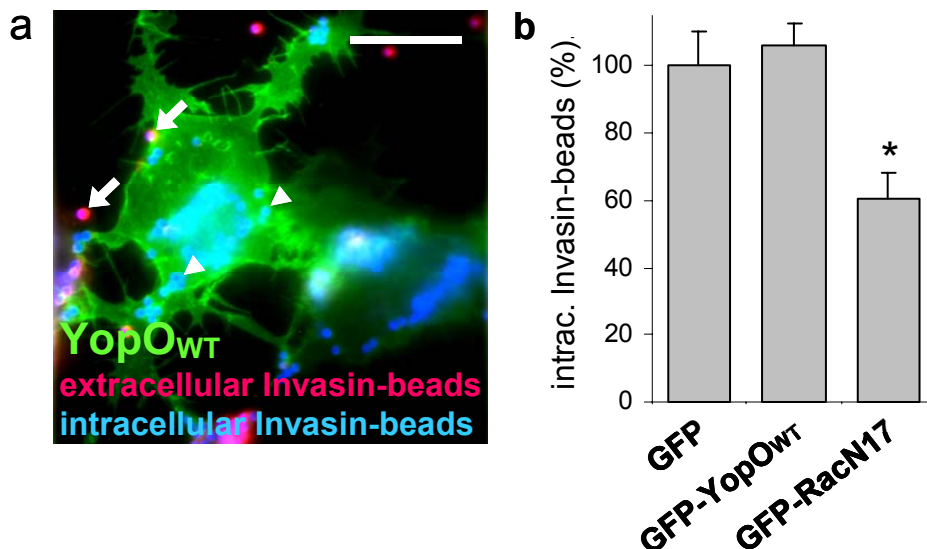
FIGURE 19. **Invasin-mediated internalization is not inhibited by YopO.**
a) Immunofluorescence image of GFP-YopO expressing endothelial cell (HBMEC, green) with internalized (blue) and extracellular Invasin-beads (red). External Invasin beads were stained red with AlexaFluor 568 secondary antibody (arrows). Internalized Invasin-beads appear in blue due to their default property (arrowheads). GFP-YopO expressing cell shows early signs of rounding/arborization. The bar represents 10 μm.
b) Statistical evaluation of Invasin-bead internalization for GFP, GFP-YopOwt and GFP-RacN17 expressing cells. Uptake is shown as the percentage of total cell associated Invasin-beads that is intracellular. Internalization was normalized to GFP control that was set to 100%. Significant reduction in internalization for GFP-RacN17 expressing cells is indicated by an asterisk. Values are mean ± S.D. of 3 experiments with 90 cells evaluated per experiment.

A GFP-YopOwt expressing cell with Invasin-beads stained for discrimination of intra- and extracellular localization is shown in figure 19a. Outside staining with an anti-Invasin antibody shows extracellular beads in red (arrows). Phagocytosed intracellular beads are distinguishable inside the transfected cell (green) as blue spheres (arrowheads). Although the

GFP-YopO transfected cell shows morphological signs of rounding/arborization, uptake of Invasin-beads (arrowheads) was not inhibited.

Statistical analysis of internalization experiments showed that there is no detectable inhibition of Invasin-bead uptake by GFP-YopO (figure 19b). Cells expressing GFP-YopO were as efficient in internalizing Invasin-beads as GFP expressing control cells. Due to the accuracy of the method (see standard deviation/error bars) the slightly higher internalization in GFP-YopO transfected cells ($106 \pm 6\%$) can be regarded identical to the internalization in GFP control cells (set to 100%). GFP-RacN17 transfected cells showed significantly lower uptake ($60 \pm 8\%$) compared to GFP control cells, confirming the established role of Rac in invasin-mediated uptake.

These data suggest that YopO is not able to inhibit bacterial internalization mediated by invasin.

3.3 YadA mediated phagocytosis

3.3.1 Adhesion of YadA-*E. coli* to fibronectin (FN) and collagen (COL)

YadA was shown to mediate adhesion to matrix proteins like fibronectin and collagen. A recent publication relates invasion in Hep-2 cells to the ability of *Y. pseudotuberculosis* YadA to bind fibronectin (Heise and Dersch 2006). That study revealed that *Y. enterocolitica* YadA showed low fibronectin binding and minimal invasion in Hep-2 cells. The YadA-*E. coli* strain (DH5A-pBR-A1) used in this study is expressing *Y. enterocolitica* O:8 YadA on its surface (Roggenkamp, Neuberger et al. 1995).

To characterize fibronectin and collagen binding of the YadA-*E. coli* strain used in this work, adhesion assays on fibronectin and collagen coated surfaces were performed. YadA-*E. coli* and control bacteria (DH5A-pBR) were incubated with surface-coated glass coverslips, washed, fixed and immunofluorescently stained. Adhesion was evaluated from fluorescent staining. Normalized values are displayed in figure 20. YadA-*E. coli* shows stronger adhesion to collagen ($100 \pm 27\%$) than to fibronectin ($42 \pm 18\%$).

In line with the previously published results adhesion of the YadA-*E. coli* strain to fibronectin coated coverslips was lower than adhesion to collagen coated coverslips (figure 20). The parental *E. coli* strain (DH5A-pBR) was used as a control and showed minimal adhesion.

FIGURE 20
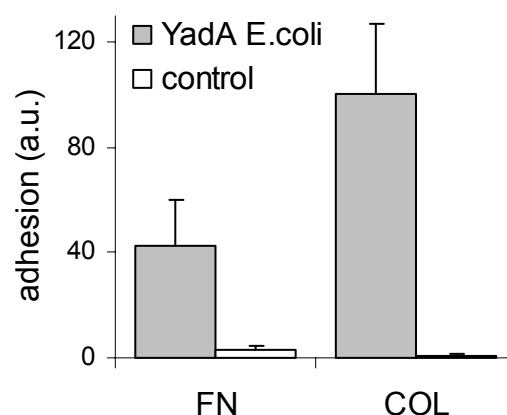
FIGURE 20. **Adhesion of YadA-*E. coli* to fibronectin (FN) and collagen (COL).**
Quantification of YadA-*E. coli* (DH5A-pBR-A1) adhesion to the ECM proteins fibronectin (FN) and collagen (COL) on glass coverslips. The non-adhesive parental strain DH5A-pBR was used as control. Adhesion was quantified by measurement of immunofluorescence of adhered bacteria and is displayed in arbitrary units. Values are mean $\pm$ S.D. of 3 experiments with 10 objective fields measured per condition.

3.3.2 Internalization of YadA-*E. coli* is independent of fibronectin

YadA dependent internalization was studied in Hep-2 cells with the YadA protein from *Y. pseudotuberculosis* and shown to be dependent on fibronectin. The YadA protein from *Y. enterocolitica* was shown to be non-invasive in that cell type (Heise and Dersch 2006). Primary endothelial cells (HUVEC) used in this study to assay YadA-mediated internalization showed slow but considerable uptake mediated by the *Y. enterocolitica* YadA protein.

To investigate internalization mediated by *Y. enterocolitica* YadA, YadA-*E. coli* and the parental control strain were attached to fibronectin knockout cells (FN-/-) or the parental control fibroblastic cell line (FN+/+) under serum free conditions. Internalization quantified by double fluorescence staining shows considerable uptake of YadA-*E. coli* in both cell lines (figure 21). Internalization is visualized for FN-/- cells in figure 21a.

FIGURE 21
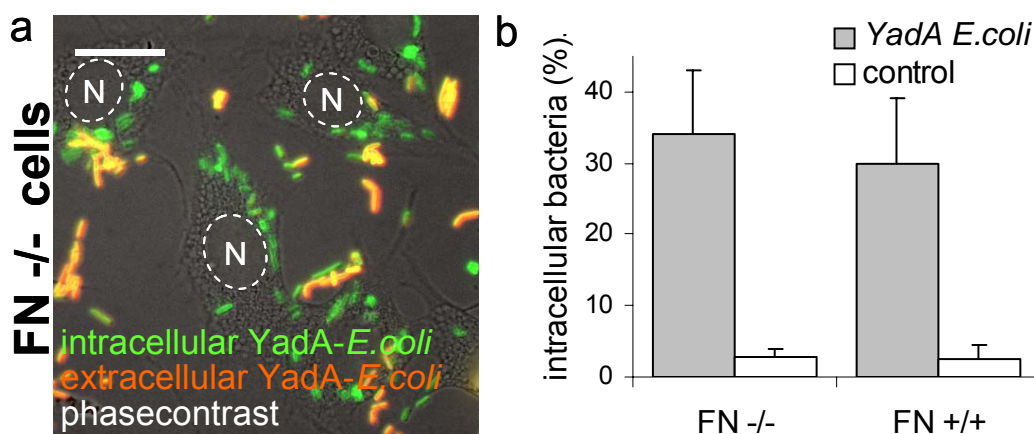
FIGURE 21. **Internalization of YadA-*E. coli* is independent of fibronectin.**
a) Phasecontrast image of FN-/- fibroblasts merged with fluorescence images showing attached external YadA-*E. coli* (orange) and internalized YadA-*E. coli* (green). Extracellular and internalized YadA-*E. coli* were stained with AlexaFluor 568- (red) and AlexaFluor 488- (green) labeled secondary antibody, respectively. The bar represents 10 μm.
b) Quantification of YadA-*E. coli* (DH5A-pBR-A1) and DH5A-pBR (control, non-adhesive parental strain) internalization in fibronectin knockout (FN-/-) and control (FN+/+) cells. Uptake is shown as the percentage of total cell associated bacteria that is intracellular. Internalization was quantified by immunofluorescence staining. Values are mean ± S.D. of 3 experiments with at least 90 cells evaluated per experiment.

After 90 minutes $30 \pm 9\%$ of the FN+/+ attached YadA-*E. coli* and $34 \pm 9\%$ of the FN-/- attached YadA-*E. coli* were intracellular (figure 21b). The parental *E. coli* control strain showed minimal internalization of $3 \pm 1\%$ for FN-/- and $2 \pm 4\%$ for FN+/+ even when attached at a 100-fold higher ratio compared to YadA-*E. coli*.

Uptake of YadA-*E. coli* therefore can be considered as specifically mediated by *Y. enterocolitica* YadA and to proceed independently of fibronectin.

3.3.3 Localization of YopO to the YadA uptake structure

Upon uptake of YadA-*E. coli* in GFP-YopOwt expressing cells, localization of YopO at the site of bacterial internalization can be observed.

FIGURE 22
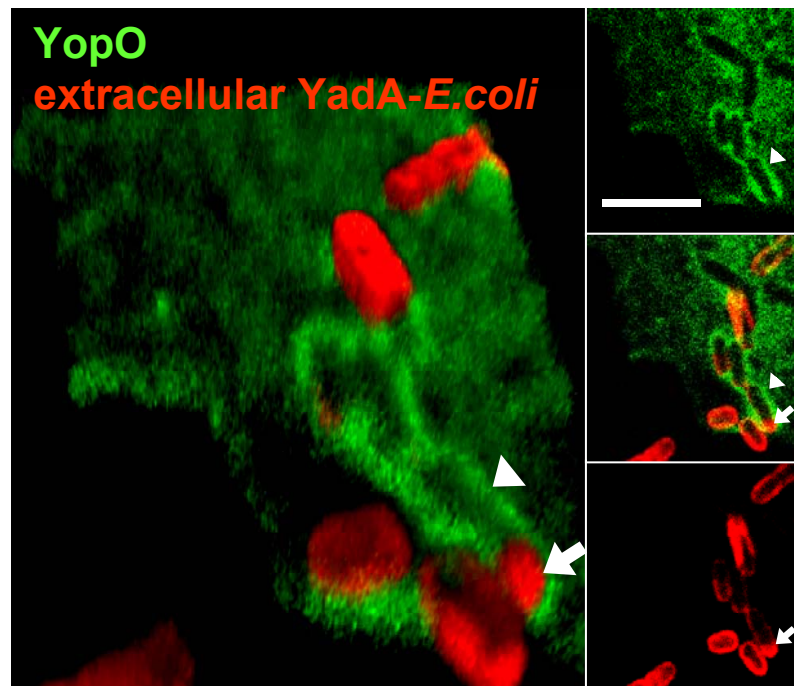
FIGURE 22. **YopO localizes to YadA-induced uptake structure.**
Left image shows 3 dimensional reconstruction of a confocal stack of an endothelial cell (HUVEC) expressing GFP-YopO (green) during phagocytosis of YadA-*E. coli* (red). Thumbnails on the right show channels (green, merge, red) of one confocal plane. The bar represents 5 μm. Outside staining of YadA-*E. coli* in red shows extracellular bacterial surface in bright red and the GFP-YopO protein (green) that is recruited to the site of bacterial uptake. A small extracellular fraction of a partially phagocytosed bacterium (arrow) is distinguishable from the intracellular part that is defined by the recruitment of GFP-YopO (arrowhead)

Figure 22 shows external YadA-*E. coli* stained in red and a GFP-YopOwt expressing cell. Bacterial internalization is depicted exemplarily for a single bacterium, where the external part of the bacterial cell is stained red (arrow) and the internalized part shows accumulation of GFP-YopO (arrowhead). Adjacent internalized YadA-*E. coli* show no extracellular staining in red and are visible only by the GFP-YopO accumulation around their surface.

3.3.4 YadA-induced actin polymerization is not inhibited by YopO

YopO does not inhibit actin polymerization induced upon binding of Invasin-beads (see above). Compared to invasin, indirect interaction of YadA with cells via an extracellular matrix bridge triggers substantially less prominent actin accumulation at the site of attachment. Internalization is slower and formation of the phagocytic actin cup is less pronounced. To investigate if the inhibitory effect of YopO is accompanied by disruption of F-actin at the YadA induced phagocytic cup, GFP-YopO expressing cells were evaluated for F-actin accumulation at the site of bacterial internalization by immunofluorescence staining.

FIGURE 23
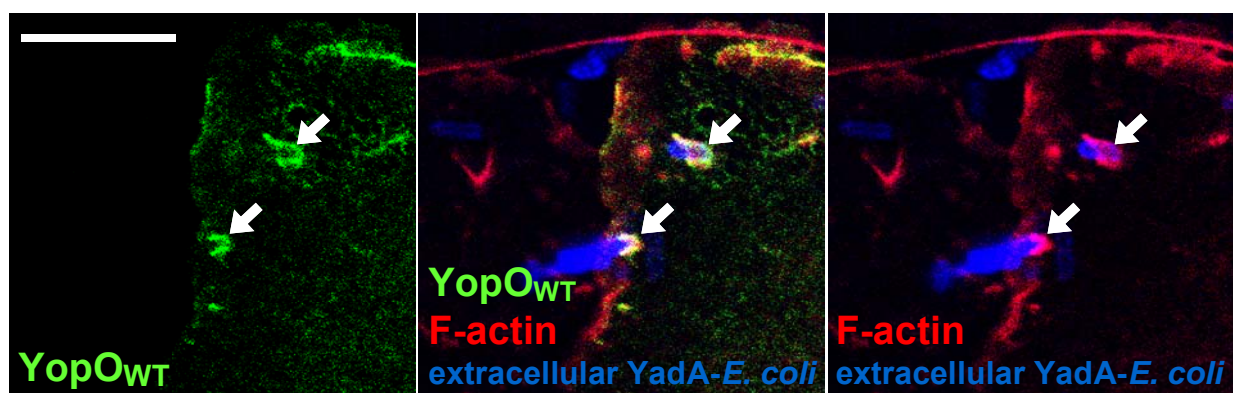
FIGURE 23. **YadA-induced actin polymerization is not inhibited by YopO.**
Image series showing GFP-YopO expressing endothelial cell (HUVEC) in green, YadA-*E. coli* stained in blue and F-actin stained in red. Green channel shows GFP-YopO expression (left), channel merge in the middle shows localization of GFP-YopO and F-actin at the site of YadA-*E. coli* attachment (yellow) and channel merge on the right shows actin polymerization at the site of YadA-*E. coli* attachment. Arrows indicate actin polymerization and YopO recruitment to YadA-*E. coli*-induced uptake structure. The bar represents 10 μm.

Confocal immunofluorescence data show that actin polymerization at the site of YadA-*E. coli* attachment is not inhibited in GFP-YopO expressing endothelial cells (figure 23). Extracellular structures of YadA-*E. coli* are visible in blue, F-actin is shown in red and GFP-YopO accumulation at the site of bacterial uptake is visible in green. Colocalization of GFP-YopO and F-actin at the site of YadA-*E. coli* internalization is visible in yellow (arrows in middle frame).

GFP-YopO is shown here to localize to YadA-induced uptake structures. *De novo* formation of F-actin cups during the phagocytic process is not inhibited by YopO.

3.3.5 YadA-mediated internalization is inhibited by YopO

To study the effects of YopO on YadA-mediated phagocytosis, GFP-YopO expressing HUVEC were inoculated with YadA-*E. coli* and after 90 minutes of invasion a double fluorescence staining method was used to identify uptake.

YadA-mediated internalization in the presence of GFP-YopO was reduced to approximately 50%. The GFP-YopO expressing cell in figure 24a shows attached YadA-*E. coli,* identified by red extracellular staining (arrows, bacteria appear orange due to overlay with green derived from GFP), with intracellular YadA-*E. coli*, identified by blue staining. In contrast to the GFP-YopO expressing cell, the neighboring untransfected control cell shows articulate internalization of YadA-*E. coli*, identified by blue staining (arrowheads).

Internalization data from three independent experiments were statistically evaluated and are shown in figure 24b. Expression of GFP-YopO caused inhibition of YadA-mediated phagocytosis. Compared to control cells GFP-YopO expressing cells showed significantly reduced internalization ($52 \pm 5\%$) pointing to an inhibitory effect of GFP-YopO. The absolute numbers for internalization after 90 minutes were $64 \pm 6\%$ for control cells and $33 \pm 5\%$ for GFP-YopO expressing cells (not shown).

FIGURE 24

a

b
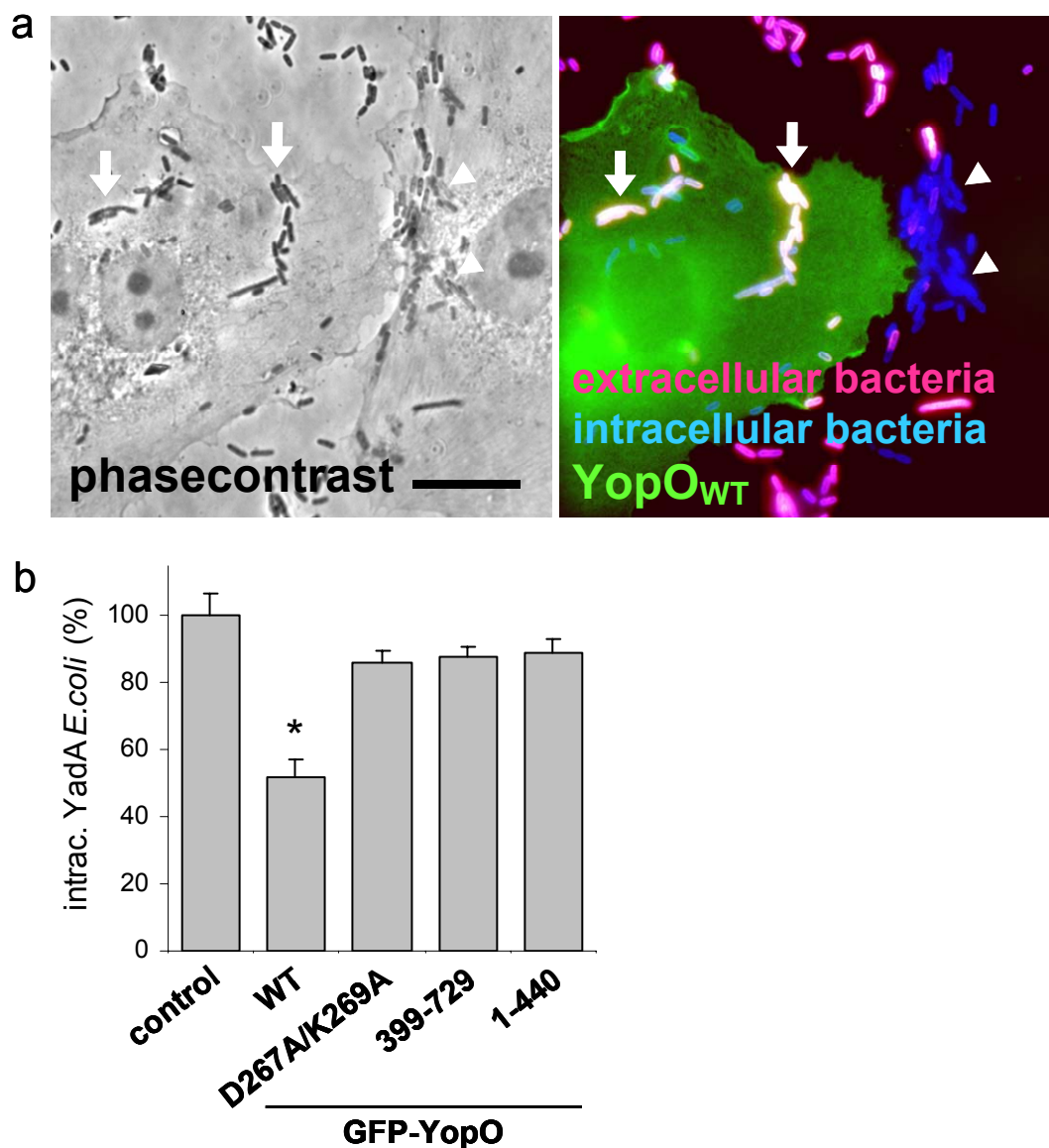
FIGURE 24. **YadA-mediated internalization is inhibited by YopO.**
a) Internalization viewed by phasecontrast (left) and fluorescence (right) images of a GFP-YopO expressing endothelial cell (HUVEC) and adjacent control cell. Inside/outside staining identifies attached external YadA-*E. coli* (red, arrows) and internalized YadA-*E. coli* (blue, arrowheads) for GFP-YopO expressing cell (green) and untransfected control cell. Intracellular bacteria appear in dark blue for untransfected control cell and light blue for GFP-YopO expressing cell. Extracellular coverslip-associated bacteria appear in red, while bacteria attached to the GFP-YopO expressing cell appear in bright red/orange (arrows). The bar represents 10 μm.
b) YadA-mediated internalization is inhibited by the kinase activity of YopO.
Quantification of YadA-*E. coli* (DH5A-pBR-A1) internalization in control cells, cells expressing GFP-YopO (WT), or the designated GFP-YopO mutant proteins. Uptake is shown as the percentage of total cell associated bacteria that is intracellular. Uptake was normalized to control cells that was set to 100%. Values are mean ± S.D. of 3 experiments with 90 cells evaluated per experiment. Asterisk indicates statistically significant difference.

3.3.6 Inhibition of YadA-mediated internalization depends on the kinase activity of YopO

To investigate to which YopO activity(ies) the inhibitory effect is connected to, YadA dependent internalization was evaluated in cells expressing GFP-YopO mutant proteins.

YadA-mediated uptake was significantly reduced ($52 \pm 5\%$ of control) only by the full length kinase-active GFP-YopOwt construct, while the kinase-dead GFP-YopOD267A/K269A ($86 \pm 3\%$ of control), the GDI-like domain containing GFP-YopO399-729 ($88 \pm 3\%$ of control) showed no significant inhibition of uptake (figure 24b) The cells expressing the GFP-YopO1-440 construct with low *in vitro* kinase activity (see above) showed an internalization capacity ($89 \pm 4\%$) as high as the control cells.

In summary only GFP-YopO with full kinase activity was able to significantly reduce YadA-mediated internalization.

3.3.7 RhoA inhibition by Edin-B does not inhibit YadA-mediated internalization

The bacterial exotoxin EDIN-B (epidermal cell differentiation inhibitor) from *Staphylococcus aureus* belongs to the group of C3 like exoenzymes that catalyze the covalent modification of Rho proteins. The specificity of the C3 exoenzymes for the ADP-ribosylation of RhoA, B, and C at asparagine residue 41 (Asn41) make these proteins useful biological tools to characterize cell biological functions of these GTPases. (Inoue, Sugai et al. 1991; Aktories, Wilde et al. 2004). Upon incubation with EDIN-B, ADP-ribosylation leads to specific inactivation of RhoA, B, C, E and Rnd3 and can be monitored in cells by depolymerization of stress fibers (Aktories, Wilde et al. 2004; Aktories and Barbieri 2005).

In mammalian cells Rho activates F-actin formation via the effector proteins mDia1 and Rho-kinase (ROCK) leading to actin filament elongation and stabilization/contraction of filamentous actin fibers. To confirm that YadA-mediated uptake is independent from the GTPase Rho, internalization of YadA-*E. coli* in endothelial cells (HUVEC) treated with the inhibitor EDIN-B was compared to internalization in untreated control cells. This should also confirm the results from above (see 3.3.6) where inactivation of Rho by transfection of the Rho GDI-like domain (YopO399-729) had no effect on YadA-mediated internalization.

FIGURE 25
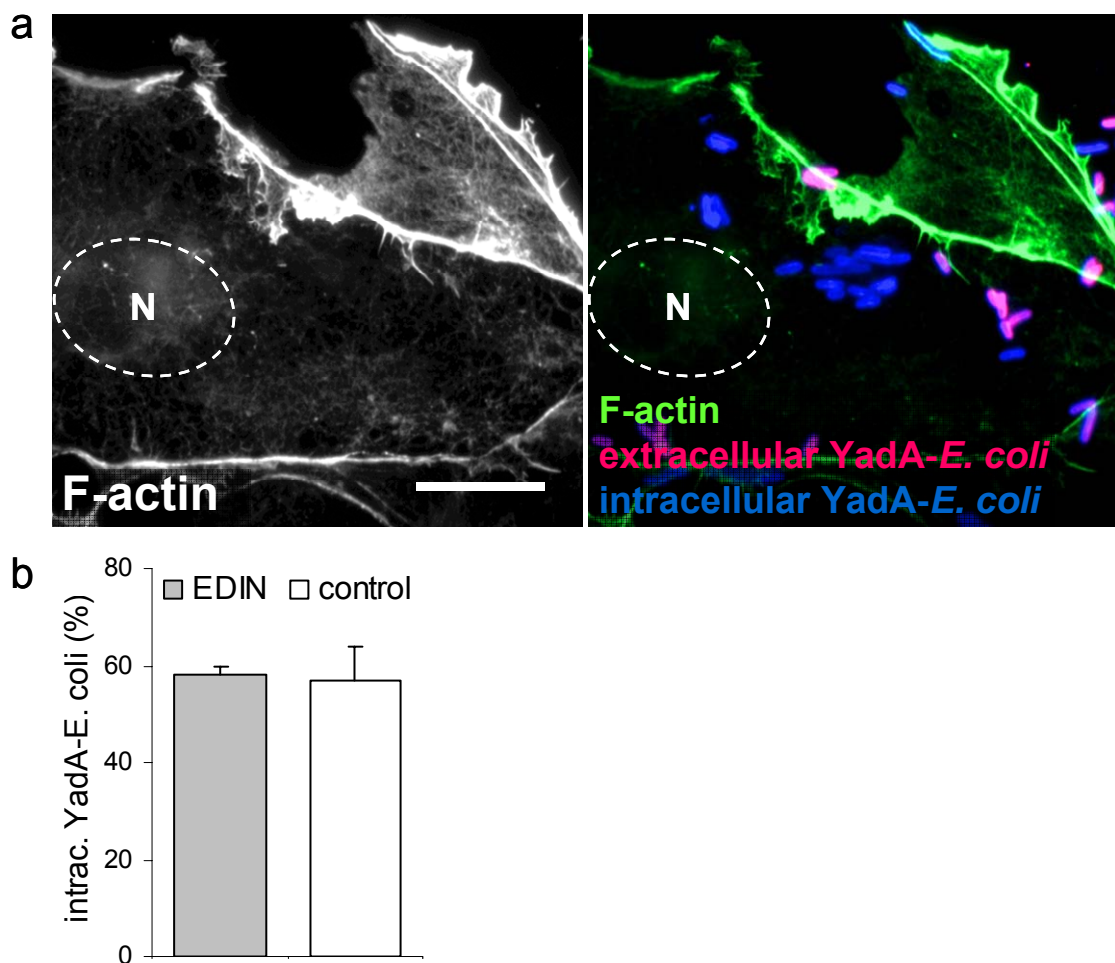
FIGURE 25. **RhoA inhibition by EDIN-B does not inhibit YadA-mediated internalization.**
a) Image series showing F-actin staining (left) and outside/inside staining (right) of endothelial cell (HUVEC) treated with EDIN-B. Green channel with FITC –phalloidin staining (left) showing F-actin disruption due to inactivation of RhoA by EDIN-B. Channel merge on the right shows cortical F-actin (green), attached extracellular YadA-*E. coli* (red) and internalized YadA-*E. coli* (blue). The bar represents 10 µm. N marks the nucleus.
b) Statistical evaluation of YadA-*E. coli* (DH5A-pBR-A1) internalization in untreated endothelial cells (HUVEC, control) and EDIN-B treated cells. Uptake is shown as the percentage of total cell associated bacteria that is intracellular Values are mean ± S.D. of 3 experiments with at least 90 cells evaluated per experiment.

Inhibition of RhoA in evaluated cells was visible through disruption of cytoplasmic F-actin structures. These cells were only visible by cortical F-actin staining (figure 25a, left frame). YadA-mediated internalization was not inhibited in HUVEC treated with EDIN-B. Uptake in cells with disrupted stress fibers is visualized by double fluorescence staining in figure 25a (right frame). Internalized YadA-*E. coli* (blue staining) can be distinguished from extracellular YadA-*E. coli* stained in red.

Statistical evaluation of internalization showed no inhibitory effect of EDIN-B treatment. Endothelial cells (HUVEC) that showed F-actin disruption due to the inhibition of RhoA

showed $58 \pm 2\%$ internalization compared to $57 \pm 7\%$ internalization in control cells (figure 25b).

These data show that inhibition of Rho by EDIN-B does not inhibit YadA-mediated internalization. GFP-YopO and EDIN-B inhibition of RhoA becomes apparent in the disruptive effect on F-actin. Because GFP-YopO is able to inhibit YadA-mediated uptake and EDIN-B is not, the target RhoA seems not to be crucial for the inhibitory effect of YopO on YadA-mediated phagocytosis.

D. DISCUSSION

Kinase activity of YopO

Bacterially produced YopO is not autophosphorylated and the role of auto-activation dependent on G-actin is unclear. One explanation for the exclusive activation only in the presence of G-actin is that *Yersinia* is protected from possible toxic effects of YopO. The absence of G-actin in the bacterial cytoplasm ensures activation of YopO only inside the mammalian host cell. A more complex explanation for the activation of YopO by G-actin takes into account the local subcellular G-actin concentration at the designated site of YopO action. Kinase activation might not only be regulated by an "all or none"-mechanism, but can be thought to be regulated at a higher degree depending on the local G-actin concentration. In this model YopO would sense G-actin concentration and fulfill its kinase function accordingly. Besides the cytoskeletal role of actin in cellular motility and phagocytosis, it has been identified as an important cofactor for RNA polymerases and additionally to regulate the localization and activity of transcriptional co-activators. The myocardin-related serum response factor (SRF) coactivator MAL associates with and is regulated by G-actin. Depending on the concentration of unpolymerized actin the coactivator MAL is targeted to the nucleus to act together with the transcription factor SRF to promote the transcription of growth-factor-regulated immediate-early genes (Miralles, Posern et al. 2003; Visa 2005). YopO has not been observed to target to the nucleus, but to the host cell membrane where it could phosphorylate target proteins dependent on the local G-actin concentration at sites important during *Yersinia* infection. An interesting site during *Yersinia* infection is the site of bacterial attachment where translocation of effector proteins via the injectisome occurs. Translocation of effector proteins from the bacterial cell through the host cell membrane is not accompanied by leakage of cytoplasmic proteins. The regulation of the injectisome-formed translocation pore was shown to be influenced by the injected effector YopE (Viboud and Bliska 2001). The GTPase-downregulating function of YopE is involved in preventing the cytotoxic pore-forming activity of the type III secretion system. The role for YopO in the regulation of this highly tuned system has not been examined. It could also be necessary and important for *Yersinia* to efficiently target a cellular substrate by a mechanism that involves dynamic regulation of YopO activity by G-actin.

Morphological effects of YopO

In this work the C-terminal GDI-like domain of YopO was shown to be responsible for F-actin disruption in host cells. F-actin disruption is independent of kinase activity and actin binding in YopO. A recent publication solved the crystal structure of a YpkA-Rac1 complex and finds that YpkA mimics host guanidine nucleotide dissociation inhibitors of Rho GTPases (Prehna, Ivanov et al. 2006). YpkA was shown *in vitro* to lock the small GTPases RhoA and Rac1 in the GDP bound, or physiologically "off", conformation and cell experiments show the disruptive role of the YpkA GDI-like domain. The data on YpkA support the results from YopO obtained in this study. Here it is additionally shown that the constitutive active RhoAV14 can rescue F-actin disruption caused by the GDI-like domain of YopO. In contrast to sequestration of endogenous RhoA, sequestration of RhoAV14 by YopO is not sufficient to block activation of effector proteins. This indicates that RhoA inactivation by YopO mechanistically is not achieved by displacement of RhoA from its site of action, but by (additional) inhibition of the GEF-induced activation of RhoA. Otherwise the interaction of RhoAV14 with effector proteins would also be blocked by displacement mediated by the Rho GDI-like domain of YopO. Although GDI can bind to the GDP- and GTP bound forms of Rho GTPases, it clearly prefers the GDP-bound form. This binding preference was shown for the interaction of YpkA with RhoA (Dukuzumuremyi, Rosqvist et al. 2000).

Rounding/arborization was shown here to be induced by the kinase activity of YopO, which is dependent on the presence of N- and C-terminal domains. Compared to the wild-type protein the kinase-dead point mutant YopOD267A/K269A caused significantly less rounding but similar F-actin disruption. N- and C-terminal truncations were unable to produce rounding at the level of wildtype YopO. The critical amino acids in YpkA responsible for GDI-like interaction with RhoA and Rac1 have been identified as Tyr591, Asn595 and Glu599 (Prehna, Ivanov et al. 2006). With this data a corresponding full length YopO mutant could be generated that will allow examination of YopO kinase activity without functional interference of the GDI-like domain. Isolated effects of the kinase activity on the actin cytoskeleton, cell morphology and cellular targets should be possible to examine with this mutant protein that shows intact three-dimensional protein structure.

Role of YopO in Fcγ-R- and CR-mediated phagocytosis

Transient expression of YopO in primary monocyte-derived macrophages is neither able to inhibit RhoA-dependent complement receptor-(CR)-mediated phagocytosis, nor Rac1 dependent Fcγ-receptor-mediated phagocytosis. Modulation of immune cell responses such as chemotaxis and phagocytosis were earlier shown to be influenced by other Yop effectors that target Rho GTPases (Cornelis and Wolf-Watz 1997; Aepfelbacher and Heesemann 2001; Juris, Shao et al. 2002). Inhibition of Rac and Rho by dominant negative GTPase mutants leads to reduced Fcγ-receptor and CR-receptor-mediated phagocytosis, respectively, in CHO cells (Caron and Hall 1998). Inhibition of Rho by YopO was evident in stress fiber disruption in endothelial cells, but did not result in significant Fcγ-R/CR3-mediated phagocytosis inhibition in primary macrophages. Potentially the mild Rho-inhibitory effect due to sequestration by a GDI-like activity does not suffice for blocking Rho activation in the context of phagocytosis. Comparing Fcγ-receptor and CR-mediated phagocytosis a slight inhibition of the Rho-dependent CR-mediated internalization by YopO could be observed, but during several independent experiments we did not find any statistically significant difference based on a 1% level of significance.

Formation of F-actin cups at the site of Fcγ-receptor-mediated phagocytosis was not disturbed upon expression of YopO in primary macrophages. In line with the results for the Fcγ-receptor-mediated uptake, this indicates that YopO does not sufficiently inactivate Rac during this specific phagocytosis mechanism.

Invasin-mediated internalization

Efficient invasin-mediated uptake was shown in non phagocytic cultured cell lines like HeLa (human epithelial), COS-1 (monkey kidney) and was also characterized in macrophages earlier (Isberg and Barnes 2001; Wiedemann, Linder et al. 2001). Endothelial cells used in this study (HUVEC and HBMEC) showed efficient bacterial internalization triggered by invasin. In macrophages inhibition of Rho, Rac or Cdc42 leads to reduced formation of Invasin-induced phagocytic cups indicating that the uptake mechanism might employ all of the three Rho GTPases (Wiedemann, Linder et al. 2001).

In contrast to the dominant negative GTPase mutant RacN17, YopO was neither able to inhibit Invasin-bead internalization, nor able to block Invasin-bead induced actin-cup formation in endothelial cells. Cells with apparent morphological signs of YopO activity showed effective Invasin-bead internalization. Obvious RhoA-dependent effects of YopO were visible in stress fiber disruption, but apparently YopO was unable to block Rho GTPase

activation upon stimulation by integrin-mediated signals. This points to incomplete blocking of Rho and Rac or an activity of YopO that goes beyond inhibition of Rho and Rac.

Invasin plays an important role in the initial step of infection when the enteropathogenic yersiniae are translocated through the M cells in the small intestine. Invasin that is repressed at host-temperature (37 °C) is thought to play a minor role in the later stages of infection. Therefore the inhibition of Invasin-mediated phagocytosis would not be the primary object in the survival strategy of enteropathogenic yersiniae.

YadA mediated internalization

In later stages of disease, when *Yersinia enterocolitica* persists in the hostile environment of lymphatic tissue, mouse experiments indicate that the adhesive surface protein YadA plays a crucial role (Kapperud, Namork et al. 1987; Pepe, Wachtel et al. 1995). In addition to conferring resistance to serum the YadA protein is also able to trigger phagocytosis. In HUVEC, this matrix-dependent internalization mediated by YadA was significantly slower than that triggered by invasin. The endothelial cell line HBMEC that was used to study Invasin-bead uptake showed attachment of YadA-*E. coli* but very low internalization for unidentified reasons (not shown). The low-invasion phenotype of *Y. enterocolitica* YadA was also reported for HEp-2 cells (Heise and Dersch 2006). In contrast, primary endothelial cells (HUVEC) showed efficient YadA-mediated internalization and were therefore used to study YadA-mediated uptake under the influence of heterologous expression of YopO. Internalization in HEp-2 cells, described for the *Yersinia pseudotuberculosis* YadA protein, is dependent on fibronectin, whereas *Yersinia enterocolitica* YadA–mediated uptake observed in this work occurred also in the absence of fibronectin. The *Y. pseudotuberculosis* YadA-uptake domain is not present in the YadA protein used in this study. Therefore an alternative matrix-dependent internalization mechanism can be inferred. Here, collagen as a matrix protein that is strongly bound by *Y. enterocolitica* YadA could serve as an alternative bridging molecule to target cellular integrin receptors. Detailed information on the ECM-binding sites of YadA is still missing. However, an approach that studied crystallographic data of the YadA-trimer structure showed that collagen binding of *Yersinia enterocolitica* YadA is very sensitive to conformational changes of 3D-trimer structure and that the collagen triple helix makes several surface contacts on two YadA-monomers within the head domain (Nummelin, Merckel et al. 2004). YadA-mediated internalization is little characterized in regard to the cellular receptors and their subsequent intracellular signaling. Whether the two *Yersinia* species only target different extracellular matrix proteins or also trigger different intracellular signaling events is

unknown. Proteins involved in YadA-induced signaling have only been roughly described for cytokine induction (Schmid, Grassl et al. 2004). Inhibitor studies showed that the signaling cascade induced by YadA or invasin that leads to IL-8 secretion, involves β1-integrins, Rho GTPases and MAP kinases (MEK1, JNK, p38). Studies of the intracellular signaling cascades specifically involved in matrix-dependent YadA-mediated uptake have not been performed.

Yersinia enterocolitica YadA-specific internalization is significantly reduced by 50% by YopO. Kinase-deficient YopO mutants that retained the ability to reduce Rho-dependent F-actin fibers lost their ability to interfere with YadA-mediated uptake. Specific inhibition of Rho by EDIN-B had no influence on YadA-mediated uptake. This points to an unidentified YopO kinase target that plays a role in this specific phagocytosis-mechanism. The Rho inactivating GDI-like domain does not seem to play a role in this specific inhibition, although a potential role for the GDI-like domain in targeting the YopO kinase to its unidentified substrate can not be ruled out. To answer the question of the role of the GDI-like domain in targeting the YopO kinase a contact-site mutant (Prehna, Ivanov et al. 2006) with retained kinase activity and membrane targeting will have to be established. The role of the N-terminal membrane localization domain in targeting the active kinase to its potential substrate will also have to be addressed.

The YopO kinase does not interfere with YadA-mediated uptake simply by inhibition of F-actin polymerization at the site of bacterial internalization. Formation of actin cups at the site of YadA-*E. coli* attachment was clearly detectable, although the dynamics of F-actin formation at the sites of bacterial internalization was not examined. Here YopO could play a role in disturbing the actin dynamics involved, thus leading to impairment of the matrix-dependent internalization process. The first recently identified YopO kinase target Otubain1 is unlikely to play a role in the inhibition of YadA-mediated internalization. Otubain1 is a cytoplasmic ubiquitin-specific cysteine protease that cleaves only isolated branched polyubiquitin chains *in vitro* and was characterized to regulate polyubiquitination and stability of GRAIL (gene related to anergy in lymphocytes), a RING-type E3 ligase that is involved in the regulation of immune responses during infection (Balakirev, Tcherniuk et al. 2003; Mueller 2004; Juris, Shah et al. 2006). This newly identified kinase target that regulates T cell growth factor production and proliferation implicates a function of YopO in immunomodulation. The role of the actin-binding activity and the Rho GDI-like domain of YopO in regulating Otubain1 phosphorylation has not been investigated. How these activities of YopO contribute to phosphorylation of Otubain1 and further how Otubain1 can influence *Yersinia* infection has not been explored.

The property of YopO to localize to the cytoplasmic membrane, the Rho GDI-like activity and the ability of YopO to interfere with YadA-mediated uptake give reason to speculate for at least one additional target of the YopO kinase. It would be reasonable to suspect a kinase target that has a function in the field of phosphorylation-state dependent outside-in signal transduction, especially in the regulation of (Rho-) GTPase and actin-dependent signaling processes. A large part of the cellular effects of YopO that have been observed are mainly induced by the Rho GDI-like domain of YopO. Targets of the only presently known kinase that is regulated by actin are starting to get discovered and YopO could serve as model for yet unidentified actin-regulated cellular kinases.

Because *Yersinia* kinase activity of YopO is relevant *in vivo* considering the loss in mouse virulence in YopO kinase-deficient mutants (Galyov, Hakansson et al. 1993; Wiley, Nordfeldth et al. 2006), studies investigating the phosphorylation of cellular substrates by the serine/threonine kinase YopO in the context of Rho- and actin-binding will have to bring answers to the question of how this essential effector protein contributes to the complex immunomodulatory manipulation of host cells by *Yersinia*.

E. MATERIALS AND METHODS

1. EQUIPMENT AND MATERIAL

1.1 Equipment

1.1.1 Laboratory Equipment

Table E3. **Laboratory Equipment**

Laboratory Equipment	
Casette for film exposure	Rego
Centrifuge	Sigma, Deisenhofen 1K1S, Table-centrifuge 3K30 with Rotor Nos. 12156 and 19776; Eppendorf table centrifuge 5417 C/ 5417 R Biofuge A, Heraeus Sepatech, Osterode, Germany
Electrophoresis/Agarose Gel chamber	Agagel, Biometra, Goettingen, Germany
Electrophoresis/SDS-PAGE	Bio-Rad, München Mini-Protean -II Cell and Western Blot Apparatus Mini-Protean 3, Bio-Rad Laboratories Hoefer SE 400, Amersham Biosciences
French Press	French Pressure Cell 40K SLM Aminco
Gel Dryer	BioRad, Munich, Germany
Glass coverlips, round (12 mm diameter)	Hartenstein GmbH, Wuerzburg, Germany
Incubator	Heraeus, BBD 6220, Hanau Typ B20
Incubator (shaking)	Thermomixer compact, Eppendorf, Hamburg, Deutschland
Microinjection and Femtotips	Transjector 5246 und Micromanipulator 5171, Eppendorf, Hamburg, Deutschland
Microscope (binocular)	Carl Zeiss, Axiovert 25
Microscope slides	Marienfeld GmbH, Lauda-Königshofen, Germany
Microwave	AEG
PCR-Cycler	PE Applied Biosystems, Weiterstadt Gene Amp 2400
pH Meter	Mettler, Toledo 320 pH Meter
Phosphoimager FLA 3000	Fujifilm, Tokyo, Japan
Photometer	Pharmacia Biotech, Ultraspec 3000
Pipettes	Eppendorf, Hamburg Research P10-P1000 Pipetman (10, 20, 200 und 1000 µl), Gilson International B.V., DenHaag, The Netherlands
Power supply	Bio-Rad, Power Pac 200
Processor for X-ray film development	Agfa Curix 60
Refrigerator	Liebherr, profi line
Scale	Sartorius, Göttingen Model R 160P and Pt 1200
Scanner ScanJet 4c/ScanJet 5470c	Hewlett Packard

Thermocycler PCR	Perkin Elmer, Gene Amp PCR System 2400
Transilluminator	Heralab, Wiesloch, UVT-20M/W
Tweezers	NeoLab Heidelberg, Germany
Ultracentrifuge	Beckmann, Optima T2 Ultracentrifuge
UV-Transilluminator	Herolab, E.A.S.Y., UVT-20M/W
Vacuum blot	Pharmacia,-LKB, Uppsala, LKB 2016 Vacu Gene^R-Chamber
Video-equipment	Sigma, Deisenhofen, EASY (Enhanced Analysis System)
Vortexer	ProScientific, Oxford, USA
Water bath	GFL Typ 1013; GFL, Burgwedel, Germany

1.1.2 Microscopical Equipment

In order to observe specimen by fluorescence-, brightfield- or phasecontrast-microscopy, two microscopic settings were used. For evaluation of morphological effects and phagocytosis a non-confocal setup, for evaluation of subcellular localization a confocal setup was employed.

Non-confocal setups for fluorescence and phasecontrast microscopy:

Leica DM IRE2 microscope equipped with 63x (oil, NA 1.4, phasecontrast) and 100x (oil, NA 1.4, phasecontrast) objectives with mercury lamp and filters for blue (365/460nm), red (570/603nm) and green (488/505nm) and a SPOT SLIDER camera system (Diagnostic Instruments, Sterling Heights, USA).

Zeiss Axioplan microscope equipped with 40x (oil, NA 1.3), 63x (oil, NA 1.4) and 100x (oil, NA 1.4) objectives with mercury lamp and filters for blue (365/460nm), red (570/603nm) and green (488/505nm) and a SPOT 1.4MP camera system (Diagnostic Instruments, Sterling Heights, USA).

Confocal setup:

Leica DMIRE2 automatic microscope equipped with 63x (water, NA1.3), 63x (oil, NA 1.4) objectives and a Leica TSC SP2 AOBS filter free confocal point scanner with Ar (458nm, 488nm, 496nm, 514nm) and HeNe (633 nm) laser lines. The confocal setup was used with green (488/505nm), red (570/603nm) and far red (633/680nm) staining.

Images were further viewed and processed using ImageJ software (Research Services Branch, NIMH), Adobe Photoshop, Volocity software (Improvision, Coventry, England) and Leica LCS Lite software (Leica Microsystems, Wetzlar, Germany).

1.2 Chemicals and Enzymes

1.2.1 Chemicals and antibiotic solutions

All chemicals and antibiotics were supplied by Amersham/GE Healthcare (Munich, Germany), Biozym (Oldendorf, Germany), Dianova (Hamburg, Germany), Fermentas (St. Leon-Rot, Germany), Invitrogen (Karslruhe, Germany), Merck (Darmstadt, Germany), Roche (Mannheim, Germany) and Sigma-Aldrich (Munich, Germany).

Table E4. **Antibiotic solutions**

antibiotic solutions

	abbreviation	dissolved in	final concentration µg/ml
Ampicillin	Amp	H2Odd	100 (*E. coli*), 400 (*Yersinia*)
Kanamycin	Kan	H2Odd	100
Nalidixic acid	Nal	0.5 N NaOH	35
Chloramphenicol	Cm	70 % EtOH	20
Streptomycin	Sm	H2Odd	100
Tetracycline	Tet	70 % EtOH	15
Gentamicin	Gen	H2Odd	50

1.2.2 Kits and Enzymes

Table E5. **Kits and Enzymes**

Kits

name	supplier
ECL Western blotting detection reagents	Amersham Biosciences, Freiburg, Germany
Plamid Miniprep Kit	Qiagen GmbH, Hilden, Germany
EndoFree Plasmid Maxi Kit	Qiagen GmbH, Hilden, Germany
QIAquick Gel Extraction Kit	Qiagen GmbH, Hilden, Germany
QIAquick PCR Purification Kit	Qiagen GmbH, Hilden, Germany
Quiaprep spin Miniprep Kit	Qiagen GmbH, Hilden, Germany
QuickChangeII Site Directed Mutagenesis Kit	Stratagene, Amsterdam, The Netherlands
HUVEC Nucleofection Kit	Amaxa, Cologne, Germany
Nuceofection solution nr.6857 for primary macrophages	Amaxa, Cologne, Germany
Complete Protease Inhibitor Cocktail Tablets	Roche, Mannheim, Germany
Alligator Quick Ligation Kit	Genaxxon GmbH, Biberach, Germany

Enzymes

name	supplier
Age I	New England Biolabs/Fermentas
*Bam*HI	New England Biolabs
Bgl II	New England Biolabs/Fermentas
Eco RI	New England Biolabs/Fermentas
Hind III	New England Biolabs
Sal I	New England Biolabs
Xho I	New England Biolabs/Fermentas
DeepVent DNA-Polymerase	New England Biolabs
T4 DNA-Ligase	Roche Diagnostics
TripleMaster PCR System	Eppendorf
AmpliTaq	Applied Biosystems
AmpliTaq Gold	Applied Biosystems

1.3 Bacterial strains and plasmids

1.3.1 Bacterial strains

Table E6. **Bacterial strains**

strain	genotype/description	reference
E. coli		
DH5A	F- endA1 glnV44 thi-1 recA1 relA1 gyrA96 deoR nupG Φ80dlacZΔM15 Δ(lacZYA-argF)U169, hsdR17(rK- mK+), λ–	Hanahan 1985
BL21	F– ompT gal dcm lon hsdSB(rB- mB-) λ	Studier & Moffat, 1986
BL21-Inv397	pGEX-4T-3-pINV397; protein expression/purification	Wiedemann et al. 2001
M15-EDIN-B	His-tagged EDIN-B protein expression/purification	Motoyuki Sugai
DH5A-pBR	DH5A with pB8-5 low-copy-number vector coding for VirF (Tet resistance)	Roggenkamp et al. (1995)
YadA-*E.coli*/ DH5A-pBR-A1	YadA-*E.coli*; DH5A-pBR with pUC-A1 (YadA from *Y. enterocolitica* O:8 full length, GenBank accession no. X13881, Amp resistance) pB8-5 low-copy-number vector coding for VirF (Tet resistance)	Roggenkamp et al. (1995)
HB101/ HB101inv-	F- mcrB mrr hsdS20(rB- mB-) recA13 leuB6 ara-14 proA2 lacY1 galK2 xyl-5 mtl-1 rpsL20(SmR) glnV44 λ-	Bolivar & Backman, 1979, Schulte, Zumbihl, et al. (1998).
Invasin-*E.coli*/ HB101inv+	Invasin-*E.coli*; HB101 carrying pInv1914; constitutively expressing invasin on bacterial surface	Schulte, Zumbihl, et al. (1998).
Yersinia enterocolitica		
WA-P	WA-314 O:8 with pYVO8 virulence plasmid, biogroup 1B, intrinsic Nalidixin resistance	Heesemann 1987
WA-C	plasmid cured WA-314	Heesemann 1987

1.3.2 Plasmids

Table E7a. **Plasmids for bacterial and mammalian expression**

plasmid	description	reference
bacterial expression		
pUC-A-1	pUC13 with insertion of 5 kb EcoRI-HindIII fragment from pYVO8, including the yadA gene (Amp resistance)	Roggenkamp et al. (1995)
pB8-5	vector with 5-kb BamHI fragment of pYVO8 encoding VirF in the low-copy-number vector pRK290B (Tet resistance)	Roggenkamp et al. (1996)
GST-Inv397	pGEX-4T-3-pINV397, GST-Invasin procaryotic protein expression for *in vitro* use	Wiedemann et al. 2001
pInv1914	invasin coding sequence under control of lpp-promotor of pNIV136 expression vector; constitutive invasin expression in bacterial outer membrane (Amp resistance)	Schulte, Zumbihl, et al. (1998). "Wortmannin…
pGEx-4T-1	prokaryotic protein expression, empty vector	Amersham
pGex4T-2	prokaryotic protein expression, empty vector	Amersham
mammalian expression		
pEGFP-N-1	mammalian expression vector; enhanced green fluorescent protein; MCS N-terminal of GFP	BD Clontech
pEGFP-C1	mammalian expression vector; enhanced green fluorescent protein; MCS C-terminal of GFP	BD Clontech
pmRFP-N1	mammalian expression vector; monomeric red fluorescent protein; MCS N-terminal of mRFP	This study
pCDNA3.1	mammalian expression vector	Invitrogen
GFP-RhoAV14	mammalian expression of constitutive active RhoA(V14/N25)	B. Schroder
GFP-RacN17	mammalian expression of dominant negative RacN17	B. Schroder

Plasmids for bacterial expression of YopO

The GST gene fusion system (Amersham/GE Healthcare, Munich, Germany) is an integrated system for the expression, purification and detection of fusion proteins produced in *E. coli*. The pGEX plasmids supplied with the system are designed for inducible, high-level intracellular expression of genes or gene fragments as fusions with *Schistosoma japonicum* GST (Glutation-S-Transferase). GST occurs naturally as a 26 kDa protein that can be expressed in *E. coli* with full enzymatic activity. Fusion proteins are easily purified from bacterial lysates by affinity chromatography using Glutathione Sepharose 4B (Amersham Biosciences/GE Healthcare, Munich, Germany). In this study N-terminally GST-tagged YopO fusions were constructed and purified.

The pGex-4T vectors encode the recognition sequence for site-specific cleavage by thrombin between the GST domain and the multiple cloning site. For biochemical analysis mutant GST-YopO fusion proteins were constructed: This includes N-and C-terminal deletion mutants and amino acid substitution mutants (see mutagenesis). The FLAG-YopO fusion proteins were a generous gift from Juris and Dixon (University of Michigan, USA). YopO

was amplified from pYV (from the WA-P strain) and sequence identity to the published
sequence on pYV8081 (accession number NP_863565) was verified.

Table E7b. **Plasmids for bacterial expression**

plasmid	description	reference
FLAG-YopO-fusions		
YopO1-729	pGEX-6p-2	Juris and Dixon (2000)
YopO1-729K269A	pGEX-6p-2	Juris and Dixon (2000)
GST-YopO-fusions		
YopOwt	pGex-4T-1 with wild type YopO1-729 (full length)	
N-terminal truncations		
YopO89-729	pGex-4T-1 with YopO89-729, (soluble protein)	This study
YopO151-729	pGex-4T-1 with Yop151-729	This study
YopO399-729	pGex-4T-1 with Yop399-729	This study
YopO441-729	pGex-4T-1 with Yop441-729	This study
YopO541-729	pGex-4T-1 with Yop541-729	This study
YopO700-729	pGex-4T-1 with Yop700-729	This study
C-terminal truncations		
YopO89-398	pGex-4T-1 with Yop89-398	This study
YopO89-440	pGex-4T-1 with Yop89-440	This study
YopO89-710	pGex-4T-1 with Yop89-710	This study
YopO151-440	pGex-4T-1 with Yop151-440	This study
point mutants YopO89-729		
D267A/K269A	pGex-4T-1 with Yop89-729D267A/K269A	This study
S95A	pGex-4T-1 with Yop89-729S95A	This study
S102A	pGex-4T-1 with Yop89-729S102	This study
T89A/S95A	pGex-4T-1 with Yop89-729T89A/S95A	This study
S90A/S95A	pGex-4T-1 with Yop89-729S90A/S95A	This study
D267A/K269A/S90A/S95A	pGex-4T-1 with Yop89-729D267A/K269A/S90A/S95A	This study

Plasmids for mammalian expression of YopO

Expression of GFP-YopO fusion proteins was accomplished by insertion of the respective
YopO fragments into vectors suitable for mammalian expression. FLAG-tagged YopO was
expressed from pCDNA3.1 carrying the *yopO* gene (generous gift from Juris and Dixon,
University of Michigan, USA) and GFP-tagged YopO was expressed from eukaryotic
expression vectors pEGFP-C1 and pEGFP-N1 (BD Clontech, Mountain View, USA) carrying
the *yopO* gene.

pEGFP carries a red-shifted variant of wild-type green fluorescent protein (GFP) which has been optimized for brighter fluorescence and higher expression in mammalian cells (excitation maximum = 488 nm; emission maximum = 507 nm).The multiple cloning site (MCS) in pEGFP-C1 is between the EGFP coding sequences and the SV40 poly A. Genes cloned into the MCS will be expressed as fusions to the EGFP C-terminus. Genes cloned into the MCS of pEGFP-N1 will be expressed as fusions to the N-terminus of EGFP.

Table E7c. **Plasmids for mammalian expression**

plasmid	description	reference
pCDNA3.1-FLAG-YopOK269A	FLAG-YopO8-729K269A	Juris and Dixon (2000)
mRFP-YopO	C-terminal fusion YopO-mRFP	This study
GFP-YopO fusions		
YopOwt (N1)	N-terminal fusion YopO1-729-EGFP	This study
YopOwt (C1)	C-terminal fusion EGFP-YopO1-729	This study
N-terminal truncations		
YopO89-729	EGFP-YopO89-729 in pEGFP-C1	This study
YopO399-729	EGFP-YopO399-729 in pEGFP-C1	This study
C-terminal truncations		
YopO1-710	EGFP-YopO1-710 in pEGFP-C1	This study
YopO1-440	EGFP-YopO1-440 in pEGFP-C1	This study
YopO89-440	EGFP-YopO89-440 in pEGFP-C1	This study
point mutants YopO1-729		
D267A/K269A	EGFP-YopO1-729D267A/K269A in pEGFP-C1	This study

1.3.3 Invasin surface-expression and adhesion of Invasin-*E. coli* (HB101inv+)

Heterologous expression of the *inv* gene of *Y. enterocolitica* O:9 is achieved in Invasin-*E. coli* (HB101inv+). The noninvasive *E. coli* HB101 (HB101inv-) strain was engineered to express *Y. enterocolitica* invasin on its surface as described by Schulte et al. (1998). Invasin surface expression in the non-invasive *E. coli* HB101 leads to specific interaction of this strain with eukaryotic cell receptors (Schulte and Autenrieth 1998; Schulte, Zumbihl et al. 1998; Grassl, Bohn et al. 2003).

For adhesion and uptake experiments, overnight cultures were diluted 1:20, bacteria were grown for 3 hours in LB at 37 °C, were collected by centrifugation and washed twice in sterile cold phosphate-buffered saline (PBS) pH 7.4. After measurement of the OD, appropriate dilutions of the bacteria in PBS were performed. Bacteria were added to the cells at a ratio of bacteria/cell = 20-60/1.

Expression of Invasin was controlled by SDS/PAGE – Western Blot in bacterial lysates and by fluorescence staining of the bacterial surface. For detection of invasin the primary α-invasin antibody (rabbit IgG) was used.

Invasin expression in HB101inv+ is illustrated in figure E1a. Immunofluorescence labeling of invasin shows expression on the bacterial surface.

FIGURE E1a.
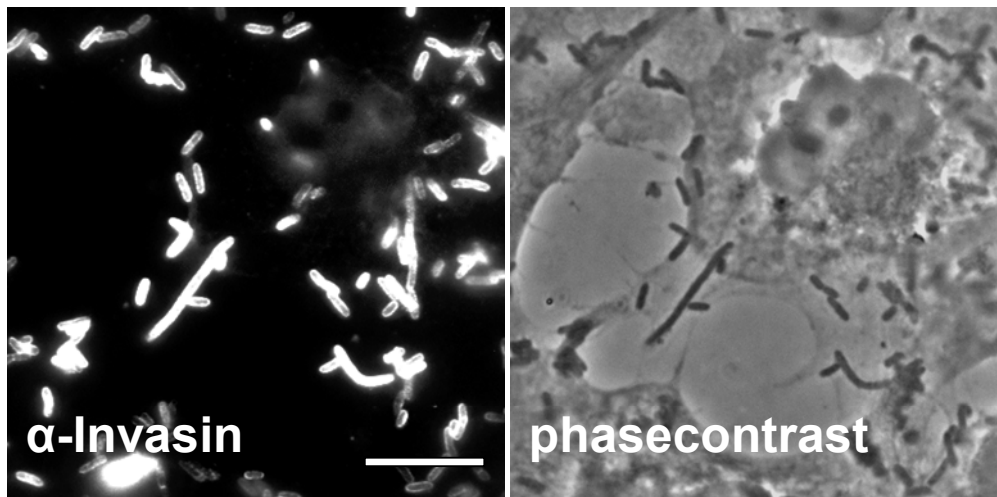
FIGURE E1a. **Invasin surface expression in Invasin-*E. coli***

Invasin-*E. coli* (HB101inv+) attached to endothelial cells (HBMEC) visualized by immunofluorescence staining (left) with anti-Invasin antibody. Phasecontrast (right) shows endothelial cells and attached Invasin-*E. coli* (HB101inv+). The bar represents 10 μm.
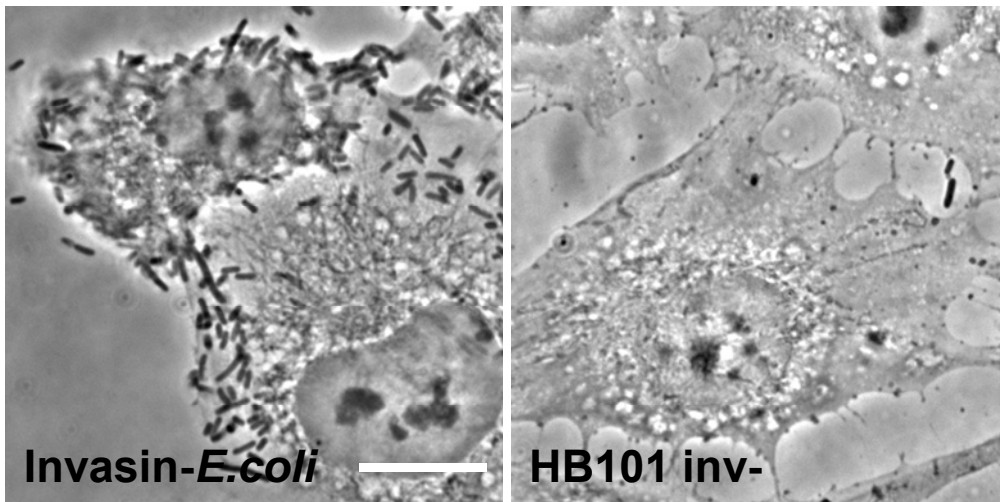
FIGURE E1b.

FIGURE E1b. **Adhesion of Invasin-*E. coli* and control strain HB101inv-**
Invasin-*E. coli* (HB101inv+) and control strain (HB101inv-) were attached to endothelial cells. After washing and fixation adhesion on endothelial cell surface was visualized by phasecontast: For Invasin-*E.coli* (left) many adhered bacteria can be seen. The parental control strain HB101inv- (right) shows no adhesion to cell surface. The bar represents 10 μm.

Attachment of HB101inv+ and the invasin-negative control strain (HB101inv-) is illustrated in figure E1b. The parental strain HB101inv- shows no adhesion in contrast to Invasin-*E. coli* (HB101inv+).

1.3.4 YadA surface-expression and adhesion of YadA-*E. coli* (DH5A-pBR-A1)

The *E. coli* DH5A strain expressing YadA from *Yersinia enterocolitica* O8 (GenBank accession no. X13881) was engineered and described in detail by Roggenkamp et al. (1996). In summary, the non-adhesive *E. coli* DH5A was engineered to incorporate YadA in the outer membrane by introducing a plasmid coding for YadA (pUC-A1) and a low-copy-number vector (pB8-5) coding for the YadA transcriptional activator VirF.

The production of YadA in YadA-*E. coli* (DH5A-pBR-A1) was verified by SDS/PAGE – Western Blot and by immunofluorescence staining. For detection of YadA the primary α-YadA antibody 9H11 was used.

FIGURE E2
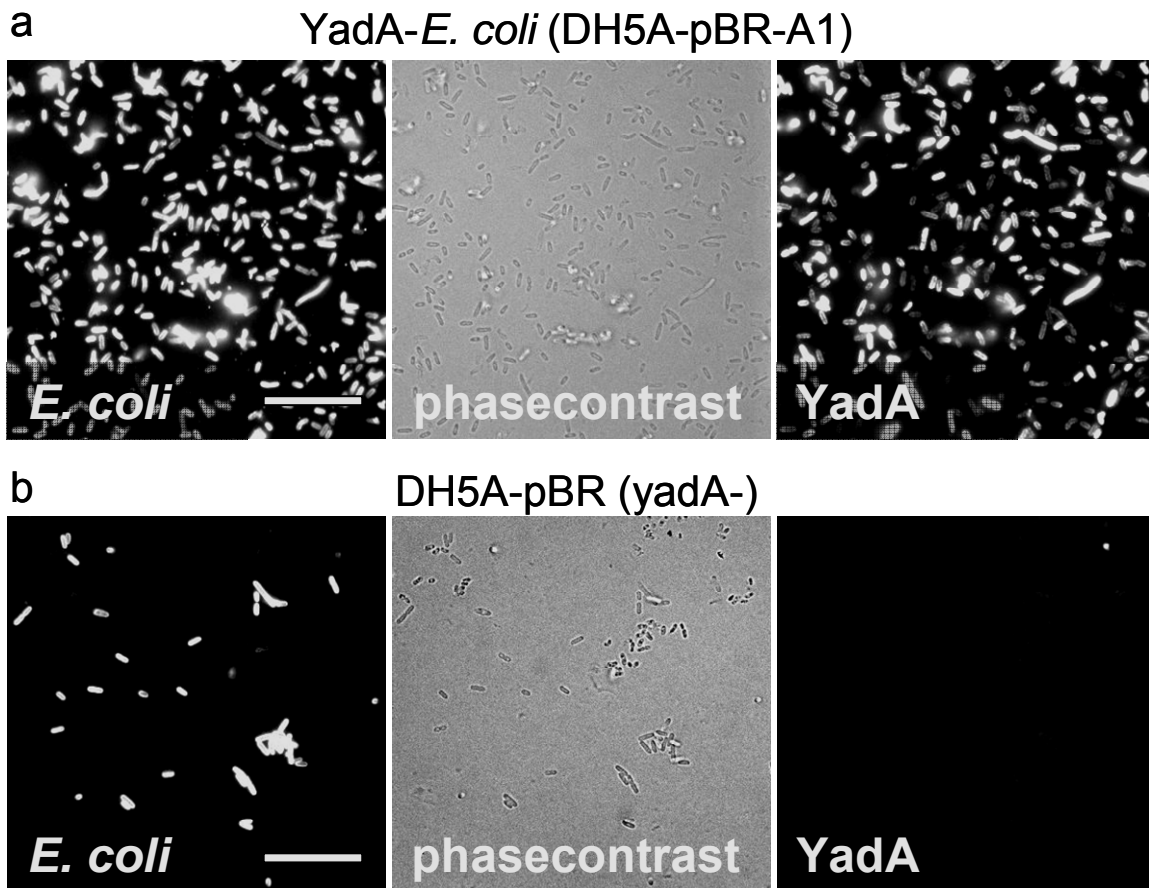
FIGURE E2. **YadA surface expression and adhesion of YadA-*E. coli* and control strain DH5A-pBR.**
a) YadA-*E. coli* (DH5A-pBR-A1) were attached to coverslips and stained with anti-*E. coli* antibody (left) and anti-YadA antibody (right). Phasecontrast image (middle) shows attached bacteria.
b) YadA-negative parental control strain (DH5A-pBR) was attached to coverslips and stained with anti-*E. coli* antibody (left) and anti-YadA antibody (right). Phasecontrast image (middle) shows low attachment of bacteria. The control strain DH5A-pBR is not detected by YadA staining (right). The bar represents 10 μm.

Immunofluorescent staining shows expression of YadA on the surface of YadA-*E. coli* (DH5A-pBR-A1, figure E2a) and specificity of the YadA antibody for the YadA epitope. The YadA-negative parental strain (DH5A-pBR) shows no detectable expression of YadA (figure E2b).

1.3.5 Antibodies for Western and Immunofluorescence

Table E8. **Antibodies**

primary antibodies

anti-	species	supplier
actin	MAB1501; anti-aktin mouse	Chemicon/Millipore
SRBC	rabbit IgG	ICN Pharmaceuticals
		WAK-Chemie Medical
SRBC	rabbit IgM	GmbH
Invasin	rabbit IgG (1:500)	Schulte et al. (2000)
YadA	mouse IgG (1:200); 9H11 (aa29-81 YadA)	Roggenkamp et al. (1995)
GST	rabbit IgG	Molecular Probes
YopO	rabbit polyclonal	Barz et al. (2000)
E. coli	rabbit IgG	Biodesign Int. Maine, USA

secondary antibodies

anti-		
rabbit	AlexaFluor® 488 IgG (H+L) goat (495/519nm)	Molecular Probes
rabbit	AlexaFluor® 568 IgG (H+L) goat (578/603nm)	Molecular Probes
rabbit	MarinaBlue® 365 IgG (H+L) goat (365/460nm)	Molecular Probes
rabbit	Cy5 IgG (H+L) goat (650/670nm)	Invitrogen
rabbit	IgG horseradish peroxidase goat	Amersham-Biosciences
mouse	AlexaFluor® 488 IgG (H+L) goat (495/519nm)	Molecular Probes
mouse	AlexaFluor® 568 IgG (H+L) goat (578/603nm)	Molecular Probes
mouse	MarinaBlue® 365 IgG (H+L) goat (365/460nm)	Molecular Probes
mouse	IgG horseradish peroxidase goat	Amersham-Biosciences
mouse	Cy5 IgG (H+L) goat (650/670nm)	Invitrogen
rat	AlexaFluor® 488 IgG (H+L) goat (495/519nm)	Molecular Probes
rat	AlexaFluor® 568 IgG (H+L) goat (578/603nm)	Molecular Probes

2. MOLECULAR BIOLOGY METHODS

2.1 Digestion of DNA with Restriction Enzymes

Restriction enzymes specifically bind to mainly palindromic recognition sites within a DNA molecule and cut it by hydrolyzing two phosphodiester bonds. Depending on the restriction enzyme "blunt" (no 5´or 3´ overhang) or "sticky" (5´and 3´overhangs) ends will be generated. The restriction enzymes were purchased together with their corresponding 5x or 10x buffers from NEB (New England Biolabs GmbH, Frankfurt, Germany), Invitrogen (Invitrogen GmbH, Karlsruhe, Germany) or Fermentas (Fermentas GmbH, St. Leon-Rot, Germany). Restriction enzyme digests were performed at temperatures recommended by the manufacturer (mostly 37 °C) in a thermo block or an incubator for 90 to 120 min. Usually 5 units of enzyme were used to cut one microgram of DNA. The digestion was performed in the presence of an appropriate 10x buffer, BSA (10 mg/ml) and H2Odd, following the manufacturer's directions. For double digestions the recommended buffers were used.

2.2 Ligation of DNA fragments

In order to ligate a vector DNA with the desired insert DNA, both cut with the same or compatible set of restriction enzymes, T4-DNA-ligase which catalyzes the formation of a phosphodiester bond between the 3'-OH and 5'-phosphate ends was applied.
Ligation reaction:

Vector DNA	10 - 100 ng
Insert DNA	3 - 10x the molar amount of vector DNA
5x ligase buffer	4 µl
T4-DNA-ligase (1 unit/µl)	1 µl
ad 10-20 µl with H2Odd	

The ligation reaction was prepared in 1.5 ml reaction tubes and incubated overnight at 16 °C.

Ligation using Alligator Ligation Kit

For fast ligation of DNA-fragments the Alligator Ligation Kit was used (Genaxxon Bioscience GmbH, Biberach, Germany). Following the manufacturer's instructions, vector and insert DNA was mixed with the two solutions provided and after 30 min of ligation the mix was added to competent cells for transformation.

2.3 Oligonucleotides/Primer

Table E9. **Oligonucleotides/Primer for cloning, sequencing and mutagenesis**

cloning into pGex4T-1/2

name	YopO site	primer sequence
YopO1-440	aa1	5´- [GATCTGAATTCATGAAAATCATGGG]-3´ (sense oligonucleotide)
YopO 1-710	aa8	5´- [ACAAGGACGACGGAATTCAGTCACCTTCG]-3´ (sense oligonucleotide)
YopO 89-729	aa89	5´-[CAGAAAACTGAATTCACTTCGCAGGAGCTAAGGTCTGATATCCCC] - 3´ (sense oligonucleotide)
YopO 89-440	aa89	5´- [GCCCAGGAATTCACTTCGCAGG]-3´ (sense oligonucleotide)
YopO 151-729	aa151	5´- [ATTAGTATAGAATTCACTAAGGATAAGCAGCGG TTGG] -3´ (sense oligonucleotide)
YopO 399-729	aa399	5´- [ACCTGATTCCGAATTCGCCAGACTCCACG] -3´ (sense oligonucleotide)
YopO 441-729	aa441	5´- [GATAACAGAATTCAAGCTTCGGGAGCTC] -3´ (sense oligonucleotide)
YopO 541-729	aa541	5´- [GAA CCT GAA TTC CAG AGG ATC CAG] -3´ (sense oligonucleotide)
YopO 89-398	aa398	5´- [TCGTGCTCGAGTCATTCGTTGGAATCAGG] -3´ (antisense oligonucleotide)
YopO 1-440	aa440	5´- [TCCCGCTCGAGTCACTTGGGTGTTATC]-3´ (antisense oligonucleotide)
YopO 1-710	aa710	5´- [TGGTTGTCAGCTCGAGTCACTTTTCTCTCTGTTCAACCA] -3´ (antisense oligonucleotide)
YopO 441-729	aa729	5´- [CTGCACTCGAGTCACATCCATTCCCG]-3´ (antisense oligonucleotide)

cloning into pEGFP-C1

name	YopO site	primer sequence
YO-C1XhoF	aa1	5´- AT GCT CGA GGC ATG AAA ATC ATG GGA –3´ (sense oligonucleotide)
N88YO-C1XhoF	aa89	5´- GCC CCT CGA GCT ACT TCG CAG –3´ (sense oligonucleotide)
N150YO-C1XhoF	aa151	5´- AGT ACT CGA GAA ACT AAG GAT AAG CAG CGG-3´ (sense oligonucleotide)
N398YO-C1XhoF	aa399	5´- AGA CCT GAT TCT CGA GAA GCC AGA CTC -3´ (sense oligonucleotide)
d440YO-C1EcoR	aa440	5´- GAG CTC GAA TTC CTA CTT GGG TGT TAT CCG –3´ (antisense oligonucleotide)
d710YO-C1EcoR	aa710	5´- TGT CAG GAA TTC TCA CTT TTC TCT CTG -3´ (antisense oligonucleotide)
YO-C1EcoRs	aa729	5´- GGC GAA TTC TCA CAT CCA TTC CCG CT –3´ (antisense oligonucleotide)

cloning into pEGFP-N1

name	YopO site	primer sequence
YO-N1XhoF	aa1	5´- GAG CTC GAG ATG AAA ATC ATG GGA ACT –3´ (sense oligonucleotide)
YO-N1EcoR	aa729	5´- G CCG AAT TCG CCA CAT CCA TTC CCG CT –3´ (antisense oligonucleotide)

Sequencing primer

name	annealing site	primer sequence
YopO internal sequencing primer		
YopO-P1	YopO aa186	5`- AAA CAT CCT AAT CTT GCC –3´ (sense oligonucleotide)
YopO-P2	YopO aa367	5´- ATC GAC CTG GTA TAG CTG G –3´ (sense oligonucleotide)
pGex vector sequencing primer		
GEX-F (GEX5)		5´- CTTTGCAGGGCTGGCAAG -3´ (sense oligonucleotide)
GEX-R(GEX3)		5´- GAGCTGCATGTGTCAGAGG -3´ (antisense oligonucleotide)
pEGFP-C1 vector sequencing primer		
EGFP-C1-F		5´- GAAGCGCGATCACATGGTC -3´ (sense oligonucleotide)
EGFP-C1-R		5´- AACCATTATAAGCTGCAATAAAC -3´ (antisense oligonucleotide)
pEGFP-N1 vector sequencing primer		
EGFP-N1-F		5´- GAGGTCTATATAAGCAGAGC -3´ (sense oligonucleotide)
EGFP-N1-R		5´- ACTTGTGGCCGTTTACGTC -3´ (antisense oligonucleotide)

Mutagenesis primer

name	mutation	primer sequence
D267A_K269A_Fw	aa267+aa269	5´- GG ATA GTA CAT AAC **GCA** ATC **GCA** CCC GGT AAT GTG G -3´
D267A_K269A_R	aa267+aa269	5´- C CAC ATT ACC GGG **TGC** GAT **TGC** GTT ATG TAC TAT CC -3´
YO-T89A_Fw	aa89	5´- GGA TCC CCG *GAA TTC* **GCG** TCG CAG GAG CTA AGG
YO-T89A_R	aa89	5´- CCT TAG CTC CTG CGA **CGC** GAA TTC AGG GGA TCC -3´
YO-S90A_Fw	aa90	5´- GGA TCC CCG GAA TTC ACT **GCG** CAG GAG CTA AGG
YO-S90A_R	aa90	5´- CCT TAG CTC CTG **CGC** AGT GAA TTC CGG GGA TCC -3´
YO-S95A_Fw:	aa95	5'- <u>CT</u> TCG CAG GAG CTA AGG <u>GCC</u> GAT ATC CCC AAT GC -3'
YO-S95A_R	aa96	5'- GC ATT GGG GAT ATC <u>GGC</u> CCT TAG CTC CTG CGA <u>AG</u> -3'
YO-S102A_Fw	aa102	5´- GG TCT GAT ATC CCC AAT GCT CTC **GCG** AAT CTC TTT GGA G -3´
YO-S102A_R	aa102	5'- C TCC AAA GAG ATT <u>CGC</u> GAG AGC ATT GGG GAT ATC AGA CC -3´

2.4 Agarose Gel Electrophoresis

Agarose gels were prepared by mixing an appropriate proportion of agarose (to a final concentration of 0.7 - 2 % (w/v) depending on the MW of the sample DNA) with 1 x TAE buffer (40 mM Tris /Acetate, pH = 8.3, 10 mM EDTA), the mixture was cooked and after cooling poured into agarose gel chambers. The DNA was then mixed with loading buffer (30% (v/v) glycerol, 0.25% (w/v) bromphenole blue, 0.25% (w/v) Xylene blue), loaded on the gel and electrophoretically separated by application of voltage (50-120 V) utilizing the 1 x TAE solution as the running buffer. Following the electrophoretic run, gels were stained in ethidium bromide solution (1 µg ethidium bromide pro ml H2Odd) and the DNA visualized under ultraviolet light. For size markers the ready to load solutions "1kb ladder" and "1kbplus ladder" from Invitrogen (Karslruhe, Germany) were used.

2.5 Extraction of DNA from Agarose Gels

To isolate DNA fragments from agarose gels, the desired DNA fragments were excised from the gel, weighed and extracted using the QIAquick Gel Extraction Kit (Qiagen, Hilden Germany) according to the protocol of the manufacturer. DNA concentration and purity grade was determined by measurement of OD260 nm and OD280 nm, respectively (Ultraspec 3000, Amersham Pharmacia Biotech).

2.6 Preparation of Calcium-Competent Bacteria

Calcium-competent cells (*E. coli*: DH5α, BL21) for heat shock transformation were produced according to a simplified method from Current Protocols (Ausubel *et al.*, 2000) as follows:

- 2 ml of an overnight culture was inoculated into 100 ml LB medium and incubated with vigorous shaking at 37 °C until an OD600 of 0.6 was reached
- Cells were collected in 50 ml falcon tubes, cooled for 15 min on ice and centrifuged in a pre-cooled centrifuge (3000 g for 10 min at 4 °C)
- cells were washed in 50 ml ice cold MgCl2 (100 mM) and incubated on ice for 30 min, followed by centrifugation (at 3000 g for 10 min at 4 °C)
- cells were washed in 50 ml ice cold CaCl2 (100mM) and incubated on ice for 30 min, followed by centrifugation (at 3000 g for 10 min at 4 °C)
- cells were resuspended in 2 ml cold CaCl2 (100 mM) and incubated on ice overnight
- after incubation 2.5 ml cold CaCl2 (100 mM) and 0.5 ml sterile glycerol (10 % glycerol final concentration) was added and mixed
- Aliquots of 50-200 µl were prepared and transferred to -80 °C for storage

2.7 Transformation of bacteria

Competent bacteria were thawed on ice, 50-100 µl of cells were mixed with plasmid DNA (0.5-50 ng) or ligation mix (1-10 µl) in sterile 1.5 ml reaction tubes and maintained on ice for 30 min. Cell membranes were disrupted by subjection of cells to a heat-pulse (42 °C) for 45-90 sec. Commercial competent cells were heat shocked following the manufacturer's recommendations. After heat shock cells were incubated on ice for 5 min. Subsequently cells were mixed with 200-1000 µl antibiotic-free LB medium (or SOC medium) and incubated at 37 °C with shaking for 60 min. Bacterial cells were then plated in 100 - 200 µl aliquots onto LB-agar plates containing the required antibiotics for selection of recombinants.

2.8 Preparation of Plasmid DNA (Miniprep and Maxiprep)

Mini-preparation of plasmid DNA (Miniprep)

In order to isolate analytical amounts of plasmid DNA, 5 ml LB medium was inoculated with a bacterial colony and incubated with shaking overnight at 37 °C. Cells were collected in a 2 ml tube by centrifugation at maximum speed for 1 min. After removing the supernatant, the pellet was processed due to the manufacturer's instructions (Quiagen, Hilden, Germany). Plasmid DNA was eluted in supplied (TRIS-buffered) elution buffer and DNA concentration and purity grade was determined by measurement of OD260 nm and OD280 nm, respectively (Ultraspec 3000, Amersham Pharmacia Biotech). The DNA was stored at -20 °C.

Maxi-preparation of plasmid DNA (Maxiprep)

Maxi-preparation was performed to obtain preparative amounts of plasmid DNA. The maxiprep was performed according to the QIAGEN Plasmid Maxi Protocol (Qiagen, Hilden Germany) with QIAgentip 500. The DNA concentration and purity grade was determined by measurement of OD260 nm and OD280 nm, respectively (Ultraspec 3000, Amersham Pharmacia Biotech). The DNA was stored at -20 °C.

2.9 Determination of DNA concentration and purity

Nucleic acids have a maximum absorption at 260 nm wavelength. The isolated DNA was diluted with distilled water (H2Odd) and the absorbance at 260 nm against H2Odd measured spectrophotometrically (Pharmacia Biotech, Ultraspec 3000).

For determination of DNA purity, the $A_{260/280}$ coefficient was photometrically determined. An $A_{260/280} < 1.8$ indicated contamination of the DNA preparation with protein, while an $A_{260/280} > 2.0$ indicated contamination with RNA.

2.10 Mutagenesis

All mutations in the YopO proteins were introduced by means of the QuickChangeII *in vitro* Mutagenesis System (Stratagene, Amsterdam, The Netherlands) according to the protocol of the manufacturer. In brief, the method relies on linear amplification of template DNA by mutagenesis-grade *PfuUltra* high fidelity DNA polymerase. Mutagenic primers are extended during temperature cycling, incorporating the mutation of interest into the newly synthesized strands. Final treatment with *Dpn* I ensures the digestion of only the dam-methylated parental strand. The mutagenic strands were finally transformed into competent cells and transformants were checked for the desired mutation(s) by DNA sequencing.

2.11 DNA Sequencing

In order to verify the correct sequence of a given DNA, 1 - 2 µg of plasmid DNA per sequencing reaction was send for sequencing, together with adequate primers to the Agowa sequencing lab (AGOWA-Gesellschaft für molekularbiologische Technologie mbH, Berlin, Germany). The ensuing chromatograms were processed with Chromas software and BLASTN and BLASTX programs provided by NCBI (National Center for Biotechnology Information). Additionally DNA sequences were analyzed using VectorNTI (Invitrogen, GmbH, Karlsruhe, Germany) and DNAMan (Lynnon Corporation, Quebec, Canada) software.

2.12 PCR

Polymerase chain reaction is an easy and quick method to specifically amplify DNA from smallest amounts of DNA. This technique was routinely used to genotype clones and to amplify fragments of a desired genomic or vector DNA.

All PCR reactions were prepared in 0.2 ml tubes (TreffLab, Degersheim, Switzerland), on ice, in a volume of 20 µl or 50 µl for preparative PCR, respectively. Polymerase enzymes were used according to the manufacturer's recommendations. A typical reaction was set up as follows:

1 µl	*template* DNA (Maxiprep 1:100)
2 µl	Taq-buffer (10x)
0.4 µl	dNTP-Mix (10 mM each)
2 µl	5' Primer (5 pmol/µl)
2 µl	3' Primer (5 pmol/µl)
0.2 µl	Taq-Polymerase (5 Units/µl)
12.4 µl	H2O

After mixing of these components the tubes were placed in the PCR machine at 95 °C and run with the following protocol. The annealing temperature was chosen dependent on the primer pair.

Initial Denaturation	5 min, 95 °C	1x
Denaturation	30 sec, 95 °C	
Annealing	30sec, 45-65 °C	12-36 cycles
Elongation	30 -90sec, 72 °C	
Final elongation	5min, 72 °C 1x	
Hold at 4 °C		

The PCR products were analyzed by agarose gel electrophoresis.

3. BIOCHEMICAL METHODS

3.1 Protein expression and purification

Plasmids were transformed into *E. coli* BL21 using a heat shock procedure. For protein expression, over night bacterial cultures were diluted 1:20 in Luria Bertani medium (LB) containing the selective antibiotic and grown at 37 °C to an OD_{600} of 0.6 to 0.8. Bacterial cultures were shifted to 18 °C and protein expression was induced by 0.4 mM IPTG (isopropyl- b-D-thiogalactopyranoside) for 3 to 4 hours. Cells were harvested (3000 g for 10 min at 4 °C) and french-pressed or sonicated in lysis buffer containing 50mM Tris, pH7.4, 100 mM NaCl, 10% glycerol (and additional 0.1% Triton X-100 for purification of GST-YopOwt and GST-YopOK269A).

The soluble fractions with the GST fusion protein from bacterial lysates were rapidly purified with Glutathione-Sepharose 4B (Amersham, Freiburg, Germany). The principle is based on the strong affinity of the GST protein for Glutathione, allowing other proteins to flow through the column packed with the Glutathione-Sepharose beads. Through several wash steps with lysis buffer, the unspecific bound proteins are washed through the column. The GST-fusion protein was either eluted under mild conditions with lysis buffer containing reduced glutathione (30mM glutathione pH8.8 in lysis buffer) or cleaved overnight at 4 °C with 50 units of thrombin per ml settled beads.

If required (e.g. for microinjection) supernatants containing the desired protein were dialyzed against buffer containing 10 mM Tris pH 7,5, 150 mM NaCl, 2 mM MgCl2, 0.1 mM DTT.

3.2 GST-Invasin expression for coating of fluorescent beads

For bacterial expression of invasin (Schulte, Grassl et al. 2000; Schulte, Kerneis et al. 2000; Wiedemann, Linder et al. 2001) *E. coli* BL21 harboring pGEX-4T-3 with an insertion of the *inv397* gene (BL21-inv397), coding for the 397 carboxy-terminal amino acids of invasin, was grown at 24 °C in LB to an OD of 0.7. Expression of the GST-Invasin fusion protein was induced with IPTG (isopropyl- b-D-thiogalactopyranoside) at a final concentration of 0.3 mM. Cells were grown for 3 additional hours at 37 °C before being harvested by centrifugation and frozen at -20 °C. Frozen cells were resuspended in lysis buffer (50 mM Tris, pH 7.4, 100 mM NaCl, 10 % glycerol) supplemented with complete protease inhibitor mix (Roche, Mannheim, Germany) and disrupted by French press. Lysates were cleared by centrifugation and GST-Inv397 was purified with glutathione Sepharose 4B (Amersham, Freiburg, Germany). GST-fused protein was eluted with reduced glutathione (30 mM, pH 8.9, in lysis buffer).

3.3 Determination of protein concentration (Bradford)

Concentration of solubilized protein was determined with the *BioRad protein Assay* (BioRad, Munich, Germany) based on the method of Bradford. The *Bio-Rad Protein Assay* is a dye-binding assay in which a differential color change of a dye occurs in response to various protein concentrations. The absorbtion maximum for the used acidic solution of Coomassie Brilliant Blue G-250 dye shifts from 465 nm to 595 nm upon binding to protein. As a standard bovine serum albumin (BSA, Sigma-Aldrich, Munich, Germany) was used in the concentrations 20 µg/ml, 15 µg/ml, 10 µg/ml, 5 µg/ml und 1 µg/ml. To 800 µl of sample or standard solution 200 µl of *dye reagent* were added and after vortexing and an incubation of 5 minutes at room temperature the absorbance at 595nm was measured.

3.4 SDS/PAGE

In SDS/PAGE (Sodium-dodecyl-sulphate/polyacrylamide gel electrophoresis) proteins are separated on the basis of their molecular weights as they migrate through a gel. SDS is an anionic detergent that denatures proteins. The SDS also disrupts hydrogen bonds, blocks hydrophobic interactions, and substantially unfolds the protein molecules by eliminating the tertiary and secondary structures. In the discontinuous gel system employed in this work, a stacking gel (non-restrictive large-pore gel, 5% acrylamide) was layered on top of a separating gel (resolving gel, 8-12% acrylamide). Samples were mixed with 5x Laemmli SDS loading buffer (2-mercapto-ethanol added for a final concentration of 5 %) incubated at 95 °C (5 min) and subjected to electrophoresis. With the aid of a protein marker (*prestained high range maker*, Peqlab, Erlangen, Germany) the molecular weight of the proteins applied could be estimated.

5x SDS-sample buffer (Laemmli)

0.5 M Tris/HCl pH 6,8	5 ml
Glycerol	2 ml
SDS	0.8 g
0.5 % Bromophenol blue	1 ml
H2Odd	2 ml

Stacking Gel (5%)

ddH2O	5.5 ml
0.5M Tris-HCl, pH6.8	1 ml
30% acrylamide	1.3 ml
10% SDS	800 μl
10% ammonium persulfate (APS)	800 μl
TEMED (Sigma)	8 μl

Resolving Gel (10%)

ddH2O	7.9 ml
0.5M Tris-HCl. pH8.8	5 ml
30% acrylamide	6.7 ml
10% SDS	200 μl
10% ammonium persulfate (APS)	200 μl
TEMED (Sigma)	8μl

SDS/PAGE running buffer (10%)

Tris-Base	30.3 g
Glycine	144 g
SDS	10 g
ad 1 l ddH2O	

3.5 Coomassie Staining

Gels were stained for 30 minutes in Coomasie staining solution (0.1% Coomassie Brilliant blue , 25% methanol, 10% acetic acid) and subsequently destained in Destain solution (33% [v/v] Methanol, 10% [v/v] glacial acetic acid).

3.6 Western Blot

Western blot is a technique that employs electrophoretic transfer of proteins separated by SDS/PAGE to a membrane and subsequent detection of the proteins by antibody-coupled chemiluminescence or autoradiography. The separated proteins were transferred to a polyvinylidene fluoride (PVDF) membrane (Immobilon–P, Millipore, Schwalbach, Germany) by electrophoretic transfer. For this, a SDS/PAGE gel was placed directly on a piece of methanol-activated PVDF membrane (10 seconds in 100% methanol) and "sandwiched" between two electrodes. For tank-blotting the gel and the membrane were submerged in a container (Mini Protean-II, BioRad, Munich Germany) with blotting buffer (25 mM Tris-Base, 96 mM Glycin) and an electric field applied (100V, 100min or 30V over night, 4 °C).

For semi-dry-blotting the gel and the membrane were transferred to a semi-dry blotting device and proteins transferred onto PVDF membrane for 1 hour at 1.2 mA/cm2.

The PVDF membrane was blocked for 1 hour or overnight at room temperature or 4 °C, respectively, in PBS pH 7.4, 3% bovine serum albumin (BSA), 0.05% Tween 20. The membrane was incubated with primary antibody for 1 hour at room temperature (or 4 °C overnight), washed three times for 5 minutes followed by incubation with horseradish peroxidase-coupled secondary antibody (1:2000 to 1:10.000) for 1 hour. After a final washing step the detection solution (ECL Western blotting detection reagent, Amersham Biosciences, Freiburg, Germany) was applied according to the protocol of the manufacturer. Detection is based on a chemoluminescence reaction in which Luminol is oxidized in the presence of H2O2 by the peroxidase conjugated to the secondary antibody. The emitted light was detected by exposing the membrane to an X-ray film (Kodak, Stuttgart, Germany). The exposed film was developed in a processor for X-ray film development (Agfa Curix 60) and, in case of quantification of chemiluminescence signals, two dimensional densitometry was performed using a Gel Doc EQ System with Quantity One software (BioRad, Munich, Germany).

3.7 Kinase Assay and Kinase Quantification

Kinase reactions were performed with 3-10 µg of GST-YopO protein or indicated fragments in 20 µl kinase buffer containing 20mM Hepes pH 7.4, 1 mM ATP, 1mM DTT, 10 mM MgCl2, 2 mM MnCl2 supplemented with 5µCi [γ-32P] adenosine 5' trisphosphate (Amersham Biosciences, Freiburg, Germany) and 3-10µg G-actin from *Dictyostelium discoideum* (generous gift from Michael Schleicher).

Reactions were incubated at 30 °C for 30 minutes and phosphorylation was stopped by addition of SDS/PAGE sample buffer and heating for 5 minutes at 95 °C. Reactions were subjected to SDS/PAGE and/or Western blot transfer and radioactivity in dried gels or on membranes was visualized and quantified using a Phosphoimager (FLA 3000, Fujifilm, Tokyo, Japan) with Aida 4.0 Image Analyzer software (Raytest, Straubenhardt, Germany) or X-ray film (Kodak, Stuttgart, Germany). For autoradiography quantification of single and double point mutant YopO proteins autophosphorylation of YopO89-729 was set to 100% and autophosphorylation of mutant proteins normalized.

3.8 Phosphorylation of artificial substrates

Kinase reactions were performed as described (see above) with designated artificial substrates (histone and myelin basic protein, MBP) added to kinase assay, run on SDS/PAGE and subjected to autoradiography.

Reactions were incubated at 30 °C for 30 minutes and phosphorylation was stopped by addition of SDS/PAGE sample buffer and heating for 5 minutes at 95 °C. Reactions were subjected to SDS/PAGE and/or Western blot transfer and radioactivity in dried gels or on membranes was visualized and quantified using a Phosphoimager (FLA 3000, Fujifilm, Tokyo, Japan) with Aida 4.0 Image Analyzer software (Raytest, Straubenhardt, Germany) or X-ray film (Kodak, Stuttgart, Germany).

4. CELL CULTURE AND CELL BIOLOGICAL METHODS

4.1 Cell culture

TableE10. **Cells and Cell Culture Media**

cells, cell lines and culture conditions

name	description	culture conditions
HBMEC	Human Brain Microvascular Endothelial Cells. Endothelial cell line.	ECGM-Endothelial Cell Growth Medium (PromoCell) with 2-10% FCS and optional 100 µg/ml penicillin and/or streptomycin
HUVEC	Human Umbilical Vein Endothelial Cells. Primary cells.	ECGM-Endothelial Cell Growth Medium (PromoCell) with 2-10 % FCS and optional 100 µg/ml penicillin and/or streptomycin
FN+/+	mouse embryo fibroblast-like cell line	Nyberg et al. 2004
FN-/-	mouse embryo fibroblast-like cell line, fibronectin gene knockout	Nyberg et al. 2004
monocytes	human monocyte-derived macrophages. Primary cells	RPMI 1640 (PromoCell) containing 20% autologous serum and optional 100 µg/ml penicillin and/or streptomycin

Cell Culture Growth Media

name	description	supplier
ECGM	Endothelial Cell Growth Medium	PromoCell, Heidelberg, Germany
OptiMem	Serum free medium	Invitrogen, Karlsruhe, Germany
RPMI	RPMI 1640 with L-glutamine	Invitrogen, Karlsruhe, Germany
FBGM	Fibroblast Growth Medium (serum free)	PromoCell, Heidelberg, Germany
additives/other		
FCS	Fetal Bovine Serum	Invitrogen, Karlsruhe, Germany
PBS	PBS with Na+ and K+	Sigma-Aldrich, Munich, Germany

HBMEC

Human Brain Microvascular Endothelial Cells -derived endothelial cell line (Greiffenberg, Goebel 2000) that was immortalized by transfection with simian virus 40 large T-antigen and described to maintain their morphologic and functional characteristics at least until passage 30. In this study HBMEC passage from 15 to 28 was used and cultivated in ECGM with 2-10% heat-inactivated serum.

HUVEC

Human Umbilical Vein Endothelial Cell – primary cells isolated from umbilical veins (see isolation of HUVEC), used from passage 2 to 6 and cultivated in ECGM with 2% heat-inactivated serum.

FN+/+ and FN(-/-) fibroblast-like cells

The fibronectin knockout cell line (FN-/-) and the cell line with undeleted floxed *fn* gene (FN+/+) are a generous gift from Reinhard Faessler (Sakai, Johnson et al. 2001; Nyberg,

Sakai et al. 2004). Primary fibroblast-like cells from a fibronectin knockout mouse embryo (E13.5 Fn (flox/flox)) were immortalised by the transfection of SV-40 large T antigen, cloned, and several immortalised and clonal fibroblast-like cell lines were generated. Clonal lines were treated with a cre-transducing adenovirus to delete the floxed Fn genes. The deletion of Fn alleles in cre-treated clones was confirmed by PCR and the lack of Fn protein expression by immunoprecipitation.

4.2 Isolation and culture of HUVEC and human monocytes

Isolation of human monocytes

Human peripheral blood monocytes were isolated by centrifugation of heparinized blood in Ficoll (Seromed, Berlin, Germany). Monocytes were isolated with magnetic anti-CD14 antibody beads and an MS1 Separation Column (Miltenyi Biotec, Bergisch Gladbach, Germany) according to the manufacturer's instructions and seeded onto coverslips (50.000 per coverslip) or into multi-well plates (Nunc, Wiesbaden Germany). Cells were cultured for 5-7 days in RPMI containing 20% autologous serum at 37 °C, 5% $CO2$ and 90% humidity. The medium was changed every 3-4 days. Within 5-7 days, monocytes differentiate into adherent, spread out macrophages (Linder, Nelson et al., 1999).

Isolation of HUVEC

Human umbilical vein endothelial cells (HUVEC) were obtained by trypsin treatment of umbilical cord veins and used at passages 2-6. The method was adapted from Jaffe *et al.*, 1973:

The cord was inspected, and all areas with clamp marks were cut off. The umbilical vein was cannulated with a blunt 2 cm long needle and the needle was secured by clamping the cord over the needle with 2 compressors. After perfusing the umbilical vein with sterile PBS to wash out the blood, the other end of the umbilical vein was clamped shut and warm 0.1 % [w/v] α-chymotrypsin in PBS was infused into the umbilical vein. The umbilical cord was incubated at 37 °C for 20 minutes. After incubation, the chymotrypsin solution containing the endothelial cells was flushed from the cord by perfusion with sterile PBS. The effluent was collected in a sterile 50 ml conical centrifuge tube (BD Biosciences) containing 2 ml of fetal calf serum (Gibco/Invitrogen, Karlsruhe, Germany) to stop the trypsinization. The cells were sedimented at 130 g for 10 min at 25 °C, resuspended in endothelial cell growth medium containing 2% serum (ECGM, PromoCell, Heildelberg, Germany), transferred to collagen-coated (Sigma-Aldrich. Munich Germany) culture flasks (Nunc, Wiesbaden, Germany) and

incubated at 37 °C, 5% CO2 and 90% humidity. After 3h non-adhered cells were removed by replacement of culture medium. Cell culture medium was replaced every 3-4 days.

4.3 Coating of glass coverslips and culture flasks

Glass cover slides (coverslips, diameter 12mm, Hartenstein, Wuerzburg, Germany) were treated with 100% ethanol moved through a Bunsen burner flame and then added to the wells of a 6-, 8-, or 12-well-plate (Nunc, Wiesbaden, Germany). To facilitate adhesion of endothelial cells, a 0.1 % solution of gelatin in PBS (Gelatin solution TypeB from bovine skin, 2%; Sigma-Aldrich, Munich, Germany) was applied and the surface was allowed to dry for at least 3 hours before cells and medium was introduced. Correspondingly the surface of culture flasks (Nunc, Wiesbaden, Germany) was treated with 0.1% gelatin solution to facilitate adhesion.

4.4 Passaging and detachment of adherent cells

After removal of growth medium, cells were washed once with sterile PBS. HUVEC/HBMEC were removed with Trypsin-EDTA (0.05% Trypsin 0.53 mM EDTA x 4 Na; GIBCO/Invitrogen, Karlsruhe, Germany) and for primary human macrophages AccutaseII (Fa. PAA Laboratories, Linz, Austria) was used. In contrast to the fast detachment of HUVEC after trypsin treatment, monocytes were incubated with AccutaseII for 15-25 minutes at 37 °C for detachment (500µl AccutasII per 10cm2 surface area). Trypsin and Accutase activity were stopped by addition of culture medium with 10% heat-inactivated serum, cells were sedimented for 5 min at 450 g at 24 °C and afterwards either cells were used for nucleofection, or resuspended in medium for seeding on coverslips or further cultivation in flasks or multi-well plates.

4.5 Freezing and thawing of cells

Freezing of cells

Cells were detached from cell culture dishes, re-suspended in pre-warmed growth medium and spun down at 450g for 5 min. The cell pellet was resuspended in sterile-filtered pre-cooled freezing medium (growth medium + 10% dimethysulfoxide, DMSO; Sigma-Aldrich, Munich, Germany). Cells were transferred to 1.5 ml cryo-vials, incubated at -20 °C for 3 hours and subsequently transferred to -80 °C and optionally into liquid nitrogen for longer storage.

Thawing of cells

Cryo-vials were removed from -80 °C or liquid nitrogen and placed into a 37 °C water bath, until the frozen medium had melted. The thawed cells were transferred into 5 ml of warm growth medium, centrifuged for 5 min at 450g, re-suspended in growth medium and transferred to culture flasks.

4.6 Transfection with Metafectene

Transfection with the polycationic agent Metafectene (Biontex, Martinsried, Germany) is based on liposome technology. Transfection of endothelial cells (HBMEC and HUVEC) was performed in serum free conditions. Prior to transfection the cells were incubated in serum free OptiMem medium (Invitrogen, Karlsruhe, Germany) for 2 hours. The transfection-mix was prepared from two solutions: One solution was prepared with vector DNA (0.5-2μg vector per 20.000 cells) in OptiMem and the second solution was prepared with Metafectene in OptiMem. The two Metafectene lipid and DNA solutions were mixed (lipd:DNA ratio in the range of 2-7:1) and added to seeded endothelial cells. After 3 hours of incubation (37 °C, 5% CO2) the transfection mix was replaced by cell growth medium (ECGM with 2% serum).

4.7 Transfection with Nucleofector (Amaxa)

Transfection of vectors, leading to transient expression of proteins, was also performed with a Nucleofector device (Amaxa Biosystems, Cologne, Germany). Transfer of vectors in eukaryotic cells by this method (a combination of electroporation and lipofection) resulted in higher cellular expression and higher transfection efficiencies compared to methods using only lipid agents. Nucleofection with the Amaxa device is the only suitable method for successful transfection of primary macrophages. Nucleofection was used in the phagocytosis assays for transfection of primary macrophages and endothelial cells (HUVEC).

Nucleofection was performed due to the manufacturer's recommendations. For macrophages the coded solution Nr.6857 was used and HUVEC were transfected with the HUVEC Nucleofector Kit. For transfection reactions the recommended amount of cells (0.5-1 million) with an average of 2 μg vector DNA per reaction was used.

4.8 Coating of fluorescent beads with invasin

For non-covalent coating of beads, purified protein was dialyzed against PBS pH 7.0. Fluorescent polystyrene microspheres (beads, diameter 1 μm, blue, Exc./Em.=350/440nm) with sulfate groups on the surface for passive adsorption of proteins were purchased from Molecular Probes (Invitrogen, Karlsruhe, Germany).

About 200 µl of beads slurry (approximately 600.000 beads/µl; were washed with 1 ml of PBS and resuspended in 500 µl of PBS. Purified GST-Inv397 fusion protein (1 mg) was added and allowed to adsorb to the beads for 3 h at room temperature (RT). After adding 500 µl of 1 % BSA (in PBS), the solution was incubated at RT for another 1 h. Next, beads were washed in PBS containing 1 % BSA and stored at 4 °C in 500 µl of PBS containing 1 % BSA.

To determine the coupling efficiency, the protein concentration of the starting solution and of the supernatant before adding BSA was determined. Integrity of coated GST-Inv397 protein was checked using Western blot analysis and Immunofluorescence.

FIGURE E3
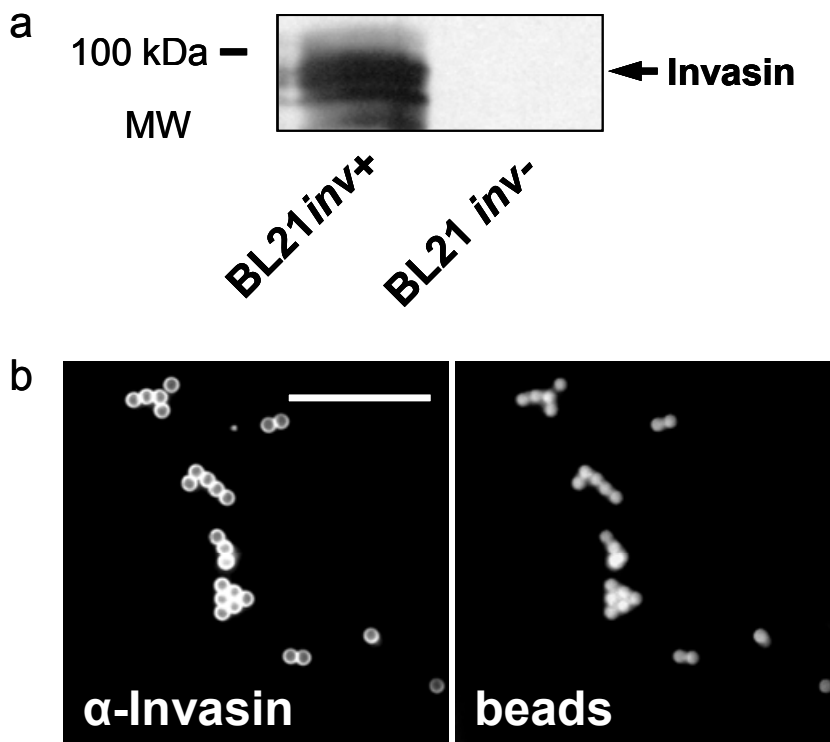
FIGURE E3. **Recombinant expression of invasin and Invasin detection on Invasin-beads.**
a) Western blot detection of purified invasin with anti-Invasin antibody after expression in BL21-Inv397 (labeled BL21*inv+*). Invasin-negative control strain (labeled BL21*inv-)* shows no expression of invasin.
b) Immunofluorescence detection of Invasin on the surface of invasin-beads. Immunofluorescence staining with anti-invasin antibody (left) shows surface staining. Beads are visible by blue autofluorescence (right). The bar represents 10 µm.

4.9 Microinjection

The protein to be injected was added to microinjection buffer (150 mM NaCl, 50 mM Tris pH 7.4, 5 mM MgCl2) with the concentration limit of 10 µg protein per µl solution. High concentrations of protein lead to highly viscous solutions that can plug up the injection needle. As a marker for injected cells rat-IgG (Dianova, Hamburg, Germany) was added to the microinjection buffer (200 ng/ml). To remove aggregates the solution to be injected was centrifuged (4 °C, 30min, 14000 x g) before it was loaded into the injection needle (Femtotip, Eppendorf, Hamburg, Germany). The Femtotip was controlled by the microinjection device (Transjector 5246 with micromanipulator 5171, Eppendorf, Hamburg, Germany) via a personal computer. Cells to be microinjected were placed on the heated stage of the microscope, the Femtotip was moved to the cell layer and computer controlled injection of cells was performed after marking the cells on the monitor screen. Approximately 90-150 cells per coverslip were injected and either immediately fixed with 3.7% (v/v) formaldehyde in PBS, or after an incubation time (37 °C, 5% CO2) of 30 to 90 minutes. Injected marker IgG was detected with AlexaFluor-coupled secondary antibodies (see below). Control experiments were done with microinjection buffer containing marker (rat IgG) and no YopO protein. For microinjection of YopO89-729 the GST-tag was cleaved off by incubation with thrombin (see above).

4.10 Immunofluorescence methods

4.10.1 Formaldehyde/Acetone fixation/permeabilization

Cells seeded on coverslips were fixed by incubation in 3.7 % [v/v] formaldehyde in PBS for 8 minutes at room temperature. After a washing step in PBS, the permeabilization was carried out in cold (-20 °C) acetone for 3 minutes. Formaldehyde fixation was performed when partial disruption of cell membranes by the common additive methanol was not critical.

4.10.2 Formaldehyde/Triton fixation/permeabilization

Cells seeded on coverslips were fixed and permeabilized in one step by incubation with 3.7% formaldehyde containing 0.18% Triton X-100 in PBS for 10 min at room temperature.

4.10.3 Paraformaldehyde fixation

Fixation of cells for minimal disruption of cell membranes was performed with freshly made 4 % paraformaldehyde in PBS. For the preparation of a 4 % paraformaldehyde solution an 8% solution was prepared by dissolving 2 g of paraformaldehyde in 25 ml of H2Odd (addition of NaOH and heating required for dissolving). Subsequently 25ml of 2x PBS were added to obtain the 4 % solution. Cells on glass coverslips were fixed in 4% parafornaldehyde for 8 minutes and transferred to PBS to remove traces paraformaldehyde. This fixation was used for the phagocytosis assays where discrimination of intra and extracellular bacteria was essential.

4.10.4 Methanol fixation

Cells seeded on coverlips were fixed and permeabilized in a one step procedure by incubation in cold (-20 °C) methanol for 60 seconds. Subsequently the coverslips were washed in PBS to remove traces of methanol.

4.10.5 Immunofluorescence staining

Indirect immunofluorescence staining of cells attached to glass coverslips was performed in a wet chamber on a layer of parafilm (American National Can, Menasha, USA). A drop (27 µl) of staining solution was placed on the parafilm and the coverslips were applied with the cellular side oriented downwards.

In general, staining with antibodies followed a two step procedure with intermediate steps for washing and blocking. Unspecific binding of antibody was blocked with 1% BSA in PBS, followed by application of the primary antibody for 45 minutes. After 3 washing/blocking steps with 1 % BSA in PBS the secondary antibody was applied for 45 minutes. After 3 terminal washing steps with PBS the coverslips were partially dried, mounted on a drop (2.7µl) of Mowiol (including *p*-Phenylendiamin as antibleach) and sealed with nail polish.

4.10.6 F-actin staining

Direct staining with labeled phallotoxins

Phalloidin that can be coupled to fluorescent dyes is a toxin from the toadstool *Amanita phalloides* that serves as a high affinity probe for F-actin (Wulf, Deboben et al. 1979). Phallotoxins interact specifically with small and large actin filaments and show minimal background staining. For F-actin staining with fluorescently-labeled phalloidin the cells were permeabilized with acetone before application of the staining solution. Dependent on other

antibodies used in the experiment one of the following three labeled phalloidins (Invitrogen/Molecular Probes, Karlsruhe, Germany) was used: AlexaFluor 568-phalloidin (Exc/Emm=578/603nm), AlexaFluor 488-phalloidin (Exc/Emm=495/519nm) or AlexaFluor 350-phalloidin (Exc/Emm=346/446nm).

Indirect staining with Actin antibody

After cell fixation and permeabilization with formaldehyde/acetone a primary α-actin antibody (MAB1501 α-actin mouse IgG; Chemicon/Millipore, Schwalbach, Germany) was used as an alternative to the fluorescently-labeled phallotoxins. With the choice of a secondary antibody, F-actin could not only be labeled in blue, green and red, but additionally with a secondary antibody labeled with the far-red fluorescent dye Cy5 (Invitrogen, Karlsruhe, Germany).

4.10.7 Inside/outside staining (double fluorescence staining)

The microscopic technique for differentiation of cell-attached (extracellular) and ingested (intracellular) bacteria or particles was adapted from a method described elsewhere (Heesemann and Laufs 1985; Wiedemann, Linder et al. 2001). This method is based upon the observation that membranes of mammalian cells are impermeable for antibodies after fixation with paraformaldehyde but become permeable after treatment with acetone. Consequently, before permeabilization extracellular bacteria can be exclusively stained by primary and secondary antibodies, and intracellular bacteria (together with extracellular bacteria) can be visualized by treatment with specific antibodies after permeabilization. This results in extracellular bacteria being stained in one color during the first step and all bacteria being stained with the second color after permeabilization. By comparison of the two fluorescent channels the number of extracellular bacteria and the number of all bacteria present can be determined microscopically.

The double fluorescence staining method was used to determine internalization of Invasin-*E. coli* (HB101inv+), internalization of invasin-beads (only outside staining necessary for blue-fluorescent Invasin-beads) and internalization of YadA-*E. coli* (DH5A-pBR-A1) into endothelial cells and fibroblast-like cells (FN-/- and FN+/+). Uptake of SRBC was determined using fluorescent outside staining and phase contrast microscopy (see below).

4.11 Quantification of Adhesion of YadA-*E. coli* to Fibronectin (FN) and Collagen (COL)

To analyze the ability of YadA (from *Yersinia enterocolitica*) to interact with extracellular matrix (ECM) proteins glass coverlips were coated with fibronectin (1 µg/ml FN in PBS pH 7.4, bovine plasma fibronectin, Calbiochem/Merck, Darmstadt, Germany) or collagen (1 mg/ml COL in PBS pH7.4, 0.1% Gelatin solution TypeB from bovine skin, Sigma-Aldrich, Munich, Germany) at room temperature overnight.

Overnight cultures of YadA-*E. coli* (DH5A-pBR-A1) were induced for YadA expression at 37 °C for 3 hours, washed in ice cold PBS pH7.4 and added in equal amounts to ECM-coated coverlips in a 12 well plate.

After 60 minutes incubation at 37 °C non-bound bacteria were removed, adherent bacteria were fixed with 4% formaldehyde in PBS for 8 minutes and stained with anti-*E. coli*-antibody followed by AlexaFluor 488-labeled secondary antibody. The YadA-negative non-adhesive parental *E. coli* strain (DH5A-pBR) was used as negative control.

Stained bacteria were quantified by a microscopic method: Therefore, 10 representative microscopic fields were captured with a Zeiss Axioplan microscope, a 40x objective lens, Spot Pursuit 1.4MP monochrome camera (Diagnostic Instruments, Inc, Sterling Heights, USA) and Spot software (Diagnostic Instruments, Inc, Sterling Heights, USA), the total area covered by bacteria measured using ImageJ software (Research Services Branch, NIMH) and the data imported into a graphic and spread sheet program (MS Excel, Unterschleissheim, Germany) for statistical analysis. The measured unit was pixel^2 (square pixel) directly reflecting the number of attached bacteria. The values for the measured area were divided by 100 and displayed as adhesion in arbitrary units. Adhesion to fibronectin (FN) was normalized to collagen (COL) that was set to 100%.

Data presented are mean +/- standard deviation (+/-S.D) of three independent experiments. For each experiment 10 objective fields per matrix protein were evaluated.

4.12 Quantification of expression of GFP-YopO mutants

YopO effects were observed at the cellular level in cells identified by green fluorescence originating from GFP-YopO fusion proteins. To ensure that different effects of GFP-YopO mutants are not based on different cellular expression levels, transfected cells (HBMEC) that had the brightness to be chosen for evaluation of cellular effects were measured for GFP-fluorescence. Fluorescence intensity of GFP directly reflects the cellular expression level of GFP-YopO mutant proteins.

Therefore, at least ten transfected cells per construct were captured with a Zeiss Axioplan microscope, a 100x objective lens (numerical aperture 1.4), Spot Pursuit 1.4MP monochrome camera (Diagnostic Instruments, Inc, Sterling Heights, USA) and Spot software (Diagnostic Instruments, Inc, Sterling Heights, USA) using identical exposure settings. Average pixel intensities of three outlined regions per cell were obtained using ImageJ software (Research Services Branch, NIMH) and imported into a spreadsheet and graphics program for statistical analysis.

FIGURE E4.
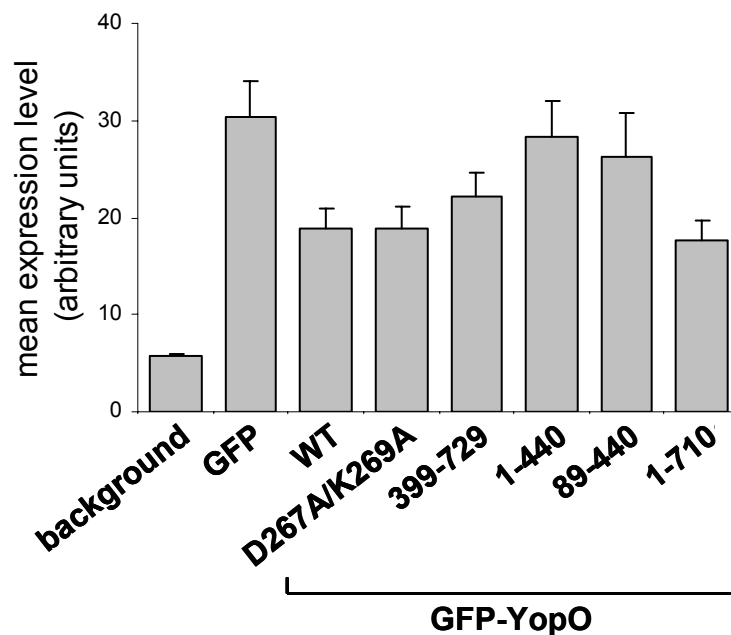
FIGURE E4. **Expression levels of evaluated GFP-YopO fusion proteins**
Mean expression level (arbitrary units) determined by immunofluorescence-intensity measurement is shown for background, GFP empty vector (GFP) and the respective GFP-YopO mutant proteins. Values are mean ± S.D. of 3 experiments with 10 cells (30 regions of interest) evaluated per experiment.

The expression levels directly reflected in the brightness of GFP fluorescence were measured for background (control with no cells present), for GFP empty vector expressing control and

for cells expressing GFP-YopOwt and the designated GFP-YopO mutant proteins. The GFP empty vector showed maximal expression, while the different GFP-YopO constructs were mostly expressed at a lower level (see figure E4). Transfection efficiency (not shown) and additionally the expression level were shown to be dependent on the size of the GFP-YopO fusion protein. The truncated GFP-YopO fusion proteins GFP-YopO1-440 and GFP-YopO89-440 showed higher expression than to the full length proteins GFP-YopOwt and GFP-YopOD267A/K279A and the C-terminally truncated GFP-YopO1-710 (figure E4). Although smaller YopO mutant proteins tended to show a higher expression level compared to the larger YopO mutant proteins, the expression levels of all GFP-YopO constructs evaluated in this study were comparable.

In conclusion, the different effects on cell morphology, F-actin disruption and phagocytosis can not be attributed to different expression levels of the YopO constructs.

4.13 Evaluation of cellular effects

4.13.1 F-actin disruption and rounding/arborization

To observe F-actin disruption caused by GFP-YopO and its mutants, endothelial cells (HBMEC) were transfected with Metafectene and 2µg of the respective vector DNA. After 20 hours of expression, cells were fixed with formaldehyde, permeabilized with acetone and stained for F-actin with AlexaFluor 568-phalloidin (see above). Cells showing GFP fluorescence were scored for unaltered phenotype showing normal stress fibers (named no phenotype in figure 10), F-actin disruption or rounding/arborization. Cells showing F-actin disruption (reduced amount and size of actin filaments) and cells showing no cytoplasmic F-actin were scored positive for F-actin disruption. Cells with completely rounded phenotype determined by phase contrast and the green fluorescence channel (apparent retraction fibers) were scored positive for rounding/arborization.

Data presented are mean +/- standard deviation (+/-S.D) of at least three independent experiments. For each experiment at least 90 cells per condition were evaluated.

4.13.2 RhoAV14 rescue assay

F-actin disruption was examined by staining of the actin cytoskeleton with an anti-actin antibody (mouse IgG, Chemicon/Millipore, Schwalbach, Germany) followed by MarinaBlue 365-coupled secondary antibody (Molecular Probes, Karlsruhe, Germany). Actin staining was evaluated in the blue channel and the green and red channels were used for GFP-RhoAV14 and mRFP-YopO, respectively.

Endothelial cells (HBMEC) were transfected with Nucleofector technology (Amaxa, Cologne, Germany) using GFP (empty vector), GFP-RhoAV14, a mixture of GFP-RhoAV14 and mRFP-YopO, mRFP-YopO or mRFP (empty vector). For single transfections 2 μg of vector and for the double transfection 1 μg of each vector was introduced. Cells were fixed 18 hours after transfection and stained with anti-actin antibody.

For statistical evaluation of transfected cells two phenotypes were distinguished: Cells showing F-actin disruption (reduced amount and size of actin filaments) and cells showing no cytoplasmic F-actin were scored positive for F-actin disruption. The other phenotype that was scored had articulate cytoplasmic F-actin fibers comparable to untransfected control cells.

Data presented in the results are mean +/- standard deviation (+/-S.D) of three independent experiments. For each experiment at least 90 cells per condition (GFP, GFP-RhoAV14, GFP-RhoAV14+mRFP-YopO, mRFP-YopO, mRFP) were evaluated.

4.14 Phagocytosis assays

4.14.1 Invasion properties of Invasin-beads and Invasin-*E. coli* (HB101inv+)

Endothelial cells (HBMEC) cultured on gelatin coated glass coverslips (Hartenstein GmbH, Wuerzburg, Germany) were inoculated with either bacteria expressing invasin on their surface (Invasin-*E. coli*/HB101inv+; ratio bacteria:cell of 60:1), or with Invasin-beads (ratio beads:cell of 50:1). For synchronization of attachment bacteria and beads were centrifuged (1 min, 18x g) onto the cells and incubated at 37 °C, 5% CO_2 in a humidified atmosphere.

Morphological effects (F-actin)

Ten minutes after centrifugation cells were fixed, permeabilized (formaldehyde/acetone) and stained for F-actin with AlexaFluor 568-phalloidin. Actin phenotype elicited at attachment sites of Invasin-*E. coli* (HB101inv+) or Invasin-beads was observed by phasecontrast and immunofluorescence microscopy.

Uptake kinetics

At time points 10, 30 and 60 minutes after attachment of bacteria or beads cells were fixed in paraformaldehyde and stained for discrimination of intra- and extracellular particles (see above). Double fluorescence staining (outside AlexaFluor 568; inside/all AlexaFluor 488) was performed for Invasin-*E. coli*. Attached extracellular Invasin-beads were stained with AlexaFluor 568 (red) secondary antibody, while all beads (including intracellular) were detected by their blue staining. Per experiment for each time point 90 cells were evaluated for attached and internalized particles. Data presented in the results are mean +/- standard deviation (+/-S.D) of three independent experiments.

4.14.2 Invasin-mediated phagocytosis

To evaluate the effect of YopO on invasin-mediated phagocytosis, Invasin-beads were attached to endothelial cells (HBMEC; ratio 50:1) expressing GFP (control), GFP-YopOwt or GFP-RacN17. Transfection of HBMEC was performed with Metafectene (Biontex, Martinsried, Germany). Invasin-beads were added 18 hours after transfection, attachment was synchronized by a 1 min, 18x g centrifugation step, after 30 minutes cells were fixed with paraformaldehyde and extracellular Invasin-beads were stained with anti-invasin primary antibody (rabbit IgG) followed by AlexaFluor 568-labeled (red) secondary antibody. Blue fluorescence of Invasin-beads makes the inside/all staining after permeabilization dispensable. Outside staining enabled to distinguish the red-labeled extracellular beads from the blue intracellular beads. In cells expressing the respective GFP protein statistical analysis of attached and internalized bacteria was performed using a microscope with the red, green and blue fluorescent channels. Internalization was normalized to the construct showing the highest internalization (GFP-YopOwt; undistinguishable from GFP within standard error) that was set to 100%.

Data presented in the results are mean +/- standard deviation (+/- S.D) of three independent experiments. For each experiment at least 90 cells per condition (GFP, GFP-YopOwt, GFP-RacN17) were evaluated. Student-t test was used to determine statistical significance (99% level).

4.14.3 FN-dependent phagocytosis

To clarify if the uptake of YadA-*E. coli* is strictly dependent on the presence of fibronectin, fibronectin knockout cells (FN-/-) and the corresponding fibronectin-positive control cells (FN+/+) were assayed for internalization of YadA-*E. coli* . The fibroblasts (a generous gift from Reinhard Faessler; (Nyberg, Sakai et al. 2004)) were grown in serum free medium (FBGM) on collagen coated surfaces for 7 days, the medium was replaced every 2 days.

Internalization was evaluated for YadA-*E. coli* (DH5A-pBR-A1) and as a control, to verify that internalization is exclusively dependent on YadA, for the parental control strain DH5A-pBR. The parental control strain showed very low adhesion and therefore was added at a ratio of 3000:1 to cells, while YadA-*E. coli* was added at a ratio of 30:1. Internalization was synchronized by centrifugation (1 minute, 18x g), cells were incubated at 37 °C for 90 minutes and fixed with paraformaldehyde. Double fluorescence staining discriminated red-labeled extracellular YadA-*E. coli* from intracellular green-labeled YadA-*E. coli*.

Statistical analysis of attached and internalized bacteria (YadA-*E. coli* or DH5A-pBR) was performed on a microscope using phasecontrast and the red and green fluorescent channels. Data presented in the results are mean +/- standard deviation (+/- S.D) of three independent experiments. For each experiment at least 90 cells per condition were evaluated. Student-t test was used to determine statistical significance (99% level).

4.14.4 FcγR- and CR-mediated phagocytosis

FcγR- and CR-mediated phagocytosis was evaluated for GFP-YopO expressing monocytes using an adapted method described before (Braun, Fraisier et al. 2004). Hereby, complement coated or IgG-coated sheep red blood cells (SRBC) were subjected to phagocytosis by macrophages in serum-free complete RPMI (Invitrogen, Karlsruhe, Germany) phagocytosis medium.

FcγR phagocytosis

SRBC (MP Biomedicals, Eschwege, Germany) were washed three times with sterile PBS (containing Ca^{2+} and Mg^{2+}; Sigma-Aldrich, Taufkirchen, Germany), resuspended in sterile PBS and then incubated with rabbit IgG anti-SRBC (ICN Pharmaceuticals, Ohio, USA) at RT for 30 minutes. After one wash in PBS, IgG-opsonized SRBC were resuspended in pre-warmed phagocytosis medium.

Opsonized IgG-SRBC were added at a ratio of 15:1 to GFP- or GFP-YopO expressing monocytes grown on glass coverslips. Phagocytosis was synchronized by centrifugation for 2 minutes at 400 g at RT and cells were subsequently incubated at 37 °C, 5% CO_2 for 10 to 60 minutes, before phagocytosis was stopped by fixation with 4% paraformaldehyde.

Outside staining of IgG-SRBC:

After fixation coverslips were washed in PBS and incubated in 1 % BSA in PBS for 5 minutes to block unspecific binding of antibody. Coverslips with IgG (rabbit IgG anti-SRBC) opsonized SRBC were incubated with AlexaFluor 568 labeled secondary antibody (anti-rabbit AlexaFluor 568 IgG (H+L) goat, Molecular Probes/Invitrogen, Karlsruhe, Germany) for red outside staining.

CR phagocytosis

SRBC (MP Biomedicals, Eschwege, Germany) were washed three times with sterile PBS (containing Ca^{2+} and Mg^{2+}; Sigma-Aldrich, Taufkirchen, Germany), resuspended in sterile PBS and then incubated with rabbit IgM anti-SRBC (WAK-Chemie Medical GmbH, Steinbach, Germany) at RT for 30 minutes. After one wash with PBS IgM-opsonized SRBC were further incubated for 20 min at 37 °C in phagocytosis medium containing 10% C5-

deficient complement (Sigma-Aldrich, Taufkirchen, Germany). Complement-coated SRBC were washed once with warm PBS and resuspended in warm phagocytosis medium. In order to activate the CR3 receptors for CR3-mediated phagocytosis, macrophages were incubated with 150 ng/ml PMA (Phorbol 12-Myristate 13-acetate, Sigma-Aldrich, Taufkirchen, Germany) in phagocytosis medium for 15 min at 37 °C before the start of phagocytosis assay. Complement coated SRBC were added to activated GFP- and GFP-YopO expressing monocytes at a ratio of 15:1. Phagocytosis was synchronized by centrifugation for 2 minutes at 400 g at RT and cells were subsequently incubated at 37 °C, 5% CO_2 for 10 to 60 minutes, before phagocytosis was stopped by fixation with 4% paraformaldehyde.

Outside staining of complement coated SRBC

After fixation coverslips with monocytes and complement opsonized SRBC were washed in PBS and incubated in 1% BSA in PBS for 5 minutes to block unspecific binding of antibody. In the first step coverslips were incubated with rabbit IgG anti-SRBC (ICN Pharmaceuticals, Ohio, USA) primary antibody and then stained with AlexaFluor 568-labeled secondary antibody (anti-rabbit AlexaFluor 568 IgG (H+L) goat, Molecular Probes/Invitrogen, Karlsruhe, Germany) for red outside staining.

Microscopic evaluation of FcγR- and CR-mediated phagocytosis

Internalized SRBC can be distinguished from attached SRBC by their appearance in phasecontrast and fluorescence microscopy, respectively (Greenberg, el Khoury et al. 1991). Phagocytosed SRBC become visible by phasecontrast as swollen particles in vacuoles, but they are almost invisible by phasecontrast when they are extracellular. Fluorescent outside staining in red (AlexaFluor 568) identifies extracellular SRBC.

Statistical analysis of attached and internalized SRBC (IgG-opsonized or complement-coated) was performed for monocytes expressing GFP or GFP-YopO. Internalization was normalized to the GFP control that was set to 100%. The results presented are mean +/- standard deviation (+/-S.D) of three independent experiments. For each experiment 90 transfected cells were evaluated. Student-t test was used to determine statistical significance (99% level).

Preliminary experiments showed that uptake of IgG- and Complement-coated SRBC was best to be evaluated after 60 minutes. Uptake after 10 and 30 minutes was considerably lower than after 60 minutes (not shown), therefore the data presented in the results refer to experiments with 60 minutes of internalization at 37 °C before fixation.

4.14.5 YadA-mediated phagocytosis

YadA-mediated internalization was examined in primary endothelial cells (HUVEC) expressing the GFP-YopO fusion proteins. To examine the effects of YopO on YadA-mediated phagocytosis YadA-*E. coli* (DH5A-pBR-A1) were attached to endothelial cells (ratio 30:1) expressing the respective GFP-fusion protein.

Transient expression of GFP-YopO fusion proteins was initiated by Nucleofection (Amaxa, Cologne, Germany; see above). YadA-*E. coli* were added to cells 19 hours after transfection. A centrifugation step (1 minute, 18x g) for synchronization of attachment was employed, subsequently cells were incubated at 37 °C (5 % CO_2). Phagocytosis was stopped after 90 minutes with 4% paraformaldehyde. For evaluation of internalization in GFP expressing cells, a double fluorescence staining method was used (see above). Outside staining was performed with mouse anti-YadA primary antibody (mouse IgG, 9H11) and red-labeled anti-mouse secondary antibody (AlexaFluor 568, goat IgG, Molecular Probes/Invitrogen, Karlsruhe, Germany). After permeabilization internalized YadA-*E. coli* were stained with rabbit anti-*E. coli* (Biodesign, Maine, USA) and mouse anti-YadA primary antibodies followed by blue anti-rabbit (MarinaBlue 365 IgG goat, Molecular Probes/Invitrogen, Karlsruhe, Germany) and anti-mouse (MarinaBlue 365 IgG goat, Molecular Probes/Invitrogen, Karlsruhe, Germany) secondary antibodies. Green fluorescence identified the cells expressing the respective GFP-YopO fusion protein, red fluorescence identified extracellular bacteria and blue fluorescence all bacteria present. Inside staining of YadA-*E. coli* with a combination of two primary antibodies (one antibody against YadA (mouse IgG, 9H11) and one against several *E. coli* epitopes (rabbit IgG, Biodesign, Maine, USA)) proved to be better for the detection of internalized bacteria. Detection of internalized bacteria when using solely the anti-YadA primary antibody was more difficult, because of the ongoing digestion of antigenic epitopes in formed phagocytic vesicles.

Internalization was statistically evaluated for green (GFP-expressing) cells and adjacent control cells showing no GFP expression. Internalization was normalized to control cells that were set to 100%. Data presented in the results are mean +/- standard deviation (+/-S.D) of three independent experiments. For each experiment at least 90 cells per condition were evaluated. Student-t test was used to determine statistical significance (99% level).

4.14.6 EDIN-B inhibition of RhoA and YadA-mediated phagocytosis

Expression of EDIN-B in *E. coli* BL21 was performed following a standard procedure. Therefore, *E. coli* bearing the plasmid for recombinant production of His-tagged EDIN-B were induced with 0.4 mM IPTG in the logarithmic growth phase and expression was performed for 3 hours at 20°C. Bacteria were harvested, lysed and the recombinant His-EDIN-B protein was purified with Ni-NTA-Agarose (Qiagen, Hilden, Germany).

YadA-mediated uptake in EDIN-B treated cells was evaluated by a double fluorescence staining method (see above). Efficiency of RhoA inactivation by EDIN-B was controlled by staining of F-actin with labeled phalloidin (see above). Cells with disrupted F-actin cytoskeleton were evaluated for YadA-*E. coli* (DH5A-pBR-A1) uptake. Endothelial cells (HUVEC) seeded on coverslips 24 hours were treated with EDIN-B (60 µg/ml in ECGM) for 22 hours to inactivate RhoA. YadA-*E. coli* were added (at a ratio of 30:1), attachment was synchronized by centrifugation (1 min, 18x g), after 90 min cells were fixed with 4% paraformaldehyde and double fluorescence staining performed. External bacteria were stained with mouse anti-YadA primary antibody (mouse IgG, 9H11) and red-labeled anti-mouse secondary antibody (AlexaFluor 568, goat IgG, Molecular Probes/Invitrogen, Karlsruhe, Germany). After permeabilization internalized YadA-*E. coli* were stained with rabbit anti-*E. coli* (Biodesign, Maine, USA) and mouse anti-YadA primary antibodies followed by blue anti-rabbit (MarinaBlue 365 IgG goat, Molecular Probes/Invitrogen, Karlsruhe, Germany) and anti-mouse (MarinaBlue 365 IgG goat, Molecular Probes/Invitrogen, Karlsruhe, Germany) secondary antibodies. F-actin staining was performed with green AlexaFluor 488-labeled phalloidin.

Internalization was statistically evaluated for EDIN-B treated cells (showing RhoA inhibition by disruption of F-actin) and for untreated control cells. Internalization was normalized to control cells that was set to 100%. Data presented in the results are mean +/- standard deviation (+/-S.D) of three independent experiments. For each experiment at least 90 cells per condition were evaluated.

F. ABBREVIATIONS

°C	degree Celsius		kb	kilo bases
A	adenine, alanine, ampere		kDa	kilo Dalton
aa	amino acid		l	liter
Ab	antibody		L	lysine
Amp	ampicillin		LB	Luria-Bertani
APS	ammoniumpersulfate		LD50	lethal dosis 50
ATP	adenosintriphosphate		LIM	protein-protein interaction motive from genes lin-11, isl-1 and mec-3
au	arbitrary units		m	milli
BG	biogroup		M	molar
BHI	Brain-Heart-Infusion		MCS	multiple cloning site
bp	base pair		min	minute
BSA	bovine serum albumin		n	nano
C	cytosine		Nal	nalidixic acid
cDNA	complementary DNA		nm	nanometer
CFU	colony forming unit		o/n	over night
CHO	chinese hamster ovarian tumor cells		OD	optical density at 600nm
CIB	calcium and integrin binding protein		OM	outer membrane
Cm	chloramphenicol		PAGE	poly-acrylamide gel electrophoresis
cm	centimeter		PBS	phosphate buffered saline
COL	collagen		PCR	polymerase chain reaction
CR	complement receptor		PFA	paraformaldehyde
D	aspartic acid		PMN	polymorphnuclear neutrophile granulocytes
Da	dalton		PMSF	phenylmethanosulfonylfluoride
dd	double distilled		PTP	protein tyrosine phosphatase
DMEM	Dulbecco's Modified Eagle Medium		pYV	*Yersinia* virulence plasmid
DNA	deoxyribonucleic acid		RFP	red fluorescent protein
dNTP	deoxynucleoside triphosphate (dATP, dCTP, dGTP, dTTP)		RNS	ribonucleic acid
DTT	dithiothreitol		rpm	revolutions per minute
ECGM	endothelial cell growth medium		RT	room temperature
ECM	extracellular matrix		S.D.	standard deviation
EDTA	ethylendiamin-N,N,N',N'-tetra acetic acid		SDS	sodiumdodecylsulfate
ELISA	Enzyme Linked Immunoabsorbent Assay		Sm	streptomycin
EtOH	ethanol		SRF	serum response factor
F-actin	filamentous actin		T	thymine
FAK	focal adhesion kinase		T	threonine
FCS	fetal calf Serum		Tab.	table
FGM	Fibroblast growth medium		TAE	Tris/Acetate/EDTA
fig.	Figure		TE	Tris/EDTA
FN	fibronectin		TEMED	N,N,N',N'-tetramethylethylenediamine
g	Gram		Tet	tetracycline
G	Guanine		Tris	Tris(hydroxymethyl)aminomethane
G-actin	globular actin		TTS	type III secretion
GAP	GTPase activating protein		U	units, uracil
GDI	Guanine nucleotide dissociation inhibitor		UV	ultra violet
GEF	GTP exchange factor		V	Volt
GFP	green fluorescent protein		v/v	volume/volume
GST	Glutathion-S-Transferase		Vol.	volume
h	Hour		W	watt
H2O	water		w/v	weight/volume
H2Odd	bidestilled water		WASP	Wiskott Aldrich syndrome protein
HPI	high Pathogenicity island		WT	wild type
Ig	immunoglobulin		Yop	*Yersinia* outer protein
IM	inner membrane		YpkA	*Yersinia* protein kinase A
IPTG	1-Isopropyl-β-D-1-thiogalaktoside		μ	micro
Kan	kanamycin			

G. REFERENCES

Achtman, M., K. Zurth, et al. (1999). "Yersinia pestis, the cause of plague, is a recently emerged clone of Yersinia pseudotuberculosis.[erratum appears in Proc Natl Acad Sci U S A 2000 Jul 5;97(14):8192]." Proc Natl Acad Sci U S A **96**(24): 14043-8.

Aepfelbacher, M. (2004). "Modulation of Rho GTPases by type III secretion system translocated effectors of Yersinia." Rev Physiol Biochem Pharmacol **152**: 65-77.

Aepfelbacher, M. and J. Heesemann (2001). "Modulation of Rho GTPases and the actin cytoskeleton by Yersinia outer proteins (Yops)." Int J Med Microbiol **291**(4): 269-76.

Aepfelbacher, M., C. Trasak, et al. (2003). "Characterization of YopT effects on Rho GTPases in Yersinia enterocolitica-infected cells." J Biol Chem **278**(35): 33217-23.

Aepfelbacher, M., R. Zumbihl, et al. (1999). "The tranquilizing injection of Yersinia proteins: a pathogen's strategy to resist host defense." Biol Chem **380**(7-8): 795-802.

Aili, M., E. L. Isaksson, et al. (2006). "Functional analysis of the YopE GTPase-activating protein (GAP) activity of Yersinia pseudotuberculosis." Cell Microbiol **8**(6): 1020-33.

Aili, M., M. Telepnev, et al. (2003). "In vitro GAP activity towards RhoA, Rac1 and Cdc42 is not a prerequisite for YopE induced HeLa cell cytotoxicity." Microb Pathog **34**(6): 297-308.

Aizawa, S. I. (2001). "Bacterial flagella and type III secretion systems." FEMS Microbiol Lett **202**(2): 157-64.

Aktories, K. and J. T. Barbieri (2005). "Bacterial cytotoxins: targeting eukaryotic switches." Nat Rev Microbiol **3**(5): 397-410.

Aktories, K., C. Wilde, et al. (2004). "Rho-modifying C3-like ADP-ribosyltransferases." Rev Physiol Biochem Pharmacol **152**: 1-22.

Aleksic, S. and J. Bockemuhl (1990). "[Microbiology and epidemiology of Yersinia infections]." Immun Infekt **18**(6): 178-85.

Alrutz, M. A., A. Srivastava, et al. (2001). "Efficient uptake of Yersinia pseudotuberculosis via integrin receptors involves a Rac1-Arp 2/3 pathway that bypasses N-WASP function." Mol Microbiol **42**(3): 689-703.

Anderson, D. M. and O. Schneewind (1997). "A mRNA signal for the type III secretion of Yop proteins by Yersinia enterocolitica." Science **278**(5340): 1140-3.

Anderson, D. M. and O. Schneewind (1999). "Type III machines of Gram-negative pathogens: injecting virulence factors into host cells and more." Curr Opin Microbiol **2**(1): 18-24.

Andersson, K., N. Carballeira, et al. (1996). "YopH of Yersinia pseudotuberculosis interrupts early phosphotyrosine signalling associated with phagocytosis." Mol Microbiol **20**(5): 1057-69.

Andor, A., K. Trulzsch, et al. (2001). "YopE of Yersinia, a GAP for Rho GTPases, selectively modulates Rac-dependent actin structures in endothelial cells." Cell Microbiol **3**(5): 301-10.

Aota, S., M. Nomizu, et al. (1994). "The short amino acid sequence Pro-His-Ser-Arg-Asn in human fibronectin enhances cell-adhesive function." J Biol Chem **269**(40): 24756-61.

Autenrieth, I. B. and R. Firsching (1996). "Penetration of M cells and destruction of Peyer's patches by Yersinia enterocolitica: an ultrastructural and histological study." J Med Microbiol **44**(4): 285-94.

Badger, J. L. and V. L. Miller (1998). "Expression of invasin and motility are coordinately regulated in Yersinia enterocolitica." J Bacteriol **180**(4): 793-800.

Balakirev, M. Y., S. O. Tcherniuk, et al. (2003). "Otubains: a new family of cysteine proteases in the ubiquitin pathway." EMBO Rep **4**(5): 517-22.

Balligand, G., Y. Laroche, et al. (1985). "Genetic analysis of virulence plasmid from a serogroup 9 Yersinia enterocolitica strain: role of outer membrane protein P1 in resistance to human serum and autoagglutination." Infect Immun **48**(3): 782-6.

Barnes, P. D., M. A. Bergman, et al. (2006). "Yersinia pseudotuberculosis disseminates directly from a replicating bacterial pool in the intestine." J Exp Med **203**(6): 1591-601.

Barz, C., T. N. Abahji, et al. (2000). "The Yersinia Ser/Thr protein kinase YpkA/YopO directly interacts with the small GTPases RhoA and Rac-1." FEBS Lett **482**(1-2): 139-43.

Ben-Efraim, S., M. Aronson, et al. (1961). "NEW ANTIGENIC COMPONENT OF PASTEURELLA PESTIS FORMED UNDER SPECIFIED CONDITIONS OF pH AND TEMPERATURE." J Bacteriol **81**(5): 704-14.

Bishop, A. L. and A. Hall (2000). "Rho GTPases and their effector proteins." Biochem J **348 Pt 2**: 241-55.

Black, D. S. and J. B. Bliska (1997). "Identification of p130Cas as a substrate of Yersinia YopH (Yop51), a bacterial protein tyrosine phosphatase that translocates into mammalian cells and targets focal adhesions." Embo J **16**(10): 2730-44.

Black, D. S. and J. B. Bliska (2000). "The RhoGAP activity of the Yersinia pseudotuberculosis cytotoxin YopE is required for antiphagocytic function and virulence." Mol Microbiol **37**(3): 515-27.

Black, D. S., L. G. Montagna, et al. (1998). "Identification of an amino-terminal substrate-binding domain in the Yersinia tyrosine phosphatase that is required for efficient recognition of focal adhesion targets." Mol Microbiol **29**(5): 1263-74.

Black, R. E., R. J. Jackson, et al. (1978). "Epidemic Yersinia enterocolitica infection due to contaminated chocolate milk." N Engl J Med **298**(2): 76-9.

Bliska, J. B. and D. S. Black (1995). "Inhibition of the Fc receptor-mediated oxidative burst in macrophages by the Yersinia pseudotuberculosis tyrosine phosphatase." Infect Immun **63**(2): 681-5.

Bliska, J. B., M. C. Copass, et al. (1993). "The Yersinia pseudotuberculosis adhesin YadA mediates intimate bacterial attachment to and entry into HEp-2 cells." Infect Immun **61**(9): 3914-21.

Bokoch, G. M. and B. A. Diebold (2002). "Current molecular models for NADPH oxidase regulation by Rac GTPase." Blood **100**(8): 2692-6.

Bolin, I., L. Norlander, et al. (1982). "Temperature-inducible outer membrane protein of Yersinia pseudotuberculosis and Yersinia enterocolitica is associated with the virulence plasmid." Infect Immun **37**(2): 506-12.

Bolin, I. and H. Wolf-Watz (1984). "Molecular cloning of the temperature-inducible outer membrane protein 1 of Yersinia pseudotuberculosis." Infect Immun **43**(1): 72-8.

Boquet, P. and E. Lemichez (2003). "Bacterial virulence factors targeting Rho GTPases: parasitism or symbiosis?" Trends Cell Biol **13**(5): 238-46.

Bottone, E. J. (1997). "Yersinia enterocolitica: the charisma continues." Clin Microbiol Rev **10**(2): 257-76.

Bottone, E. J. (1999). "Yersinia enterocolitica: overview and epidemiologic correlates." Microbes Infect **1**(4): 323-33.

Brakebusch, C. and R. Fassler (2003). "The integrin-actin connection, an eternal love affair." Embo J **22**(10): 2324-33.

Braun, V., V. Fraisier, et al. (2004). "TI-VAMP/VAMP7 is required for optimal phagocytosis of opsonised particles in macrophages." Embo J **23**(21): 4166-76.

Brenner, D. J. (1979). "Speciation in *Yersinia*." Contrib Microbiol Immunol **5**: 33-43.

Brubaker, R. R. (1991). "Factors promoting acute and chronic diseases caused by *yersiniae*." Clin Microbiol Rev **4**(3): 309-24.

Carniel, E., I. Guilvout, et al. (1996). "Characterization of a large chromosomal "high-pathogenicity island" in biotype 1B Yersinia enterocolitica." J Bacteriol **178**(23): 6743-51.

Caron, E. and A. Hall (1998). "Identification of two distinct mechanisms of phagocytosis controlled by different Rho GTPases." Science **282**(5394): 1717-21.

Castellano, F., P. Chavrier, et al. (2001). "Actin dynamics during phagocytosis." Semin Immunol **13**(6): 347-55.

Clark, M. A., B. H. Hirst, et al. (1998). "M-cell surface beta1 integrin expression and invasin-mediated targeting of Yersinia pseudotuberculosis to mouse Peyer's patch M cells." Infection & Immunity **66**(3): 1237-43.

Cornelis, G., Y. Laroche, et al. (1987). "Yersinia enterocolitica, a primary model for bacterial invasiveness." Rev Infect Dis **9**(1): 64-87.

Cornelis, G., J. C. Vanootegem, et al. (1987). "Transcription of the yop regulon from Y. enterocolitica requires trans acting pYV and chromosomal genes." Microb Pathog **2**(5): 367-79.

Cornelis, G. R. (2002). "Yersinia type III secretion: send in the effectors." J Cell Biol **158**(3): 401-8.

Cornelis, G. R. (2002). "The Yersinia Ysc-Yop 'type III' weaponry." Nat Rev Mol Cell Biol **3**(10): 742-52.

Cornelis, G. R. (2006). "The type III secretion injectisome." Nat Rev Microbiol **4**(11): 811-25.

Cornelis, G. R., A. Boland, et al. (1998). "The virulence plasmid of Yersinia, an antihost genome." Microbiol Mol Biol Rev **62**(4): 1315-52.

Cornelis, G. R. and H. Wolf-Watz (1997). "The Yersinia Yop virulon: a bacterial system for subverting eukaryotic cells." Mol Microbiol **23**(5): 861-7.

Cover, T. L. and R. C. Aber (1989). "Yersinia enterocolitica." N Engl J Med **321**(1): 16-24.

Cowan, C., H. A. Jones, et al. (2000). "Invasion of epithelial cells by Yersinia pestis: evidence for a Y. pestis-specific invasin." Infect Immun **68**(8): 4523-30.

Dequeker, J., R. Jamar, et al. (1980). "HLA-B27, arthritis and Yersinia enterocolitica infection." J Rheumatol **7**(5): 706-10.

Dersch, P. and R. R. Isberg (1999). "A region of the Yersinia pseudotuberculosis invasin protein enhances integrin-mediated uptake into mammalian cells and promotes self-association." Embo J **18**(5): 1199-213.

Dukuzumuremyi, J. M., R. Rosqvist, et al. (2000). "The Yersinia protein kinase A is a host factor inducible RhoA/Rac-binding virulence factor." J Biol Chem **275**(45): 35281-90.

Economou, A. (1999). "Following the leader: bacterial protein export through the Sec pathway." Trends Microbiol **7**(8): 315-20.

Eitel, J. and P. Dersch (2002). "The YadA protein of Yersinia pseudotuberculosis mediates high-efficiency uptake into human cells under environmental conditions in which invasin is repressed." Infect Immun **70**(9): 4880-91.

El Tahir, Y. and M. Skurnik (2001). "YadA, the multifaceted Yersinia adhesin." Int J Med Microbiol **291**(3): 209-18.

Emody, L., J. Heesemann, et al. (1989). "Binding to collagen by Yersinia enterocolitica and Yersinia pseudotuberculosis: evidence for yopA-mediated and chromosomally encoded mechanisms." J Bacteriol **171**(12): 6674-9.

Evdokimov, A. G., D. E. Anderson, et al. (2001). "Unusual molecular architecture of the Yersinia pestis cytotoxin YopM: a leucine-rich repeat protein with the shortest repeating unit." J Mol Biol **312**(4): 807-21.

Fallman, M., K. Andersson, et al. (1995). "Yersinia pseudotuberculosis inhibits Fc receptor-mediated phagocytosis in J774 cells." Infect Immun **63**(8): 3117-24.

Fincham, V. J., M. James, et al. (2000). "Active ERK/MAP kinase is targeted to newly forming cell-matrix adhesions by integrin engagement and v-Src." Embo J **19**(12): 2911-23.

Flugel, A., H. Schulze-Koops, et al. (1994). "Interaction of enteropathogenic Yersinia enterocolitica with complex basement membranes and the extracellular matrix proteins collagen type IV, laminin-1 and -2, and nidogen/entactin." J Biol Chem **269**(47): 29732-8.

Frederiksen, W. (1964). "A study of some *Yersinia pseudotuberculosis*-like bacteria (*Bacterium enterocoliticum* and *Pasteurella X*." Proc. 14th. Scand. Congr. Path. Microbiol **108**.

Fredriksson-Ahomaa, M., A. Stolle, et al. (2006). "Molecular epidemiology of Yersinia enterocolitica infections." FEMS Immunol Med Microbiol **47**(3): 315-29.

Fu, Y. and J. E. Galan (1999). "A salmonella protein antagonizes Rac-1 and Cdc42 to mediate host-cell recovery after bacterial invasion." Nature **401**(6750): 293-7.

Galyov, E. E., S. Hakansson, et al. (1993). "A secreted protein kinase of Yersinia pseudotuberculosis is an indispensable virulence determinant." Nature **361**(6414): 730-2.

Galyov, E. E., S. Hakansson, et al. (1994). "Characterization of the operon encoding the YpkA Ser/Thr protein kinase and the YopJ protein of Yersinia pseudotuberculosis." J Bacteriol **176**(15): 4543-8.

Goehring, U. M., G. Schmidt, et al. (1999). "The N-terminal domain of Pseudomonas aeruginosa exoenzyme S is a GTPase-activating protein for Rho GTPases." J Biol Chem **274**(51): 36369-72.

Grassl, G. A., E. Bohn, et al. (2003). "Interaction of Yersinia enterocolitica with epithelial cells: invasin beyond invasion." Int J Med Microbiol **293**(1): 41-54.

Greenberg, S., J. el Khoury, et al. (1991). "A fluorescence technique to distinguish attached from ingested erythrocytes and zymosan particles in phagocytosing macrophages." J Immunol Methods **139**(1): 115-22.

Grosdent, N., I. Maridonneau-Parini, et al. (2002). "Role of Yops and adhesins in resistance of Yersinia enterocolitica to phagocytosis." Infect Immun **70**(8): 4165-76.

Guan, K. L., R. S. Haun, et al. (1990). "Cloning and expression of a protein-tyrosine-phosphatase." Proc Natl Acad Sci U S A **87**(4): 1501-5.

Hakansson, S., E. E. Galyov, et al. (1996). "The Yersinia YpkA Ser/Thr kinase is translocated and subsequently targeted to the inner surface of the HeLa cell plasma membrane." Mol Microbiol **20**(3): 593-603.

Hakansson, S., K. Schesser, et al. (1996). "The YopB protein of Yersinia pseudotuberculosis is essential for the translocation of Yop effector proteins across the target cell plasma membrane and displays a contact-dependent membrane disrupting activity." Embo J **15**(21): 5812-23.

Hamburger, Z. A., M. S. Brown, et al. (1999). "Crystal structure of invasin: a bacterial integrin-binding protein." Science **286**(5438): 291-5.

Hamid, N., A. Gustavsson, et al. (1999). "YopH dephosphorylates Cas and Fyn-binding protein in macrophages." Microb Pathog **27**(4): 231-42.

Han, Y. W. and V. L. Miller (1997). "Reevaluation of the virulence phenotype of the inv yadA double mutants of Yersinia pseudotuberculosis." Infect Immun **65**(1): 327-30.

Hanski, C., U. Kutschka, et al. (1989). "Immunohistochemical and electron microscopic study of interaction of Yersinia enterocolitica serotype O8 with intestinal mucosa during experimental enteritis." Infect Immun **57**(3): 673-8.

Heesemann, J., U. Gross, et al. (1986). "Immunochemical analysis of plasmid-encoded proteins released by enteropathogenic Yersinia sp. grown in calcium-deficient media." Infect Immun **54**(2): 561-7.

Heesemann, J., K. Hantke, et al. (1993). "Virulence of Yersinia enterocolitica is closely associated with siderophore production, expression of an iron-repressible outer membrane polypeptide of 65,000 Da and pesticin sensitivity." Mol Microbiol **8**(2): 397-408.

Heesemann, J. and R. Laufs (1985). "Double immunofluorescence microscopic technique for accurate differentiation of extracellularly and intracellularly located bacteria in cell culture." J Clin Microbiol **22**(2): 168-75.

Heise, T. and P. Dersch (2006). "Identification of a domain in Yersinia virulence factor YadA that is crucial for extracellular matrix-specific cell adhesion and uptake." Proc Natl Acad Sci U S A **103**(9): 3375-80.

Hoffmann, R., K. van Erp, et al. (2004). "Transcriptional responses of murine macrophages to infection with Yersinia enterocolitica." Cell Microbiol **6**(4): 377-90.

Hoiczyk, E. and G. Blobel (2001). "Polymerization of a single protein of the pathogen Yersinia enterocolitica into needles punctures eukaryotic cells." Proc Natl Acad Sci U S A **98**(8): 4669-74.

Hoiczyk, E., A. Roggenkamp, et al. (2000). "Structure and sequence analysis of Yersinia YadA and Moraxella UspAs reveal a novel class of adhesins." EMBO Journal **19**(22): 5989-99.

Hultgren, S. J., S. Abraham, et al. (1993). "Pilus and nonpilus bacterial adhesins: assembly and function in cell recognition." Cell **73**(5): 887-901.

Inoue, S., M. Sugai, et al. (1991). "Molecular cloning and sequencing of the epidermal cell differentiation inhibitor gene from Staphylococcus aureus." Biochem Biophys Res Commun **174**(2): 459-64.

Iriarte, M. and G. R. Cornelis (1998). "YopT, a new Yersinia Yop effector protein, affects the cytoskeleton of host cells." Mol Microbiol **29**(3): 915-29.

Isberg, R. R. and P. Barnes (2001). "Subversion of integrins by enteropathogenic Yersinia." J Cell Sci **114**(Pt 1): 21-28.

Isberg, R. R., Z. Hamburger, et al. (2000). "Signaling and invasin-promoted uptake via integrin receptors." Microbes Infect **2**(7): 793-801.

Isberg, R. R. and J. M. Leong (1990). "Multiple beta 1 chain integrins are receptors for invasin, a protein that promotes bacterial penetration into mammalian cells." Cell **60**(5): 861-71.

Isberg, R. R., D. L. Voorhis, et al. (1987). "Identification of invasin: a protein that allows enteric bacteria to penetrate cultured mammalian cells." Cell **50**(5): 769-78.

Jaffe, A. B. and A. Hall (2005). "Rho GTPases: biochemistry and biology." Annu Rev Cell Dev Biol **21**: 247-69.

Juris, S. J., A. E. Rudolph, et al. (2000). "A distinctive role for the Yersinia protein kinase: actin binding, kinase activation, and cytoskeleton disruption." Proc Natl Acad Sci U S A **97**(17): 9431-6.

Juris, S. J., K. Shah, et al. (2006). "Identification of otubain 1 as a novel substrate for the Yersinia protein kinase using chemical genetics and mass spectrometry." FEBS Letters **580**(1): 179-83.

Juris, S. J., F. Shao, et al. (2002). "Yersinia effectors target mammalian signalling pathways." Cell Microbiol **4**(4): 201-11.

Kampik, D., R. Schulte, et al. (2000). "Yersinia enterocolitica invasin protein triggers differential production of interleukin-1, interleukin-8, monocyte chemoattractant protein 1, granulocyte-macrophage colony-stimulating factor, and tumor necrosis factor alpha in epithelial cells: implications for understanding the early cytokine network in Yersinia infections." Infect Immun **68**(5): 2484-92.

Kaplan, G. (1977). "Differences in the mode of phagocytosis with Fc and C3 receptors in macrophages." Scand J Immunol **6**(8): 797-807.

Kapperud, G., E. Namork, et al. (1987). "Plasmid-mediated surface fibrillae of Yersinia pseudotuberculosis and Yersinia enterocolitica: relationship to the outer membrane protein YOP1 and possible importance for pathogenesis." Infect Immun **55**(9): 2247-54.

Kerschen, E. J., D. A. Cohen, et al. (2004). "The plague virulence protein YopM targets the innate immune response by causing a global depletion of NK cells." Infect Immun **72**(8): 4589-602.

Khandelwal, P., K. Keliikuli, et al. (2002). "Solution structure and phosphopeptide binding to the N-terminal domain of Yersinia YopH: comparison with a crystal structure." Biochemistry **41**(38): 11425-37.

Knapp, W. (1988). Die Gattung *Yersinia* - Yersiniosen. Lehrbuch der Medizinischen Mikrobiologie. H.Brandis und G.Pulverer (ed.)**:** 348-358.

Krall, R., Y. Zhang, et al. (2004). "Intracellular membrane localization of pseudomonas ExoS and Yersinia YopE in mammalian cells." J Biol Chem **279**(4): 2747-53.

Lambert de Rouvroit, C., C. Sluiters, et al. (1992). "Role of the transcriptional activator, VirF, and temperature in the expression of the pYV plasmid genes of Yersinia enterocolitica." Mol Microbiol **6**(3): 395-409.

Leahy, D. J., I. Aukhil, et al. (1996). "2.0 A crystal structure of a four-domain segment of human fibronectin encompassing the RGD loop and synergy region." Cell **84**(1): 155-64.

Letzelter, M., I. Sorg, et al. (2006). "The discovery of SycO highlights a new function for type III secretion effector chaperones." Embo J **25**(13): 3223-33.

Leung, K. Y., B. S. Reisner, et al. (1990). "YopM inhibits platelet aggregation and is necessary for virulence of Yersinia pestis in mice." Infect Immun **58**(10): 3262-71.

Lloyd, S. A., M. Norman, et al. (2001). "Yersinia YopE is targeted for type III secretion by N-terminal, not mRNA, signals." Mol Microbiol **39**(2): 520-31.

Logsdon, L. K. and J. Mecsas (2003). "Requirement of the Yersinia pseudotuberculosis effectors YopH and YopE in colonization and persistence in intestinal and lymph tissues." Infect Immun **71**(8): 4595-607.

Makoveichuk, E., P. Cherepanov, et al. (2003). "pH6 antigen of Yersinia pestis interacts with plasma lipoproteins and cell membranes." J Lipid Res **44**(2): 320-30.

Marra, A. and R. R. Isberg (1997). "Invasin-dependent and invasin-independent pathways for translocation of Yersinia pseudotuberculosis across the Peyer's patch intestinal epithelium." Infect Immun **65**(8): 3412-21.

May, R. C., E. Caron, et al. (2000). "Involvement of the Arp2/3 complex in phagocytosis mediated by FcgammaR or CR3." Nat Cell Biol **2**(4): 246-8.

May, R. C. and L. M. Machesky (2001). "Phagocytosis and the actin cytoskeleton." J Cell Sci **114**(Pt 6): 1061-77.

McDonald, C., P. O. Vacratsis, et al. (2003). "The yersinia virulence factor YopM forms a novel protein complex with two cellular kinases." J Biol Chem **278**(20): 18514-23.

McGee, K., M. Zettl, et al. (2001). "A role for N-WASP in invasin-promoted internalisation." FEBS Lett **509**(1): 59-65.

Mecsas, J., B. Raupach, et al. (1998). "The Yersinia Yops inhibit invasion of Listeria, Shigella and Edwardsiella but not Salmonella into epithelial cells." Mol Microbiol **28**(6): 1269-81.

Miller, E. J. and S. Gay (1987). "The collagens: an overview and update." Methods Enzymol **144**: 3-41.

Miller, V. L., J. B. Bliska, et al. (1990). "Nucleotide sequence of the Yersinia enterocolitica ail gene and characterization of the Ail protein product." J Bacteriol **172**(2): 1062-9.

Miller, V. L. and S. Falkow (1988). "Evidence for two genetic loci in Yersinia enterocolitica that can promote invasion of epithelial cells." Infect Immun **56**(5): 1242-8.

Miller, V. L., J. J. Farmer, 3rd, et al. (1989). "The ail locus is found uniquely in Yersinia enterocolitica serotypes commonly associated with disease." Infect Immun **57**(1): 121-31.

Miller, V. L., B. B. Finlay, et al. (1988). "Factors essential for the penetration of mammalian cells by *Yersinia*." Curr Top Microbiol Immunol **138**: 15-39.

Miralles, F., G. Posern, et al. (2003). "Actin dynamics control SRF activity by regulation of its coactivator MAL." Cell **113**(3): 329-42.

Monack, D. M., J. Mecsas, et al. (1998). "Yersinia-induced apoptosis in vivo aids in the establishment of a systemic infection of mice." J Exp Med **188**(11): 2127-37.

Moore, R. L. (1979). "The molecular taxonomy of Yersinia enterocolitica." Contrib Microbiol Immunol **5**: 8-11.

Motin, V. L., A. M. Georgescu, et al. (2002). "Genetic variability of Yersinia pestis isolates as predicted by PCR-based IS100 genotyping and analysis of structural genes encoding glycerol-3-phosphate dehydrogenase (glpD)." J Bacteriol **184**(4): 1019-27.

Mueller, D. L. (2004). "E3 ubiquitin ligases as T cell anergy factors." Nat Immunol **5**(9): 883-90.

Mukherjee, S., G. Keitany, et al. (2006). "Yersinia YopJ acetylates and inhibits kinase activation by blocking phosphorylation." Science **312**(5777): 1211-4.

Mulder, B., T. Michiels, et al. (1989). "Identification of additional virulence determinants on the pYV plasmid of Yersinia enterocolitica W227." Infect Immun **57**(8): 2534-41.

Navarro, L., N. M. Alto, et al. (2005). "Functions of the Yersinia effector proteins in inhibiting host immune responses." Curr Opin Microbiol **8**(1): 21-7.

Neutra, M. R., N. J. Mantis, et al. (2001). "Collaboration of epithelial cells with organized mucosal lymphoid tissues." Nature Immunology **2**(11): 1004-9.

Nobes, C. D. and A. Hall (1995). "Rho, rac, and cdc42 GTPases regulate the assembly of multimolecular focal complexes associated with actin stress fibers, lamellipodia, and filopodia." Cell **81**(1): 53-62.

Nummelin, H., M. C. Merckel, et al. (2004). "The Yersinia adhesin YadA collagen-binding domain structure is a novel left-handed parallel beta-roll." Embo J **23**(4): 701-11.

Nyberg, P., T. Sakai, et al. (2004). "Interactions with fibronectin attenuate the virulence of Streptococcus pyogenes." Embo J **23**(10): 2166-74.

Orth, K. (2002). "Function of the Yersinia effector YopJ." Curr Opin Microbiol **5**(1): 38-43.

Orth, K., L. E. Palmer, et al. (1999). "Inhibition of the mitogen-activated protein kinase kinase superfamily by a Yersinia effector." Science **285**(5435): 1920-3.

Pepe, J. C. and V. L. Miller (1993). "Yersinia enterocolitica invasin: a primary role in the initiation of infection." Proc Natl Acad Sci U S A **90**(14): 6473-7.

Pepe, J. C., M. R. Wachtel, et al. (1995). "Pathogenesis of defined invasion mutants of Yersinia enterocolitica in a BALB/c mouse model of infection." Infect Immun **63**(12): 4837-48.

Perry, R. D. and J. D. Fetherston (1997). "Yersinia pestis--etiologic agent of plague." Clin Microbiol Rev **10**(1): 35-66.

Persson, C., N. Carballeira, et al. (1997). "The PTPase YopH inhibits uptake of Yersinia, tyrosine phosphorylation of p130Cas and FAK, and the associated accumulation of these proteins in peripheral focal adhesions." Embo J **16**(9): 2307-18.

Persson, C., R. Nordfelth, et al. (1999). "Localization of the Yersinia PTPase to focal complexes is an important virulence mechanism." Mol Microbiol **33**(4): 828-38.

Pierson, D. E. and S. Falkow (1993). "The ail gene of Yersinia enterocolitica has a role in the ability of the organism to survive serum killing." Infect Immun **61**(5): 1846-52.

Prehna, G., M. I. Ivanov, et al. (2006). "Yersinia virulence depends on mimicry of host rho-family nucleotide dissociation inhibitors." Cell **126**(5): 869-80.

Raftopoulou, M. and A. Hall (2004). "Cell migration: Rho GTPases lead the way." Dev Biol **265**(1): 23-32.

Ray, S. M., S. D. Ahuja, et al. (2004). "Population-based surveillance for Yersinia enterocolitica infections in FoodNet sites, 1996-1999: higher risk of disease in infants and minority populations." Clin Infect Dis **38 Suppl 3**: S181-9.

Revell, P. A. and V. L. Miller (2000). "A chromosomally encoded regulator is required for expression of the Yersinia enterocolitica inv gene and for virulence." Mol Microbiol **35**(3): 677-85.

Ridley, A. J., H. F. Paterson, et al. (1992). "The small GTP-binding protein rac regulates growth factor-induced membrane ruffling." Cell **70**(3): 401-10.

Roberts, A. W., C. Kim, et al. (1999). "Deficiency of the hematopoietic cell-specific Rho family GTPase Rac2 is characterized by abnormalities in neutrophil function and host defense." Immunity **10**(2): 183-96.

Roggenkamp, A., H. R. Neuberger, et al. (1995). "Substitution of two histidine residues in YadA protein of Yersinia enterocolitica abrogates collagen binding, cell adherence and mouse virulence." Mol Microbiol **16**(6): 1207-19.

Roggenkamp, A., K. Ruckdeschel, et al. (1996). "Deletion of amino acids 29 to 81 in adhesion protein YadA of Yersinia enterocolitica serotype O:8 results in selective abrogation of adherence to neutrophils." Infect Immun **64**(7): 2506-14.

Rosqvist, R., K. E. Magnusson, et al. (1994). "Target cell contact triggers expression and polarized transfer of Yersinia YopE cytotoxin into mammalian cells." Embo J **13**(4): 964-72.

Rosqvist, R., M. Skurnik, et al. (1988). "Increased virulence of Yersinia pseudotuberculosis by two independent mutations." Nature **334**(6182): 522-4.

Ruckdeschel, K. (2002). "Immunomodulation of macrophages by pathogenic Yersinia species." Arch Immunol Ther Exp (Warsz) **50**(2): 131-7.

Ruckdeschel, K., G. Pfaffinger, et al. (2006). "The proteasome pathway destabilizes Yersinia outer protein E and represses its antihost cell activities." J Immunol **176**(10): 6093-102.

Ruckdeschel, K., A. Roggenkamp, et al. (1996). "Differential contribution of Yersinia enterocolitica virulence factors to evasion of microbicidal action of neutrophils." Infect Immun **64**(3): 724-33.

Sakai, T., K. J. Johnson, et al. (2001). "Plasma fibronectin supports neuronal survival and reduces brain injury following transient focal cerebral ischemia but is not essential for skin-wound healing and hemostasis." Nat Med **7**(3): 324-30.

Sauvonnet, N., B. Pradet-Balade, et al. (2002). "Regulation of mRNA expression in macrophages after Yersinia enterocolitica infection. Role of different Yop effectors." J Biol Chem **277**(28): 25133-42.

Scheffzek, K., M. R. Ahmadian, et al. (1998). "Structural analysis of the GAP-related domain from neurofibromin and its implications." Embo J **17**(15): 4313-27.

Schleifstein, J. I. and M. B. Coleman (1939). "An unidentified microorganism resembling *B. lignier*i and *Past. pseudotuberculosis*, and pathogenic for man." N Y State J Med **39**: 1749-1753.

Schmid, Y., G. A. Grassl, et al. (2004). "Yersinia enterocolitica adhesin A induces production of interleukin-8 in epithelial cells." Infect Immun **72**(12): 6780-9.

Schubert, S., J. Bockemuhl, et al. (2003). "First isolation of virulent Yersinia enterocolitica O8, biotype 1B in Germany." Eur J Clin Microbiol Infect Dis **22**(1): 66-8.

Schubert, S., A. Rakin, et al. (2004). "The Yersinia high-pathogenicity island (HPI): evolutionary and functional aspects." Int J Med Microbiol **294**(2-3): 83-94.

Schulte, R. and I. B. Autenrieth (1998). "Yersinia enterocolitica-induced interleukin-8 secretion by human intestinal epithelial cells depends on cell differentiation." Infect Immun **66**(3): 1216-24.

Schulte, R., G. A. Grassl, et al. (2000). "Yersinia enterocolitica invasin protein triggers IL-8 production in epithelial cells via activation of Rel p65-p65 homodimers." Faseb J **14**(11): 1471-84.

Schulte, R., S. Kerneis, et al. (2000). "Translocation of Yersinia entrocolitica across reconstituted intestinal epithelial monolayers is triggered by Yersinia invasin binding to beta1 integrins apically expressed on M-like cells." Cell Microbiol **2**(2): 173-85.

Schulte, R., R. Zumbihl, et al. (1998). "Wortmannin blocks Yersinia invasin-triggered internalization, but not interleukin-8 production by epithelial cells." Med Microbiol Immunol (Berl) **187**(1): 53-60.

Schulze-Koops, H., H. Burkhardt, et al. (1993). "Outer membrane protein YadA of enteropathogenic yersiniae mediates specific binding to cellular but not plasma fibronectin." Infect Immun **61**(6): 2513-9.

Schulze-Koops, H., H. Burkhardt, et al. (1992). "Plasmid-encoded outer membrane protein YadA mediates specific binding of enteropathogenic yersiniae to various types of collagen." Infect Immun **60**(6): 2153-9.

Schulze-Koops, H., H. Burkhardt, et al. (1995). "Characterization of the binding region for the Yersinia enterocolitica adhesin YadA on types I and II collagen." Arthritis Rheum **38**(9): 1283-9.

Schwartz, M. (2004). "Rho signalling at a glance." J Cell Sci **117**(Pt 23): 5457-8.

Shao, F., P. M. Merritt, et al. (2002). "A Yersinia effector and a Pseudomonas avirulence protein define a family of cysteine proteases functioning in bacterial pathogenesis." Cell **109**(5): 575-88.

Shao, F., P. O. Vacratsis, et al. (2003). "Biochemical characterization of the Yersinia YopT protease: cleavage site and recognition elements in Rho GTPases." Proc Natl Acad Sci U S A **100**(3): 904-9.

Simonet, M., S. Richard, et al. (1990). "Electron microscopic evidence for in vivo extracellular localization of Yersinia pseudotuberculosis harboring the pYV plasmid." Infect Immun **58**(3): 841-5.

Simonet, M., B. Riot, et al. (1996). "Invasin production by Yersinia pestis is abolished by insertion of an IS200-like element within the inv gene." Infect Immun **64**(1): 375-9.

Skrzypek, E., C. Cowan, et al. (1998). "Targeting of the Yersinia pestis YopM protein into HeLa cells and intracellular trafficking to the nucleus." Mol Microbiol **30**(5): 1051-65.

Skrzypek, E., T. Myers-Morales, et al. (2003). "Application of a Saccharomyces cerevisiae model to study requirements for trafficking of Yersinia pestis YopM in eucaryotic cells." Infect Immun **71**(2): 937-47.

Snellings, N. J., M. Popek, et al. (2001). "Complete DNA sequence of Yersinia enterocolitica serotype 0:8 low-calcium-response plasmid reveals a new virulence plasmid-associated replicon." Infect Immun **69**(7): 4627-38.

Sodeinde, O. A., Y. V. Subrahmanyam, et al. (1992). "A surface protease and the invasive character of plague." Science **258**(5084): 1004-7.

Sory, M. P., A. Boland, et al. (1995). "Identification of the YopE and YopH domains required for secretion and internalization into the cytosol of macrophages, using the cyaA gene fusion approach." Proc Natl Acad Sci U S A **92**(26): 11998-2002.

Straley, S. C. and W. S. Bowmer (1986). "Virulence genes regulated at the transcriptional level by Ca2+ in Yersinia pestis include structural genes for outer membrane proteins." Infect Immun **51**(2): 445-54.

Straley, S. C. and R. D. Perry (1995). "Environmental modulation of gene expression and pathogenesis in Yersinia." Trends in Microbiology **3**(8): 310-7.

Symons, M. and J. Settleman (2000). "Rho family GTPases: more than simple switches." Trends Cell Biol **10**(10): 415-9.

Tahir, Y. E., P. Kuusela, et al. (2000). "Functional mapping of the Yersinia enterocolitica adhesin YadA. Identification Of eight NSVAIG - S motifs in the amino-terminal half of the protein involved in collagen binding." Mol Microbiol **37**(1): 192-206.

Tamm, A., A. M. Tarkkanen, et al. (1993). "Hydrophobic domains affect the collagen-binding specificity and surface polymerization as well as the virulence potential of the YadA protein of Yersinia enterocolitica." Mol Microbiol **10**(5): 995-1011.

Tardy, F., F. Homble, et al. (1999). "Yersinia enterocolitica type III secretion-translocation system: channel formation by secreted Yops." Embo J **18**(23): 6793-9.

Tertti, R., M. Skurnik, et al. (1992). "Adhesion protein YadA of Yersinia species mediates binding of bacteria to fibronectin." Infect Immun **60**(7): 3021-4.

Trasak, C., G. Zenner, et al. (2007). "Yersinia Protein Kinase YopO Is Activated by A Novel G-actin Binding Process." J Biol Chem **282**(4): 2268-2277.

Trcek, J., G. Wilharm, et al. (2002). "Yersinia enterocolitica YopQ: strain-dependent cytosolic accumulation and post-translational secretion." Microbiology **148**(Pt 5): 1457-65.

Trulzsch, K., T. Sporleder, et al. (2004). "Contribution of the major secreted yops of Yersinia enterocolitica O:8 to pathogenicity in the mouse infection model." Infect Immun **72**(9): 5227-34.

Van Aelst, L. and C. D'Souza-Schorey (1997). "Rho GTPases and signaling networks." Genes Dev **11**(18): 2295-322.

Van Nhieu, G. T. and R. R. Isberg (1991). "The Yersinia pseudotuberculosis invasin protein and human fibronectin bind to mutually exclusive sites on the alpha 5 beta 1 integrin receptor." J Biol Chem **266**(36): 24367-75.

Viboud, G. I. and J. B. Bliska (2001). "A bacterial type III secretion system inhibits actin polymerization to prevent pore formation in host cell membranes." Embo J **20**(19): 5373-82.

Viboud, G. I. and J. B. Bliska (2005). "Yersinia outer proteins: role in modulation of host cell signaling responses and pathogenesis." Annu Rev Microbiol **59**: 69-89.

Visa, N. (2005). "Actin in transcription. Actin is required for transcription by all three RNA polymerases in the eukaryotic cell nucleus." EMBO Rep **6**(3): 218-9.

Von Pawel-Rammingen, U., M. V. Telepnev, et al. (2000). "GAP activity of the Yersinia YopE cytotoxin specifically targets the Rho pathway: a mechanism for disruption of actin microfilament structure." Mol Microbiol **36**(3): 737-48.

Wattiau, P., B. Bernier, et al. (1994). "Individual chaperones required for Yop secretion by Yersinia." Proc Natl Acad Sci U S A **91**(22): 10493-7.

Wauters, G., K. Kandolo, et al. (1987). "Revised biogrouping scheme of Yersinia enterocolitica." Contrib Microbiol Immunol **9**: 14-21.

Wiedemann, A., S. Linder, et al. (2001). "*Yersinia enterocolitica* invasin triggers phagocytosis via beta1 integrins, CDC42Hs and WASp in macrophages." Cell Microbiol **3**(10): 693-702.

Wiley, D. J., R. Nordfeldth, et al. (2006). "The Ser/Thr kinase activity of the Yersinia protein kinase A (YpkA) is necessary for full virulence in the mouse, mollifying phagocytes, and disrupting the eukaryotic cytoskeleton." Microb Pathog **40**(5): 234-43.

Winblad, S. (1969). "Erythema nodosum associated with infection with Yersinia enterocolitica." Scand J Infect Dis **1**(1): 11-6.

Woestyn, S., A. Allaoui, et al. (1994). "YscN, the putative energizer of the Yersinia Yop secretion machinery." J Bacteriol **176**(6): 1561-9.

Wong, K. W. and R. R. Isberg (2005). "Yersinia pseudotuberculosis spatially controls activation and misregulation of host cell Rac1." PLoS Pathog **1**(2): e16.

Wulf, E., A. Deboben, et al. (1979). "Fluorescent phallotoxin, a tool for the visualization of cellular actin." Proc Natl Acad Sci U S A **76**(9): 4498-502.

Wurtele, M., E. Wolf, et al. (2001). "How the Pseudomonas aeruginosa ExoS toxin downregulates Rac." Nat Struct Biol **8**(1): 23-6.

Yang, Y. and R. R. Isberg (1993). "Cellular internalization in the absence of invasin expression is promoted by the Yersinia pseudotuberculosis yadA product." Infect Immun **61**(9): 3907-13.

Yang, Y., J. J. Merriam, et al. (1996). "The psa locus is responsible for thermoinducible binding of Yersinia pseudotuberculosis to cultured cells." Infect Immun **64**(7): 2483-9.

Yao, T., J. Mecsas, et al. (1999). "Suppression of T and B lymphocyte activation by a Yersinia pseudotuberculosis virulence factor, yopH." J Exp Med **190**(9): 1343-50.

Yu, J. and J. B. Kaper (1992). "Cloning and characterization of the eae gene of enterohaemorrhagic Escherichia coli O157:H7." Mol Microbiol **6**(3): 411-7.

Zav'yalov, V. P., V. M. Abramov, et al. (1996). "pH6 antigen (PsaA protein) of Yersinia pestis, a novel bacterial Fc-receptor." FEMS Immunol Med Microbiol **14**(1): 53-7.

Zhang, W. L., B. Kohler, et al. (2002). "Genetic diversity of intimin genes of attaching and effacing Escherichia coli strains." J Clin Microbiol **40**(12): 4486-92.

Zhu, M., F. Shao, et al. (2004). "The crystal structure of Pseudomonas avirulence protein AvrPphB: a papain-like fold with a distinct substrate-binding site." Proc Natl Acad Sci U S A **101**(1): 302-7.

H. ACKNOWLEDGEMENTS

This work would have never been possible without the help of many people. I wish to express my sincere gratitude to:

My supervisor, Prof. Dr. M. Aepfelbacher for giving me the opportunity to work in his group, for his confidence, his help and continues support throughout my doctoral studies in Munich and in Hamburg. Thank you for stimulating discussions, critical and careful reading of the manuscript and for giving me the opportunity to gather experience in the field of microscopical applications.

Thank you to PD Dr. Angelika Böttger for accepting to be my supervisor at the biological department, for carefully reviewing this work and being generous with her time.

I am also grateful to Prof. Dr. Michael Schleicher for reviewing this work and to Prof. Dr. Elisabeth Weiß and Prof. Dr. Thomas Cremer for accepting to be a member of the thesis committee.

PD Dr. Klaus Ruckdeschel and PD Dr. Stefan Linder for cooperation and discussions and Prof. Dr. Dr. J. Heesemann for supporting my work at the Max von Pettenkofer Institute.

All the the current and former members of the "Aepfelbacher group", the "Linder Lab" and the "Ruckdeschel group", for continues help and support, innumerous little favours, the motivating atmosphere and encouragement:
Claudia Trasak, Sabrina Schubert, Gülnihal Yüksekdag, Heiko Ilchmann, Barbara Schröder, Petra Kopp, Vanessa van Vliet, Barbara Böhlig, Anna Osiak, Rudi Hase, Gudrun Pfaffinger, Kathleen Richter.
The people in Hamburg at the UKE: Bernhard Roppenser, Franzi Albrecht, Bernd Zobiak, Stefan Feisthauer, Martin Kuhns, Johannes Knobloch and everybody I forgot to mention.

Andi Schroeder for always having the time for advice and for helping me to establish assays and microscopy techniques. I appreciate his endurance for the discussions on microscopical hardware and fast food joints.

I appreciate Nicole´s confidence in me and I am thankful for her gift to make my day brighter.

Mein größter Dank gilt meiner Familie und ganz besonders meinen Eltern:
Für ihre Liebe, Ihr Vertrauen und Ihre stetige und bedingungslose Unterstützung in meinem Leben. *Ohne Euch wäre ich nicht da wo ich jetzt bin. Danke.*

I. CURRICULUM VITAE

PERSONAL INFORMATION

LAST NAME: Zenner
FIRST NAME: Gerhardt
ADDRESS: Papenstr. 122
                  22089 Hamburg
DATE OF BIRTH: 14.04.1975
NATIONALITY: German
PLACE OF BIRTH: Arad, Romania

EDUCATION

2006	-	present	**Universitätsklinikum Hamburg - Eppendorf**
			wissenschaftlicher Mitarbeiter, continuing work for doctoral dissertation (Dr. rer. nat.)
2003	-	2006	**Ludwig Maximilians Universität - Munich**
			Max von Pettenkofer Institute, doctoral dissertation: "Cellular effects of the multidomain serine/threonine kinase from *Yersinia enterocolitica*"
2002	-	2003	**University of Wisconsin - Milwaukee, USA**
			Assistant researcher position at the College of Health Sciences
1995	-	2002	**Ludwig Maximilians Universität - Munich**
			Diplom Biologe; Fields of study: Microbiology, Cell biology, Pharmacology and Toxicology
1994	-	1995	**Military Service - Pocking**
1990	-	1994	**Tassilo Gymnasium - Simbach am Inn**
1982	-	1990	**Grade school, Hans-Leinberger Gymnasium - Landshut**
1979	-	1982	**Kindergarten and Romanian grade school - Arad, Romania**